Forecasted versus In Situ Dielectric Constants for Soil

A Thesis

Presented to

The Faculty of the Graduate School

At the University of Missouri

In Partial Fulfillment

Of the Requirements for the Degree

Master of Science

By

DAVID WILLIAMS, EIT

Dr. John J. Bowders, Jr. P.E., Thesis Supervisor

July 2016

The undersigned, appointed by the dean of the Graduate School,

have examined the Thesis entitled

FORECASTED VERSUS IN SITU DIELECTRIC CONSTANTS FOR SOIL

Presented by David Williams, EIT

A candidate for the degree of

Master of Science

And hereby certify that, in their opinion, it is worthy of acceptance.

Professor John J. Bowders, PE

Professor Robert L. Druce

Professor R. David Hammer

Acknowledgements

I would like to take this time to express my sincere appreciation to Dr. John J. Bowders, Jr., PE, for his tireless work throughout my thesis process. His guidance, encouragement, and dedication throughout not only my graduate studies, but undergraduate as well, have been an immense help. Dr. Bowders shear enthusiasm and work ethic in the field of engineering have increased the professional standards I will hold myself to moving forward.

I would also like to thank my parents, Lowell and Camelia Williams, as well as my brother, Lucas and sister, Marsha; although a simple thanks is surely not enough. Their never-ending support and advice through thick and thin has been extremely helpful to my success. Also, their encouragement and freedom to be who I wanted to be has certainly helped put me where I am today. I feel truly lucky to have been raised by my parents as many of the values and beliefs I have today are from them.

It would be completely ignorant of me to not thank my wife, Whitney, and my daughter , Madison. Their unwavering love, support and encouragement has been extremely helpful throughout my educational and professional studies. I am truly blessed to have them in my life, as they continually gives me strength to strive for success. The best is yet to come.

I must thank the University of Missouri (MU), Geotechnical Engineering Professors, Dr. Erik Loehr, Dr. Brent Rosenblad, and Dr. R. David Hammer. Their practical teachings in and out of the classroom, have built the solid foundation I will carry into my professional career. Future successes will certainly occur because of them.

The Office of Naval Research (ONR) deserves thanks for funding my graduate research. Also, the students and faculty from the MU Electrical Engineering department, should be thanked

Table of Contents

List of Figures

List of Tables

FORECASTED VERSUS *IN SITU* DIELECTRIC CONSTANTS FOR SOIL

David A. Williams

Dr. John J. Bowders, Jr., PE, Thesis Supervisor

Abstract

Some nondestructive testing (NDT) techniques in civil engineering applications employ electromagnetic (EM) wave methods. These techniques have proven to be effective for many applications including investigating and characterizing the subsurface (Bowders et al., 1982a), identifying steel reinforcement locations in pavements and testing the integrity of concrete foundations. Civil engineering subsurface characterizations typically propagate EM waves in the radio to microwave range (3 kHz to 300 GHz).

The dielectric constant of a soil determines the velocity of EM waves traveling through the soil. Dielectric constant is the real part of the relative permittivity of soil and is a measure of the soil's ability to be polarized by an electrical field. Several empirical models exist to predict the dielectric constant of soils and all show the dielectric constant to be strongly related to the soil's volumetric water content.

The objective of this project is to quantify the accuracy of forecasted dielectric constants of soil by comparing with *in situ* measured dielectric constants. A field test site at McBaine, Missouri (MO) was instrumented with commercially available sensors for measuring soil and meteorological conditions. Sensors measured the soil's dielectric constant, temperature, electrical conductivity, volumetric water content (using the measured dielectric constant in Topp et al's, 1980, predictive model), air temperature, relative humidity, solar irradiance, wind speed, and

precipitation. Measurements of meteorological and *in situ* soil conditions began on April 24th, 2012 and have been recorded for over one year.

The meteorological conditions at McBaine, MO and the soil properties associated with the field site were documented in this study. Measured meteorological conditions and soil properties were used in the moisture migration model and existing empirical dielectric constant models to forecast the dielectric constant of soil. The forecasts were compared with *in situ* measurements of dielectric constant. Forecasted and measured dielectric constants were different and the soil with the higher clay content had the least agreement (percentage difference between 80 to 100 percent), while the soil with the higher sand content had the best agreement (percentage difference less than 20 percent).

The differences lead to a discussion of the variables affecting forecasted and measured values. The laboratory characterization of McBaine, MO soils and what was observed at the field site indicated the soil's tendency to shrink-swell during wetting and drying events. The expansive nature and blocky structure created macropores thus enabling preferential flow of water through the soil. The inability of WinUnSat-H to model moisture migration through soils with macropores and the model uncertainty associated with the dielectric constant predictive models was indicated by the differences between forecasted and measured dielectric constants.

The discussion brought to light elements of the McBaine, MO field site that were not accounted for in the forecasted dielectric constants, but were factors in the measured dielectric constants. Substituting the one-dimensional moisture migration model (WinUnSat-H) with a two- or three-dimensional model, as well as measuring the *in situ* volumetric water content as a starting point for simulations may improve the accuracy of forecasted dielectric constants.

1 Introduction

1.1 Overview

Some nondestructive testing (NDT) techniques in civil engineering applications employ electromagnetic (EM) wave methods. These techniques have proven to be effective for many applications including investigating and characterizing the subsurface, identifying steel reinforcement locations in pavements, and testing the integrity of concrete foundations. For example, concrete foundations can be compromised when voids and/or cracks form out of eyesight. Propagated EM waves can help determine the size and location of voids and/or cracks in concrete structures (Bungey et al., 2006). Nondestructive test methods are beneficial because of their ability to produce a continuous evaluation of the material being analyzed. Nondestructive testing is valuable in situations where physical sampling could alter the quantity being measured or affect the function of the material.

Civil engineering subsurface characterizations typically propagate EM waves in the radio to microwave range. These waves have frequencies ranging from 3 kilohertz (kHz) to 300 megahertz (MHz) and 300 MHz to 300 gigahertz (GHz), respectively (Koerner et al., 1982b). Radio and microwave frequencies have a distinct advantage over other frequency ranges (visible or infrared) because they penetrate through vegetative cover and deeper into a soil subsurface (Behari, 2005). The visible and infrared frequency ranges, which range from 10^{12} Hz to 10^{15} Hz, are most accurate when little to no vegetative cover is present (Behari, 2005).

The real part of relative permittivity of soil is also called the dielectric constant. The dielectric constant is a measure of the material's ability to be polarized by an electrical field and determines the EM wave velocity (Behari, 2005). Wave velocities in near-surface soil are directly proportional to an EM wave's wavelength and frequency, with wavelength having a relationship

with penetration depth (Troch et al., 1996). Longer wavelengths penetrate further into a subsurface than shorter wavelengths at similar wave velocities. The dielectric constants of a soil impact properties of refracted and reflected EM energy, and consequently penetration depth.

Numerous studies have shown the dielectric constant of a soil is dependent on the amount of moisture in the medium (Okrasinski et al., 1978). Constantly changing meteorological conditions and soil properties affect the amount of moisture, and thus affect the dielectric constant, of soil. Numerous empirical and semi-empirical predictive models, which involve various soil properties for determining the dielectric constant of soil, are currently in use. Generally, the models produce predictions for a discrete point in time and therefore cannot provide continuous real-time information showing changes in a soil's dielectric properties over time. *In situ* sensors allow real-time discrete measurements of the dielectric constant of soils over time. The sensors show changes with respect to time, but only indirectly account for various meteorological conditions. Sensors make individual measurements at predetermined time intervals.

Meteorological conditions, measured at weather monitoring stations, are separated spatially and typically are not constructed at sites of interest. Remotely acquiring meteorological data from weather monitoring stations present spatial and temporal variability. There has been little attention given to determining a soil's dielectric constant using remotely acquired meteorological data.

1.2   Objective

The objective of this project is to quantify the accuracy of the forecasted dielectric constants for soil based on meteorological data by comparing them with *in situ* measured dielectric constants. The objective is to 'ground-truth' the forecasted dielectric constants of soil. *In situ* measurements of a soil's dielectric constant were compared to forecasted dielectric constants of

soil using recorded meteorological data. The dielectric constant forecasting in this study was conducted by coupling empirical and semi-empirical predictive models with a soil moisture migration model.

1.3 Scope of Investigation

A field test site at McBaine, Missouri (MO) was instrumented with commercially available sensors for measuring soil and meteorological conditions beginning April 24th, 2012. *In situ* soil measurements included: dielectric constant, soil temperature, bulk electrical conductivity, and volumetric water content. Meteorological measurements included: wind speed, wind direction, solar irradiance, precipitation, air temperature, and relative humidity. The ongoing measurements were recorded at five minute intervals.

In situ measurements over the period from June 1st, 2013 to June 30th, 2013 represent common field events where moisture, and consequently dielectric constant, change over a relatively short time with changing meteorological and soil conditions. The moisture migration computer model, WinUnsat-H, was used to simulate moisture changes at McBaine, MO over the same period of time and the simulated moisture contents were used in conjunction with dielectric constant predictive models to forecast the soil's dielectric constant.

1.4 Organization of the Thesis

The thesis contains measurements from instrumentation installed at the McBaine, MO test site to record meteorological and soil conditions, as well as forecasted results. Comparisons of forecasted dielectric constants with *in situ* measurements are described and discussed in the thesis. A review of the literature pertaining to dielectric constants of soils is presented in Chapter 2. Instruments installed at the McBaine, MO test site, laboratory characterization of soils, and the moisture migration model, WinUnsat-H, are described in Chapter 3. Meteorological recordings

and soil characterization results of McBaine, MO are presented with forecasted and *in situ* measured dielectric constants in Chapter 4. Results from the meteorological recordings and laboratory characterization at McBaine, MO are discussed in Chapter 5. Forecasted and *in situ* measured dielectric constants of soil for the McBaine, MO test site are also discussed in Chapter 5. Conclusions and recommendations based on the work presented herein are provided in Chapter 6.

2 Literature Review

2.1 Introduction

This chapter contains background on the dielectric constant of soils. A brief introduction describing electromagnetic waves and dielectric constant is given, followed by a review of the predictive models currently used to forecast the dielectric constant of soils. Two published studies conducted to measure the change in dielectric constant of soil versus depth with time are also described. Modeling subsurface moisture movement in soil using a numerical computer model is also presented.

2.2 Background

Electromagnetic (EM) waves are light waves formed when an electric field couples with an orthogonal magnetic field (Figure 2.1). The waves are characterized by their wavelength and frequency (Figure 2.2). Wavelength characterizes the distance between similar points on a wave, such as crest to crest or trough to trough, and is measured in units of length. Frequency is the number of occurrences of a repeating point per second, and is measured in units of Hertz (cycles per second, s^{-1}). When EM waves propagate through a vacuum, the wave velocity is the speed of light. Using a constant wave velocity, a particular wavelength or frequency is determined based on the relationship shown in Equation 2.1.

$$c = \lambda \times f \qquad \qquad \textbf{Equation 2.1}$$

where,

c = speed of light, constant [3.0×10^8 m/s],

λ = EM wavelength [m], and

f = EM frequency [Hz or s^{-1}]
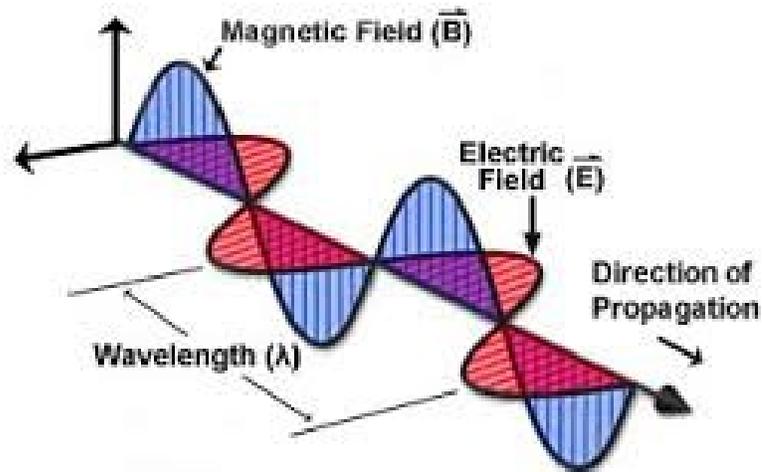
Figure 2.1: Idealized Propagating Electromagnetic Wave (http://micro.magnet.fsu.edu/primer/java/wavebasics/)
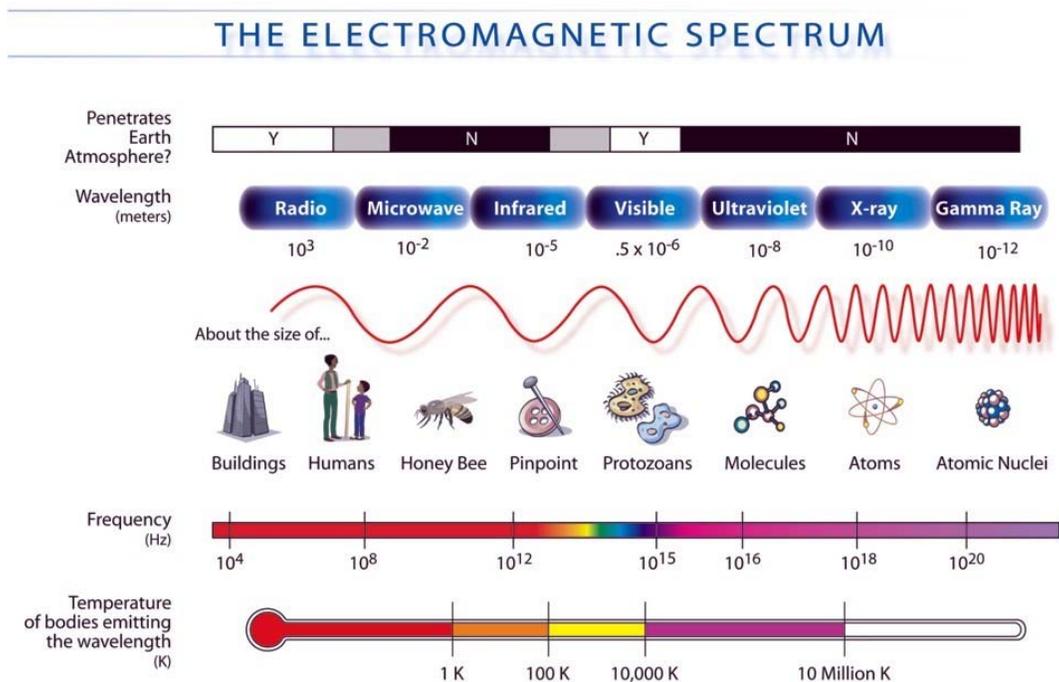
Figure 2.2: Electromagnetic Waves and Corresponding Wavelengths and Frequencies (http://mynasadata.larc.nasa.gov/science-processes/electromagnetic-diagram/)

EM waves propagate, and attenuate through a medium. The magnitude and direction of each characteristic is determined by a medium's permittivity. Permittivity is a measure of the ability of a material to be polarized by an electrical field and determines the EM wave velocity (Behari, 2005) (Equation 2.2). The relative permittivity, also called the real part of complex permittivity, can be expressed as the ratio of a material's actual permittivity to the permittivity of a vacuum (Equation 2.3).

$$V_{rf} = \frac{c}{\sqrt{\varepsilon'}}$$

Equation 2.2

where,

V_{rf} = radio frequency wave velocity $[\frac{L}{T}]$,

c = speed of light, constant [3.0 x 10^8 m/s], and

ε' = real part of relative permittivity

$$\varepsilon_r = \frac{\varepsilon_a}{\varepsilon_o}$$

Equation 2.3

where,

ε_r = relative permittivity of a medium,

ε_a = actual permittivity of a medium, and

ε_o = permittivity in a vacuum

Relative permittivity is a complex function containing both real and imaginary parts as shown in Equation 2.4.

$$\varepsilon = \varepsilon' - j\varepsilon''$$ **Equation 2.4**

where,

ε = complex relative permittivity,

ε' = real part of relative permittivity,

$j = \sqrt{-1}$, and

ε'' = imaginary part of relative permittivity

In water, the real part of relative permittivity shows little frequency dependence up to three GHz. Beyond three GHz the real part of relative permittivity decreases. The imaginary part of relative permittivity represents the loss of energy and begins increasing at around 1 GHz, and continues increasing up to 17 GHz (Curtis, 2001). The real part of relative permittivity is also termed dielectric constant.

Nondestructive testing (NDT) techniques in civil engineering applications employ EM wave methods. These techniques have proven to be effective for many applications including investigating and characterizing the subsurface (Bowders et al., 1982a, Koerner et al., 1982a, Bowders et al., 1982b, Koerner et al., 1982b, Bowders et al., 1983), identifying steel reinforcement locations in pavements, and testing the integrity of concrete foundations and pavements. For example, concrete foundations are integral parts of a successful structure and when voids and/or cracks form unknowingly, the structure can be compromised. Propagated EM waves can help determine the sizes and locations of voids and/or cracks in concrete structures (Bungey et al., 2006). These techniques are beneficial because of their ability to produce a continuous image without disturbing the material being tested. Nondestructive testing is valuable in situations where physical sampling could alter the quantity being measured or affect the function of the material.

Civil engineering subsurface characterizations typically propagate EM waves in the radio to microwave range. These waves have frequencies ranging from 3 kilohertz (kHz) to 300 megahertz (MHz) and 300 MHz to 300 gigahertz (GHz), respectively (Koerner et al., 1982b). Radio and microwave frequencies have a distinct advantage over other frequency ranges (visible or infrared) because they penetrate through vegetative cover and deeper into a soil subsurface (Behari, 2005). The visible and infrared frequency ranges (Figure 2.2) are most accurate when little to no vegetative cover is present (Behari, 2005)

2.3   Dielectric Constant of Soil

Dielectric constant represents the capacitance (ability to store electrical charge) of a medium (Hilhorst, 1998). A medium with a small dielectric constant (air $\approx$ 1) has a low ability to polarize and hold an electrical charge. Small dielectric constant mediums impede EM waves and are good insulators. A medium with a large dielectric constant (water $\approx$ 80) has a high ability to polarize and hold an electrical charge. Large dielectric constant mediums propagate EM waves with less impedance and are good conductors.

The dielectric constants of soils are affected by measurement frequency and variables of the soil, such as texture, structure, soluble salts, water content, temperature, and density (Topp et al., 1980). Each parameter helps describe the three phases of soil; soil particles (solids), liquid water (liquids), and air (gas) (Figure 2.3). Relationships have been developed based on weights and volumes of the three phases and give information pertaining to soil composition (Table 2.1). Deionized water has a dielectric constant of 80.1 when measured at a temperature of 20 °C and 1 GHz. Air, when measured at the same temperature and frequency, has a dielectric constant of 1.006. The dielectric constant of soil particles (solids), when measured at the same temperature and frequency, is typically between 2 and 5 (Thomas, 1966).
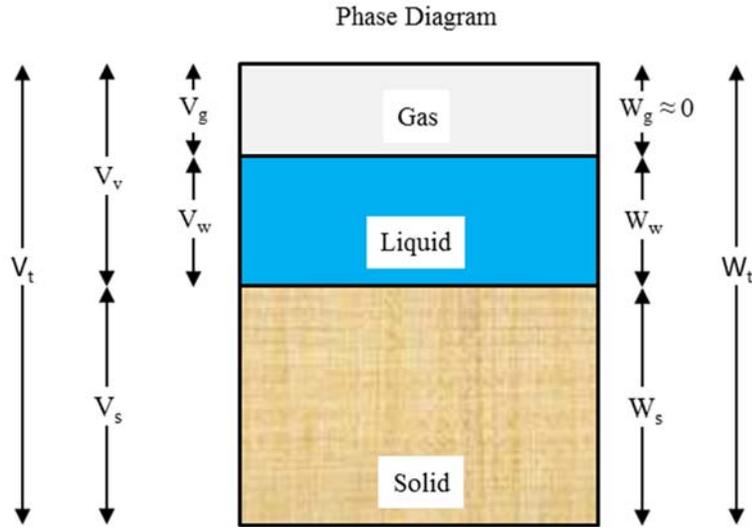
Figure 2.3: Relationships Among Separate Soil Phases

where,

V_t = total volume of all three phases,

V_g = volume of gas,

V_w = volume of liquid,

V_s = volume of soil particles,

V_v = volume of voids (liquid and gas),

W_t = total weight of all three phases,

W_g = weight of gas (≈ 0),

W_w = weight of water, and

W_w = weight of soil particles

Table 2.1: Weight - Volume Relationships Developed from Phase Diagram

Index Property	Equation	Significance
Density, γ_T	$\gamma_T = \dfrac{W_T}{V_T}$	Weight of solid, liquid, and gas per volume
Specific Density of Solids, G_s	$G_s = \dfrac{\gamma_s}{\gamma_w} = \dfrac{\frac{W_s}{V_s}}{\frac{W_w}{V_w}}$	Ratio of solid's density to that of water
Void Ratio, e	$e = \dfrac{V_v}{V_s}$	Amount of voids relative to solids
Porosity, n	$n = \dfrac{V_v}{V_T}$	Maximum void ratio for solid, liquid, and gas system
Degree of Saturation, S_r	$S_R = \dfrac{V_w}{V_v} \times 100\%$	Percentage of voids filled by liquid
Gravimetric Water Content, w_c	$w_c = \dfrac{W_w}{W_s} \times 100\%$	Measure of the amount of liquid by weight
Volumetric Water Content, θ	$\theta = \dfrac{V_w}{V_T} \times 100\%$	Measure of the amount of liquid by volume

Previous studies have developed empirical, semi-empirical, and theoretical models to predict both the real and imaginary parts of dielectric constant in soils; however, input variables used to determine a soil's dielectric constant are valid only for one snapshot in time. In reality, meteorological conditions are constantly changing, which results in a change in input variables. Three of the more commonly used predictive models for forecasting the dielectric constant in soils are described briefly in subsequent sections.

2.3.1 Topp et al. (1980) Model

The Topp et al. (1980) model is an empirical approximation of the real part of the dielectric constant ε'. The model is simplistic in that is uses one variable: volumetric water content. Topp et al. (1980) used time domain reflectometry (TDR) over a frequency range of 20 MHz to 1 GHz to measure the dielectric constant of five types of porous media: sandy loam, clay loam, an organic soil, vermiculite clay mineral, and two different sizes of glass beads. Particle size distributions for the sandy loam and clay loam soil are shown in Figure 2.4.
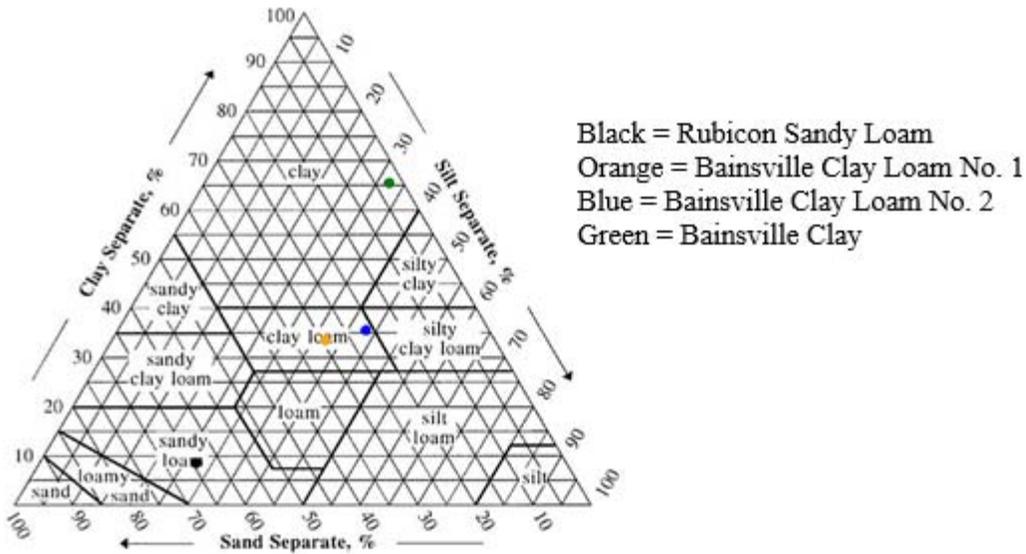
Figure 2.4: USDA Textural Descriptions of Soil Tested by Topp et al. (1980)

From the tests performed by Topp et al. (1980), a relationship between volumetric water content and dielectric constant was developed. The volumetric water content is the single input variable even though Topp et al. (1980) recognized that other soil parameters (especially specific surface area) affect a soil's dielectric constant to a lesser degree. The generalized equation is shown as Equation 2.5.

$$\varepsilon' = 3.03 + 9.3\theta + 146.0\theta^2 - 76.7\theta^3 \qquad \textbf{Equation 2.5}$$

where,

ε' = real part of dielectric constant, and

θ = volumetric water content

Figure 2.5 shows the relationship between dielectric constant and volumetric water content for the sandy loam and clay loam soils. The solid line refers to the generalized equation (Equation 2.5) developed by Topp et al. (1980), and the dashed lines are plus and minus 0.025 of the volumetric water content determined by the generalized equation. These soils varied in texture and density, but still maintained a strong dependence on volumetric water content. Topp et al.

12

(1980) conducted experiments to study the effect of density, texture and temperature and concluded a soil's dielectric constant was almost independent of these various parameters.
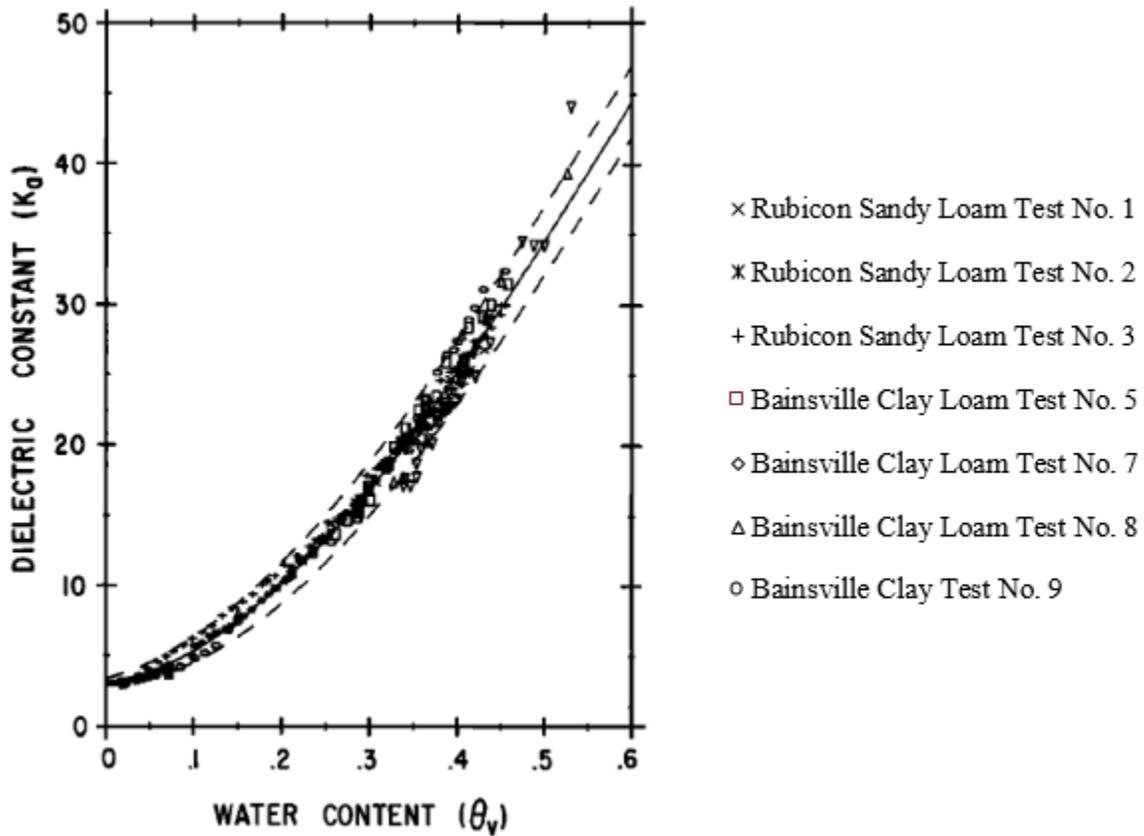
Figure 2.5: Generalized Relationship of the Seven Mineral Soils between Volumetric Water Content and Dielectric Constant (Topp et al., 1980)

Topp et al. (1980) also conducted an experiment on vermiculite; a clay mineral. Figure 2.6 shows Topp et al. (1980) results of the vermiculite's relationship of volumetric water content versus dielectric constant. The vermiculite's relationship followed a similar, but not identical, trend to the generalized equation (Equation 2.5) by Topp et al. (1980). Above volumetric water contents of 0.25 the vermiculite resided outside the plus 0.025 volumetric water content dashed line of the generalized equation (Equation 2.5) described. The clay materials tested by Topp et al. (1980) showed the effect specific surface area had on a soil's dielectric constant. Specific surface

area (SSA) refers to the surface area per unit mass of a soil solid particle. Clay-sized minerals have larger SSA's than sand- and silt-sized minerals.
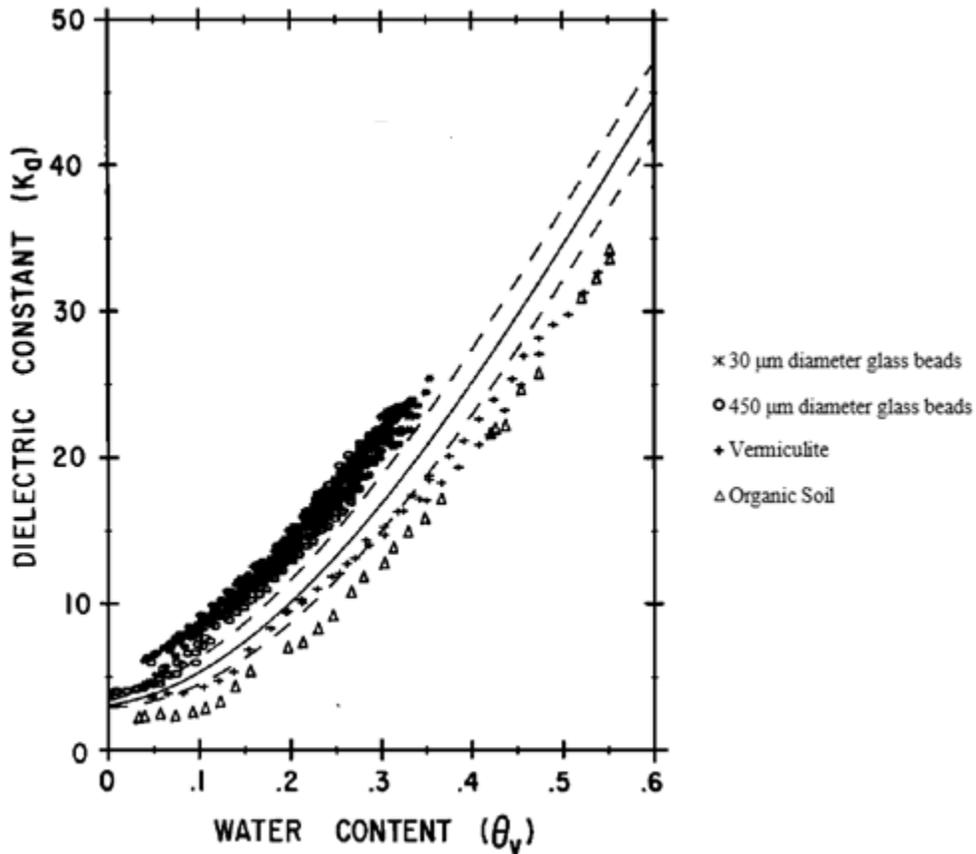
Figure 2.6: Measured Dielectric Constant versus Volumetric Water Content for Vermiculite Clay as Determined by Topp et al. (1980)

2.3.2 Peplinski et al. (1995) and Hendrickx et al. (2003) Model

The Peplinski et al. (1995) model is a semi-empirical predictive model for both the real and imaginary parts of dielectric constant. This model expands the dielectric mixing model determined for the frequency range of 1.4 GHz to 18 GHz (Dobson et al., 1985). The updated dielectric mixing model incorporates measurement frequency and six soil parameters: volumetric water content, bulk density of soil, specific density of solids, sand fraction, clay fraction, and effective electrical conductivity. Peplinski et al. (1995) used the dielectric probe technique over a

frequency range of 0.3 GHz to 1.3 GHz to measure the dielectric constant of four soil mixtures as

listed in Table 2.2.

Table 2.2: Sand, Silt, and Clay Size-Fraction from USDA Classifications of Soil Mixtures for Dielectric Tests (Peplinski et al., 1995)

Soil Mixtures	Sand (%)	Silt (%)	Clay (%)
Field 1	50	35	15
Field 3	30	60	10
Field 4	15	65	20

A relationship between volumetric water content and the real and imaginary parts of

dielectric constant over the lower frequency range was developed (Peplinski et al., 1995). The

generalized model with a linear correction for the real part of dielectric constant is shown in

Equation 2.6.

Figure 2.7 and Figure 2.8 show results of the generalized equation over various volumetric

water contents at frequencies of 0.3 GHz and 1.3 GHz. Peplinski et al. (1995) showed that the

predictive model developed by Dobson et al. (1985) is applicable over the lower frequency range

if a linear correction is applied.

$$\varepsilon' = 1.15 \times [1 + \frac{\rho_b}{\rho_s}(\varepsilon_s^\alpha) + \theta^{\beta'} \varepsilon'^\alpha_{fw} - \theta]^{1/\alpha} - 0.68 \qquad \text{\textbf{Equation 2.6}}$$

where,

ρ_b = dry density of soil [g/cm^3],

ρ_s = specific density of solids,

ε_s = real part of dielectric constant of solids,

α = empirically derived constant [0.65], and

β' = an empirically derived constant based on soil type (Equation 2.7), and

ε'_{fw} = real part of dielectric constant of free water (Equation 2.8)

15

$$\beta' = 1.2748 - 0.519 \times S - 0.152 \times C \qquad \textbf{Equation 2.7}$$

where,

S = sand percent by dry mass [decimal fraction], and

C = clay percent by dry mass [decimal fraction]
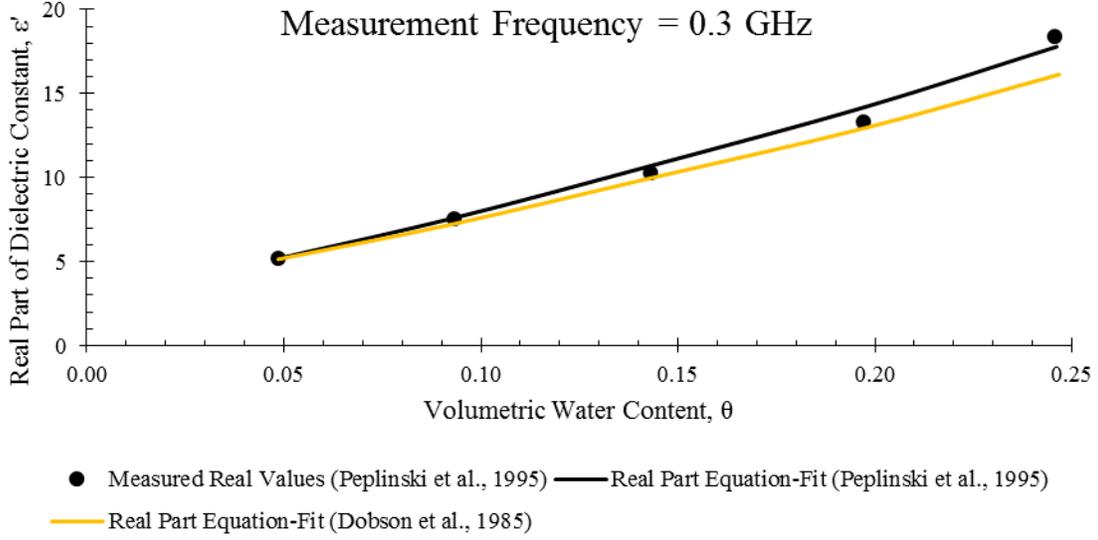
Figure 2.7: Comparison of Real Parts of Dielectric Constant for Peplinski et al. (1995) and Dobson et al. (1985) Models at Frequencies of 0.3 GHz for Field 1 Soil Mixture of 50% Sand, 35% Silt, and 15% Clay (Table 2.2) (Peplinski et al., 1995)

$$\varepsilon'_{fw} = (\varepsilon_w)_{f \to \infty} + \frac{(\varepsilon_w)_{f \to 0} - (\varepsilon_w)_{f \to \infty}}{1 + (2\pi f \tau_w)^2} \qquad \textbf{Equation 2.8}$$

where,

$(\varepsilon_w)_{f \to \infty}$ = high frequency limit of dielectric constant of free water [4.9],

$(\varepsilon_w)_{f \to 0}$ = static dielectric constant of free water,

f = measurement frequency [Hz or s^{-1}], and

τ_w = dielectric relaxation time of water [s]

16
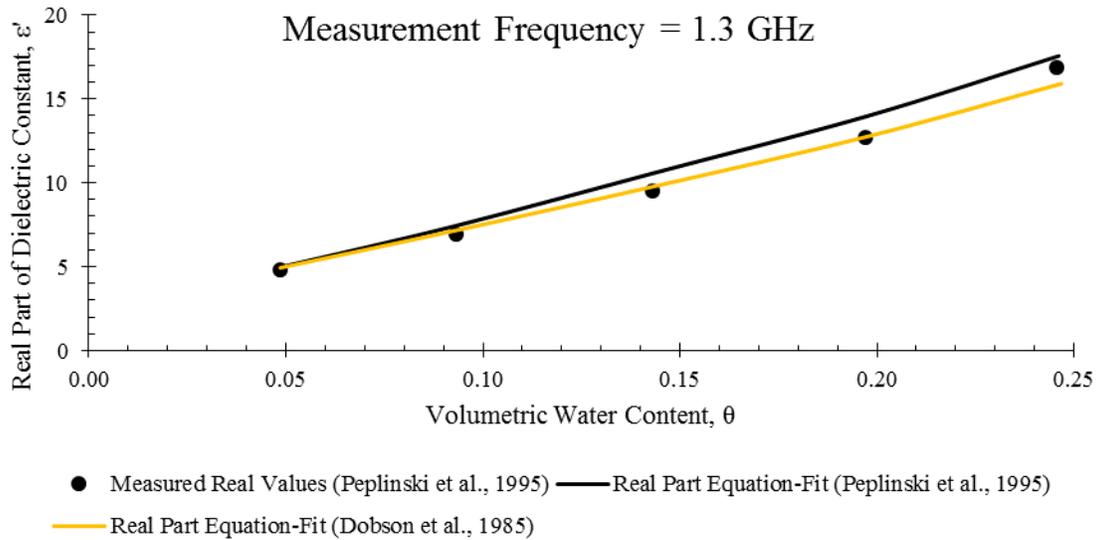
Figure 2.8: Comparison of Real Parts of Dielectric Constant for Peplinski et al. (1995) and Dobson et al. (1985) Models at Frequencies of 1.3 GHz for Field 1 Soil Mixture of 50% Sand, 35% Silt, and 15% Clay (Table 2.2) (Peplinski et al., 1995)

Peplinski et al. (1995) also indicated a soil's SSA controls its dielectric properties due to the molecular layers of water being bound near the soil surface. The bound water near a soil's surface (especially for clay due to their negative surface charge) is described as an adsorbed cation (Peplinski et al., 1995). Peplinski et al. (1995) conducted an experiment with three different clay minerals as they have high SSA's when compared to silt and sand (Table 2.3). The soil mixtures were similar except for their clay mineralogy; 50 % sand, 35 % silt, and 15 % clay by grain-size fraction. Peplinski et al. (1995) found that as the SSA increased, bound water also increased, and conversely dielectric constant decreased (Figure 2.9). However, the empirical dielectric constant predictive model described by Peplinski et al. (1995) did not include experiments with a soil that had a clay majority constituent (Table 2.2).

17

Table 2.3: Three Clays used by Peplinski et al. (1995) to determine Effect of Specific Surface Area on Dielectric Constant

Clay Type	Specific Surface Area (m²/g)
Georgia Kaolin	5 to 20
Kentucky Ball	21
Western Bentonite	~700
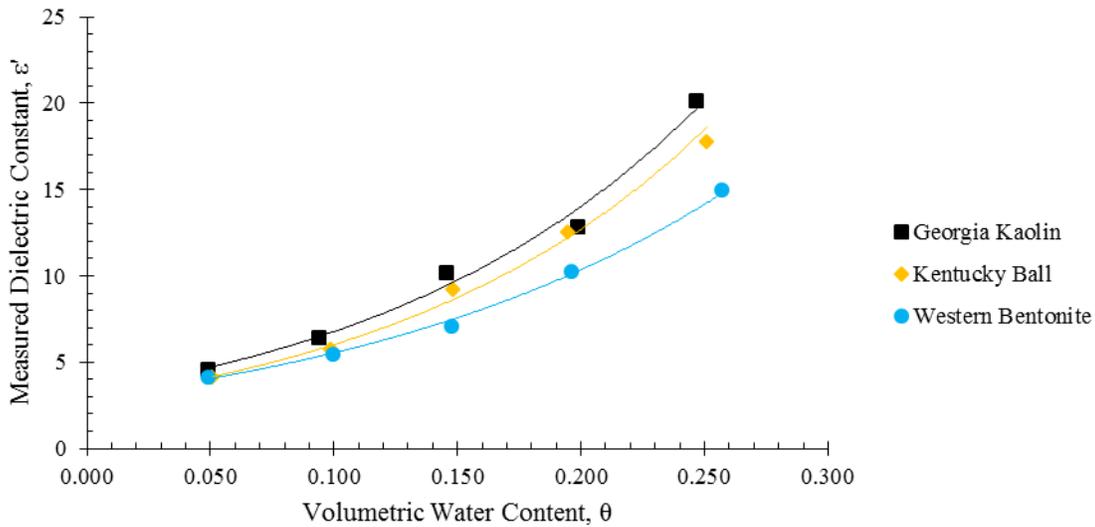
Figure 2.9: Measured Dielectric Constant versus Volumetric Water Content for Three Soils with same Sand, Silt, and Clay Fraction (Different Clay Mineral) by Peplinski et al. (1995)

Hendrickx et al. (2003) updated the empirically derived predictive model by implementing an expression for the dielectric constant of soil particles. The single variable function is based on the specific density of solids (Equation 2.9).

$$\varepsilon_s = (1.01 + 0.44 \times \rho_s)^2 - 0.062 \qquad \text{Equation 2.9}$$

2.3.3 Hilhorst, Wagner, and Schueurmann (1998) Model

Hilhorst (1998) introduced the most comprehensive and theoretically based model for predicting dielectric constants of soils. The model uses a weighted average for each component within a soil medium. There are two key points that differentiate the Hilhorst (1998) model from models discussed previously. First, the model incorporates the soil water characteristic curve

18

(SWCC) as an input parameter and a depolarization factor to construct a strictly theoretical model. The predictive model also uses measurement frequency and nine soil parameters: volumetric water content, bulk density of soil, specific density of solids, sand fraction, silt fraction, clay fraction, temperature, specific surface area, and porosity.

Hilhorst (1998) compared the theoretical predictive model to results from an "average soil" and the vermiculite tested by Topp et al. (1980). The generalized model for the real part of dielectric constant is shown as Equation 2.10.

Figure 2.10 shows the real part of dielectric constant based on the generalized equations developed by Hilhorst (1998) and Topp et al. (1980) over various volumetric water contents. Hilhorst (1998) held private conversations with Topp to determine a measurement frequency of 150 MHz was used. The "average soil" and vermiculite were also given estimated SWCC's. Hilhorst (1998) showed that the developed predictive model has some differences with the generalized model from Topp et al. (1980) over a wide range of dielectric constants and soil textures, but a similar trend is followed.

Equation 2.10

$$\varepsilon' = \frac{1}{3(2n - \theta_k)} \sum_{i=1}^{k} \left[\frac{(\varepsilon_{f \to 0} - \varepsilon_{f \to \infty})}{1 + j \frac{f}{f_{r0} e^{\frac{(p_{m(i)} + p_{m(i-1)}) \times V}{2RT}}}} (\theta_i - \theta_{i-1}) \right]$$

$$+ (\theta_k \varepsilon_{wf \to \infty}) + (1 - n)\varepsilon_s + (n - \theta)\varepsilon_a$$

where,

n = porosity,

f_{r0} = reference dielectric relaxation frequency of free water at a temperature of 20 degrees Celsius [Hz or s^{-1}],

p_m = matric suction exerted on a water molecule [Pa],

V = partial molar volume [m^3],

R = universal gas constant [8.3145 J/K*mol],

T = absolute temperature [K], and

ε_a = dielectric constant of air [≈ 1.006]
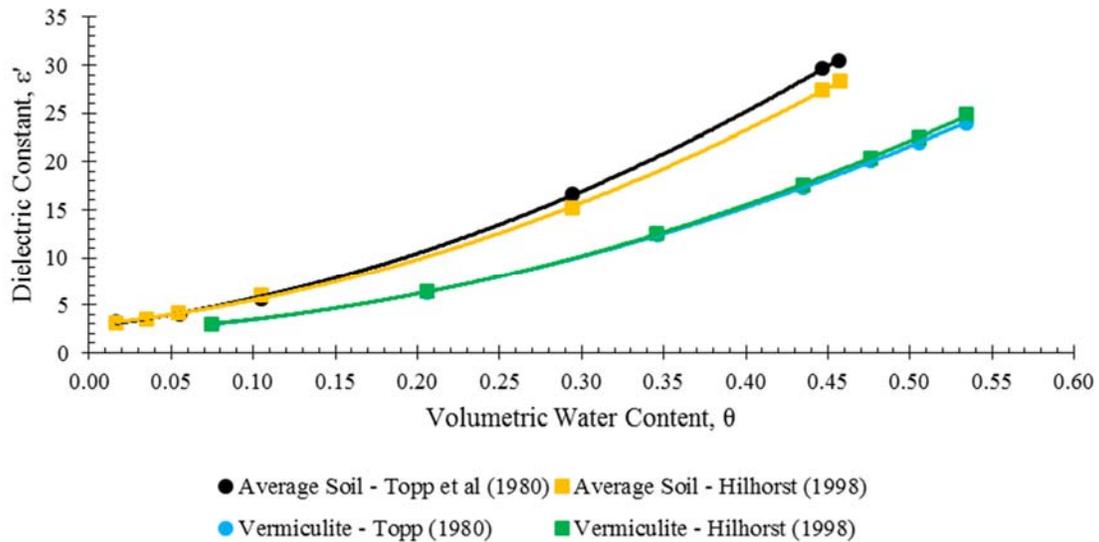
Figure 2.10: Volumetric Water Content versus Dielectric Constant Comparison Calculated Using Hilhorst (1998) and Topp (1980) Predictive Models

2.4   Dielectric Constant of Soil versus Depth over Time

The relative proportions of a soil's three phases vary continuously over depth and time (Figure 2.11). As water is supplied to the soil surface over time, by precipitation or irrigation, water infiltrates the soil. As water infiltrates the soil, the proportion of liquid increases while the gas portion decreases. Infiltrated water exits near-surface soils by evapotranspiration into the atmosphere or by drainage through a soil subsurface (Hillel, 1982). For the purpose of this thesis, near-surface soils are considered to be the first one meter of soil below the ground surface.

The effect of volumetric water content on the dielectric constant of soil is well documented (Thomas, 1966, Topp et al., 1980). Volumetric water content is not a static parameter. It is often the change in water content with respect to time that controls a soil's dielectric constant.

20
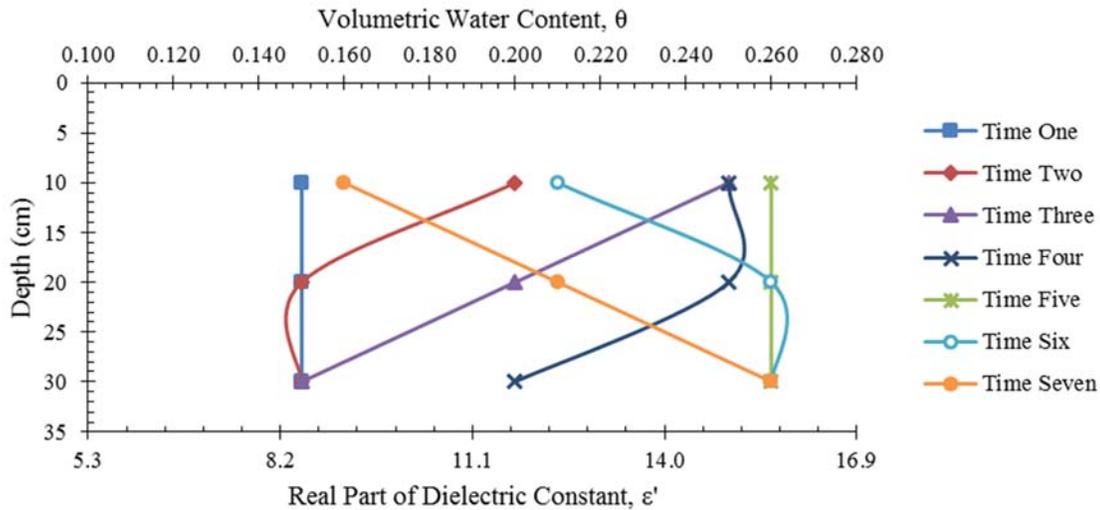
Figure 2.11: Generalized Description of Infiltrating and Exiting Moisture in Near-Surface Soils

Numerous studies have been conducted on providing continuous real-time soil moisture measurements. Baker and Allmaras (1990) developed an analog and digital TDR system interfaced with a personal computer to automate soil moisture measuring system using time-domain reflectometry (TDR). The analog TDR functioned by a program from the datalogger but required an operator to toggle a switch from the TDR. The digital TDR system was completely automated and controlled by a personal microcomputer and could be programmed to cycle through waveguides at certain time intervals. Waveguides are structures that guide electromagnetic waves. Dielectric constants of the soils were analyzed by identifying the reflection points on the digitized waveform (Equation 2.11). To determine a soil's volumetric water content, the generalized equation developed by Topp et al. (1980) was used.

$$\varepsilon' = \left(\frac{L_a}{L}\right)^2$$ **Equation 2.11**

where,

L_a = apparent distance between the initial and final reflections, and

L = waveguide length

21

Baker and Allmaras (1990) installed four sensors each at depths of 10 cm, 30 cm and 50 cm at four sites in an alfalfa field at the University of Minnesota Agricultural Experiment Station, The literature did not reveal a soil type for each site. Hourly measurements performed by the digital TDR system on May 8th, 1989, at a depth of 10 cm, are shown in Figure 2.12. A total of 22.4 mm of precipitation fell on that day. The results show an increase in volumetric water content especially between hours 10 through 12, from rainfall infiltrating into the soil subsurface.

An investigation was performed by Starr and Paltineanu (1998) concerning automated multisensor capacitance soil moisture probes. The probes measure the dielectric constant of soil by capacitance, in which the permanent dipoles of water in the dielectric medium are aligned by an electrical field and become polarized (Paltineanu and Starr, 1997).
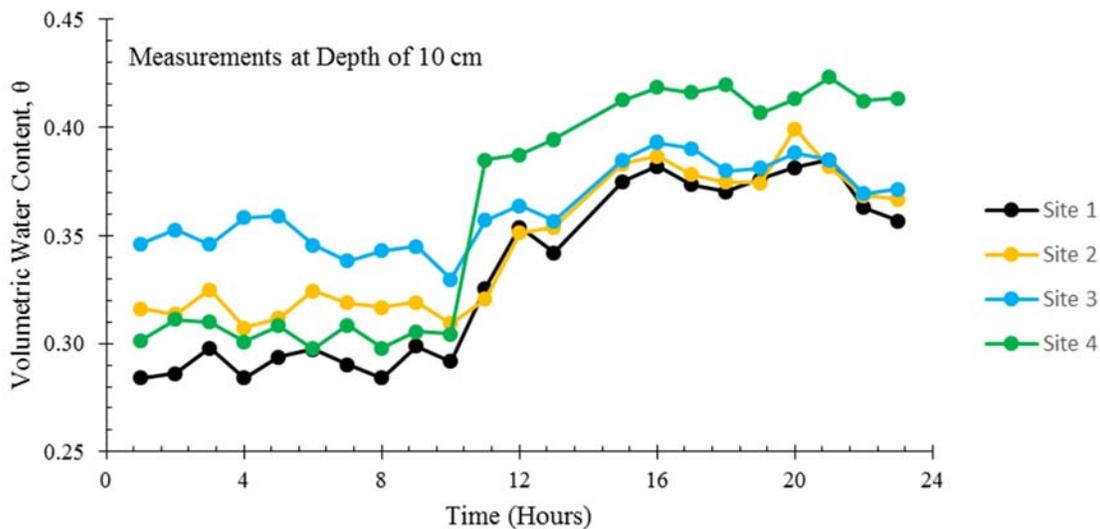
Figure 2.12: Volumetric Water Content Measurements over Time made by Digital TDR system (Baker and Allmaras, 1990)

Starr and Paltineanu (1998) installed capacitance soil moisture sensors created by EnviroScan® (Sentek PTY, Ltd., Kent Town, South Australia). The probes were installed at depths of 10 cm, 20 cm, 30 cm, and 50 cm, in a Mattepex silt loam. The loam contained 35% sand, 56% silt, 9% clay, and less than 1% organics. The probes were connected to a datalogger and

dielectric constant readings were recorded at 10 minute intervals. The Topp et al. (1980) model

was used to determine the volumetric water content. Measurements performed by the capacitance

probe during an irrigation event are shown in Figure 2.13. The results show the irrigation event

infiltrated down to the 30 cm sensor, but did not reach the 50 cm sensor over the recorded time

interval. Starr and Paltineanu (1998) noted the response of each sensor in the measured zone

exhibited higher hydraulic conductivities than typically expected from a silt-loam soil. This

increased rate of response is attributed to substantial filling of macropores (Starr and Paltineanu,
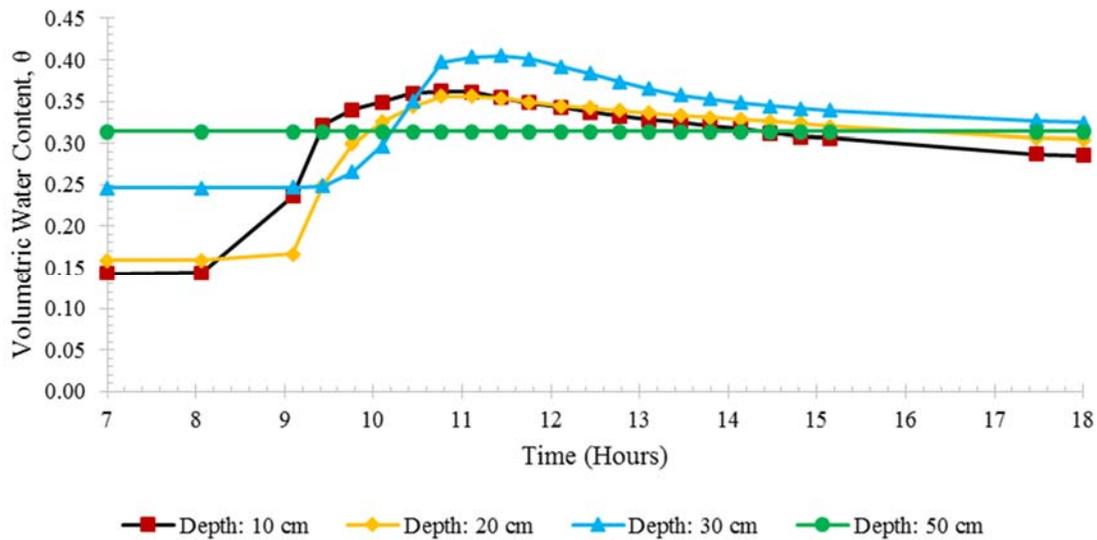
1998).

Figure 2.13: Volumetric Water Content Distribution versus Depth over Time using Capacitance Soil Moisture Sensors (Starr and Paltineanu, 1998)

2.5   Moisture Migration Modeling using UnSat-H

The continuous real-time information provided by soil moisture instruments has proven to

be effective in measuring the dielectric constant in soil. However, the numerous commercial soil

moisture sensors available cannot *forecast* the dielectric constant of near-surface soils, rather they

make physical measurements at predetermined time intervals. Moisture migration versus depth

over time becomes extremely important because volumetric water content is critical in the

determination of the dielectric constant of soil. Predicting moisture movement through soils in the unsaturated zone above a groundwater table has become more common in the fields of science and engineering. The unsaturated condition refers to partially saturated soils or systems that contain the solid, liquid, and gas phase (Lu and Likos, 2004).

UnSat-H was developed at the Pacific Northwest National Laboratory (PNNL) by Fayer (2000) to numerically analyze moisture migration in arid areas and to estimate scenarios pertinent to waste disposal facilities. Theoretical equations employed by UnSat-H are solved by finite difference method using a Crank-Nicolson scheme (Fayer, 2000). Employing this method has some error as derivatives are evaluated at each interval's midpoint, but decreasing depth and time intervals produce results that approximate correct solutions (Fayer, 2000).

UnSat-H models subsurface water dynamics by taking into account soil water infiltration, redistribution, evaporation, plant transpiration, and deep drainage as one-dimensional processes, i.e., one-dimensional vertical flow. Meteorological inputs and soil characteristics are used to model moisture movement. Predicted soil moisture can be used to forecast a soil's dielectric constant.

UnSat-H initially balances water in the soil subsurface into two categories; precipitation as an input and infiltration and runoff as an output. Storage from ponding is an additional category, but is not included to simplify the UnSat-H water balance equation (Equation 2.12).

$$P - I - R_{off} = 0$$ **Equation 2.12**

where,

    P = precipitation from wetting event,

    I = infiltration into soil from wetting event, and

    R_{off} = runoff of non-infiltrating precipitation on surface

Upon infiltration, the water balance equation changes form to include soil water storage, evaporation, transpiration, and drainage (Equation 2.13).

$$I - E - T - D = \Delta S_w$$

<div align="right">**Equation 2.13**</div>

where,

E = water lost from evaporation,

T = water lost from transpiration,

D = water lost from drainage, and

ΔS_w = change in soil water storage from previously mentioned water losses over an interval of time

Using UnSat-H to predict moisture movement, and thus forecast the dielectric constant of soil, employs a differential equation derived from the modified Richards' equation (1931). The set of differential equations and boundary conditions describe the migration of moisture at every node within the soil. Boundary conditions for UnSat-H can be modeled as constant or flux, where flux exhibits more realistic meteorological conditions. Surficial conditions change by precipitation and evapotranspiration, whereas subsurface boundary conditions change by downward vertical moisture drainage. Constant surficial conditions simulate water ponding from precipitation or irrigation events, while constant lower boundary conditions mimic a groundwater table. Richards' equation (1931) for saturated flow has the one-dimensional differential form of Darcy's Law (Equation 2.14). Negative signage throughout indicates the downward vertical flow direction.

Equation 2.14

$$q_L = -K_s \frac{\partial H}{\partial z}$$

where,

q_L = flux density of liquid flowing in soil $[\frac{\frac{L^2}{L}}{T}]$,

K_s = saturated hydraulic conductivity of fluid $[\frac{L}{T}]$,

H = gravitational head $[L]$, and

z = depth below top of soil surface $[L]$

For unsaturated flow in Equation 2.14, K_s is replaced with the soil unsaturated hydraulic conductivity, K_L. Unsaturated hydraulic conductivity is a function of the soil's matric potential (Equation 2.15). A generalized plot of hydraulic conductivity versus matric potential is shown in Figure 2.14. The relationship shows that as matric potential increases, hydraulic conductivity decreases.

$$q_L = -K_{L(\psi)} \frac{\partial H}{\partial z}$$

Equation 2.15

where,

$K_{L(\psi)}$ = unsaturated hydraulic conductivity related to corresponding matric potential $[\frac{L}{T}]$

26
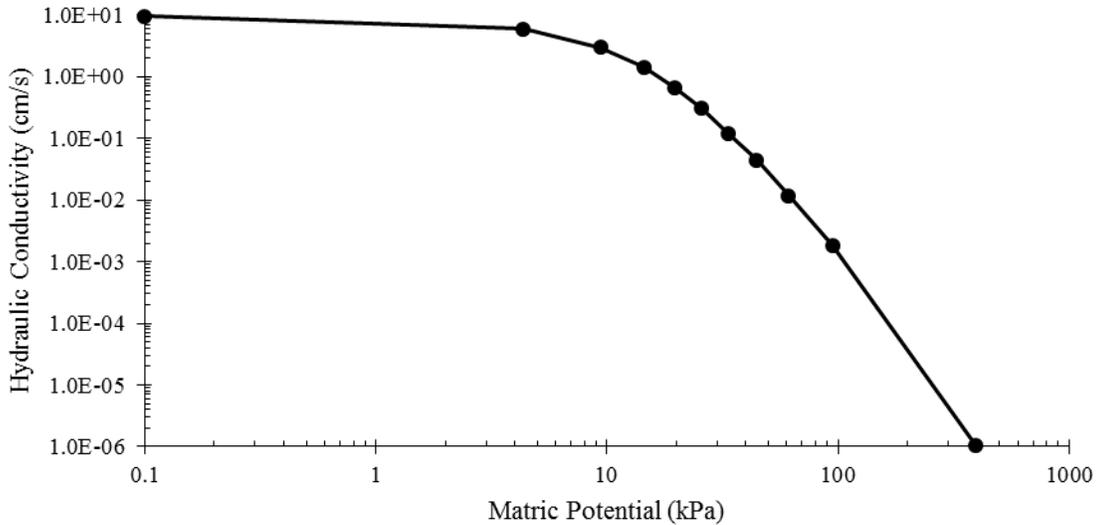
Figure 2.14: van Genuchten (1980) Equation Fit to experimental data between Hydraulic Conductivity and Matric Potential (Lu and Likos, 2004)

Moisture movement in soils are often transient conditions but still must meet continuity requirements. Continuity is where the change in volumetric water content equals the difference between flux density into the soil volume and flux density out of the soil volume. The continuity condition can be modeled for one-dimensional flow (Equation 2.16).

$$\frac{\partial \theta}{\partial t} = -\frac{\partial q_L}{\partial z} \qquad \textbf{Equation 2.16}$$

where,

θ = volumetric water content, and

t = time.

To model transient moisture flow, Equation 2.15 and Equation 2.16 are combined (Equation 2.17).

$$\frac{\partial \theta}{\partial t} = -\frac{\partial}{\partial z}\left[-K_L(\psi)\frac{\partial H}{\partial z}\right] \qquad \textbf{Equation 2.17}$$

Moisture in a soil also changes due to meteorological conditions controlling the precipitation, evaporation and transpiration. Climatological data can be used to calculate

evaporation and transpiration rates. Potential evapotranspiration (PET) is the sum of potential evaporation and potential transpiration (Equation 2.18).

$$PET = E_p + T_p$$

where,

E_p = potential evaporation, and

T_p = potential transpiration.

UnSat-H gives two options for determining moisture changes from PET. Changes can be calculated from the Penman (1948) equation reported by Doorenbos and Pruitt (1977) or input directly from measured data (Equation 2.19). PET is distributed throughout a simulated day by a sinusoidal function with the maximum at 12:00 PM and 88 percent of PET occurring between 6:00 AM and 6:00 PM (Fayer, 2000).

$$PET = \frac{sR_n}{s + \gamma} + \frac{\gamma}{s + \gamma} 0.27 \left(1 + \frac{U}{100}\right)(e_a - e_d)$$

where,

s = rate of change of the saturation vapor pressure-temperature curve,

R_n = net radiation,

γ = psychrometric constant,

U = 24-hour wind run,

e_a = saturation vapor pressure at the mean air temperature, and

e_d = actual vapor pressure.

The Penman (1948) equation contains numerous climatological components affecting evapotranspiration. Important components of the equation are often measured at a site of interest. The slope of the saturation vapor pressure-temperature curve and psychrometric constant are empirically determined weighting factors for the effect of wind, radiation, and humidity at a site.

Net radiation is determined as the difference between incoming and outgoing radiation. Radiation is dependent on many factors; latitude, time of year, time of day, and reflection characteristics of the ground surface. The 24-hour wind run accounts for wind data measured at a height different from the 2 m height determined by Penman (1948). Saturation and actual vapor pressures describe the amount, or lack thereof, of moisture in the atmosphere.

Baca and Magnuson (1990) performed verification testing of UnSat-H results by comparing them to known analytical solutions. The objective of their study was to determine if UnSat-H was accurate and fully operational for modeling the movement of moisture. One of their eight tests involved a vertical column of homogenous soil with a quasi-analytic solution for liquid water flow (Philip, 1957). Soil surface boundary conditions were kept at constant pressure to simulate full saturation and the soil specimen had a uniform water content throughout. The goal of the study was to determine if UnSat-H could correctly model the position of the wetting front when subjected to vertical infiltration. A comparison of the results of the vertical column test and the prediction of UnSat-H is shown in Figure 2.15.
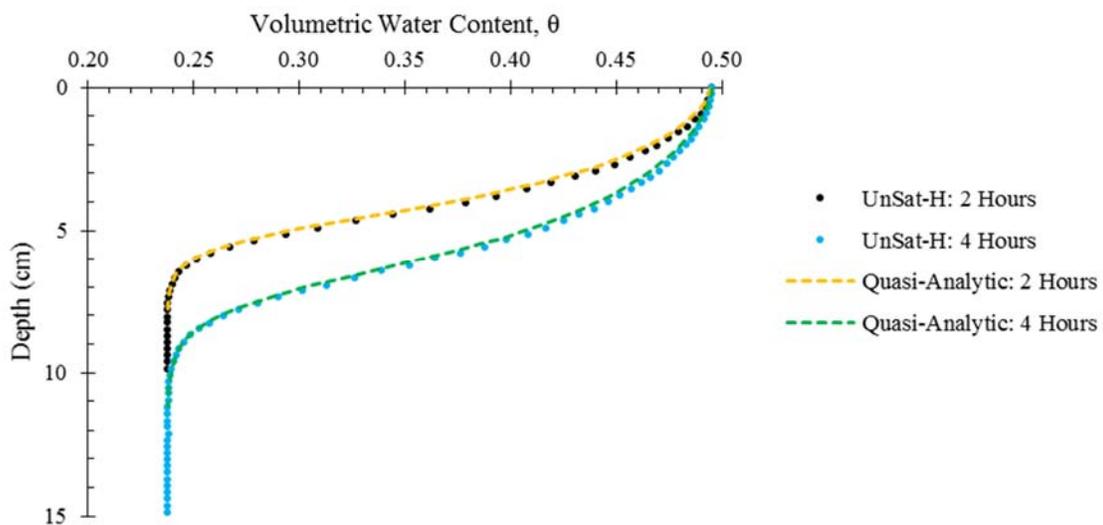
Figure 2.15: Comparison of Volumetric Water Content versus Depth 2 Hours and 4 Hours after being Subjected to a Constant Pressure (Philip, 1957, Baca and Magnuson, 1990)

Baca and Magnuson (1990) concluded that UnSat-H was a reliable numerical computer code for simulating water balance problems in the non-layered unsaturated zone with vertical flow. UnSat-H was also deemed to be fully functional with "excellent" computational stability, "reasonable" accuracy, and "acceptable" computational speed (Baca and Magnuson, 1990).

There are, however, limitations to the UnSat-H water balance modeling code. The most glaring deficiency is the one-dimensional nature of the computer code. Moisture movement in the soil subsurface can be complex in heterogeneous soils where two- and three-dimensional flow occurs (Hillel, 1998).

A soil with relatively higher hydraulic conductivity overlying a soil with a relatively lower hydraulic conductivity may present difficulties to the one-dimensional model. Positive pressures can develop in the overlying soil (from a precipitation or irrigation event) and form a perched water table (Hillel, 1980). If the overlying soil is continuous along the surface, then the infiltrating water will have the tendency to flow horizontally. This horizontal flow, which can occur in sloping soil layers as well, will be disregarded by the one-dimensional equations used by UnSat-H.

Moisture migration modeling is also difficult in soils which have a tendency to develop secondary porosities. Soils susceptible to shrink-swell are likely candidates as they tend to develop cracks, commonly called macropores (Hoogmoed and Bouma, 1980). Soils with macropores will tend to have higher infiltration and percolation rates. These differences between predicted and actual infiltration rates can cause the movement of wetting and drying fronts to be modeled at slower rates than actually occur during a precipitation event.

2.6 Summary

The literature review revealed successful studies concerning the dielectric constant of soils. In addition to determining the dielectric constant of soils with predictive models, numerous

commercial soil moisture sensors have been developed which physically measure a soil's dielectric properties over time intervals, and use one of the predictive models to determine volumetric water contents.

Successful implementation of measuring the dielectric constant of soils over time has proved beneficial in numerous applications including soil moisture measurement in agricultural fields and the determination of contamination zones in soils. However, previous studies conducted on predictive models and the development of commercial soil moisture sensors have shown the spatial and time variation of the dielectric constant of soils.

Methods for determining the dielectric constant of soil with depth over a period of time were discussed, as well as methods currently used to model moisture migration, which is a critical factor in determining the dielectric constant of soil. Studies indicate that new developments in science and engineering regarding dielectric properties of soils need accurate, and continuous real-time information provided by ground-truth data (Starr and Paltineanu, 1998). This project contributes to the need for continuous real-time information of dielectric constants of soil by using 'ground-truthed' data.

3 Materials and Methods

3.1 Introduction

Soil moisture and meteorological measurement sensors were installed at a site near McBaine, Missouri (MO) to provide 'ground-truth' data for the use of better understanding forecasted dielectric constants of near-surface soils and changes with time from remotely-acquired meteorological data. Presented in this chapter are descriptions of the site and instruments used to measure soil and meteorological conditions affecting the dielectric constant of the soil. Also presented, are the methods used to characterize the soils at the McBaine, MO test site, as well as the modeling program used to forecast moisture migration and consequently the soil's dielectric constant.

3.2 McBaine, Missouri Test Site

McBaine, MO is located in the west-central portion of Boone County, Missouri, in the Missouri River flood plain (Figure 3.1) and the surrounding landscape is largely made up of agricultural fields. The project site (38°53'49.25" N, 92°27'53.07" W), which resides near McBaine, MO, was chosen for the United States Naval Academy (USNA) to be used for above-ground radio frequency (RF) transmission measurements (Figure 3.2). Measuring instruments were positioned away from the east side toe of a section of the Missouri River levee system (Figure 3.3), which allowed agricultural equipment field access.

Figure 3.1: McBaine, MO Location in Western Boone County, Missouri (Google Maps, 2013)

Figure 3.2: Test Site Location near McBaine, MO (Google Maps, 2013)
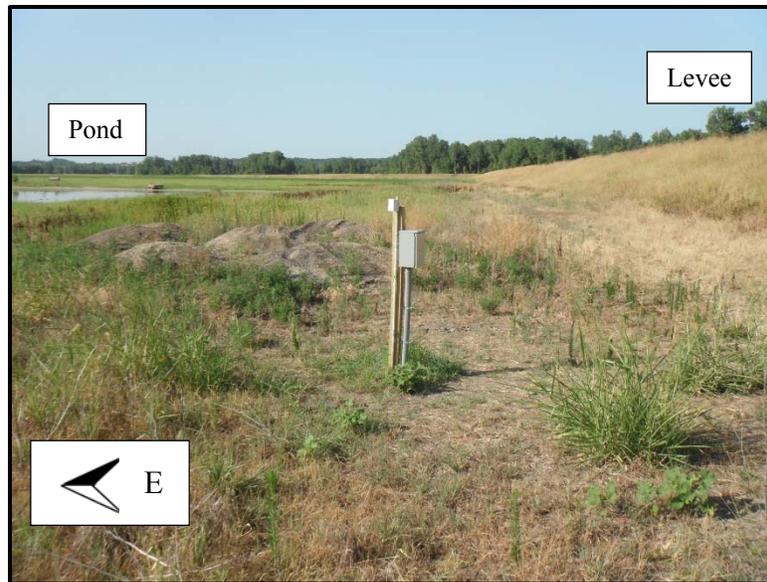
Figure 3.3: Instrumentation of Test Site 25 ft. off East Toe of Missouri River Levee System

3.2.1 Test Site Soils

The site was chosen for its clayey soils, as well as close proximity to the Missouri River and a local pond, which indicate the groundwater table is near the surface. The internet-based geographic information systems (GIS) tool established by the Center for Applied Research and Environmental Systems (CARES) indicate the soil at the test site is of the Darwin Series (CARES, 2013). The Darwin series consists of low permeability soils of clayey alluvium developed in flood plains near large rivers; for instance, the Missouri River (NRCS, USDA, 2013). The Darwin series soils are classified as fine, smectitic, and mesic Fluvaquentic Vertic Endoaquolls (NRCS, USDA, 2013). The classification of the Darwin series indicates not only the clayey soils and near surface groundwater table, but also the presence of slickensides. Slickensides are polished surfaces formed by frictional movements in the soil (Hillel, 1998).

3.2.2 Test Site Instrumentation

The measuring station at McBaine, MO was constructed in late April of 2012 and fully instrumented in early November of 2012 (Figure 3.4). In-ground soil sensors were installed by

34

excavating a test pit. Sensors developed by Decagon Devices (Decagon, 2012) were placed horizontally into the pit's undisturbed side at depths below ground surface (BGS) of 6 in., 12 in., 18 in., and 24 in. to ensure good soil to sensor contact (Table 3.1 and Figure 3.5). The test pit was backfilled with the excavated soil and compacted to its *in-situ* density. Instruments developed by Decagon Devices (Decagon, 2012) to measure meteorological conditions at the McBaine, MO test site were secured to an 8-foot long 4 in. by 4 in. cedar post embedded next to the test pit (Table 3.2). Sensor calibrations can be found in Appendix A.

Table 3.1: Decagon Devices (Decagon, 2012) Soil Moisture Sensors Installed at McBaine, MO

Sensor Name	Depth Below Ground Surface (in.)	Measurables
5TE	6, 12, 18, and 24	Dielectric Constant, Bulk Electrical Conductivity, Soil Temperature, and Volumetric Water Content (from Topp et al. (1980))
MPS-2	6, 12, 18, and 24	Matric Potential, and Soil Temperature

Figure 3.4: Instrumentation Layout of Meteorological Measuring Sensors at McBaine, MO Test Site
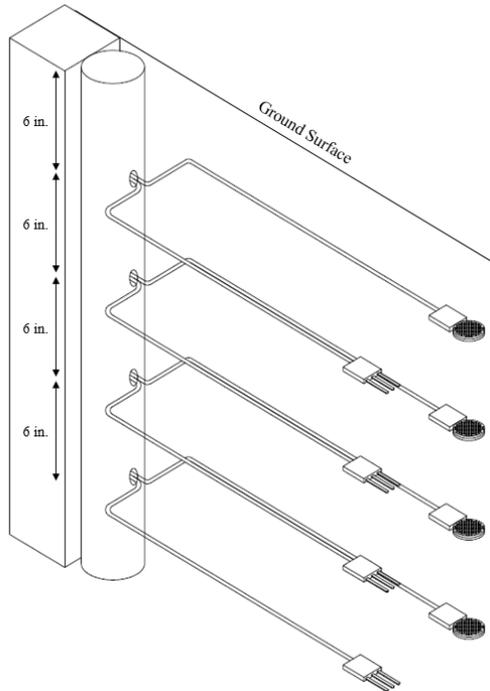
Figure 3.5: Decagon Devices "5TE" and "MPS-2" Sensor Positions Below Ground Surface

Table 3.2: Decagon Devices (Decagon, 2012) Climatological Sensors Installed at McBaine, MO

Sensor Name	Measurables
ECRN Low-Res Rain Gauge	Precipitation
VP-3	Air Temperature and Relative Humidity
Davis Cup Anemometer	Wind Speed and Direction
PYR Total Solar Radiation	Solar Irradiance

The stereo plug (Figure 3.6) attached to each soil and meteorological sensor was connected to Decagon Devices (Decagon, 2012) "Em50" automated data collection system (Figure 3.7). The "EM50" can store one MB of data or up to 36,000 scans each for five sensors. Measurements of the sensors are taken and recorded over preprogrammed time intervals, which applies to each sensor. Initially, sensors were programmed to measure and be recorded at one hour time intervals, but were switched to five minute intervals to provide better resolution with time. The data were periodically downloaded to a laptop using Decagon Devices "ECH$_2$0 Utility" software. The

program downloads both calibrated and unprocessed raw voltage output data to a Microsoft Excel® spreadsheet. Continuous real-time data from all sensors at the McBaine, MO test site has been collected since April, 23rd 2012.

Figure 3.6: Stereo Plug Connecting Sensors to Decagon Devices "EM50" Data logger

Figure 3.7: Decagon Devices "EM50" Data logger Used to Store Sensor Measurements

3.2.3 "5TE" Soil Moisture Sensor

In situ measured dielectric constants and volumetric water contents of soil present the opportunity to compare with forecasted values. Decagon Devices (Decagon, 2012) "5TE" (Figure 3.8) sensors provide continuous real-time measurements of the soil's dielectric constant,

volumetric water content (interpreted from Topp et al., 1980) model, bulk electrical conductivity, and soil temperature at McBaine, MO.

The commercial "5TE" sensor determines the dielectric constant of a soil by supplying a 70 MHz oscillating wave that charges the prongs. Capacitance of the prongs is based on the dielectric constant of the soil between them. Bulk electrical conductivity is determined by measuring the resistance between an alternating electrical current applied to two electrodes. The "5TE" sensor's two electrodes are screws positioned on separate prongs (Figure 3.8). Soil temperature is measured using a surface-mounted thermistor. The thermistor, which is underneath the overmold of the sensor, records the sensor's surface temperature, and one assumes the sensor surface has come into temperature equilibrium with the surrounding soil. Volumetric water content is interpreted using the correlation (Topp et al., 1980) with measured dielectric constant.
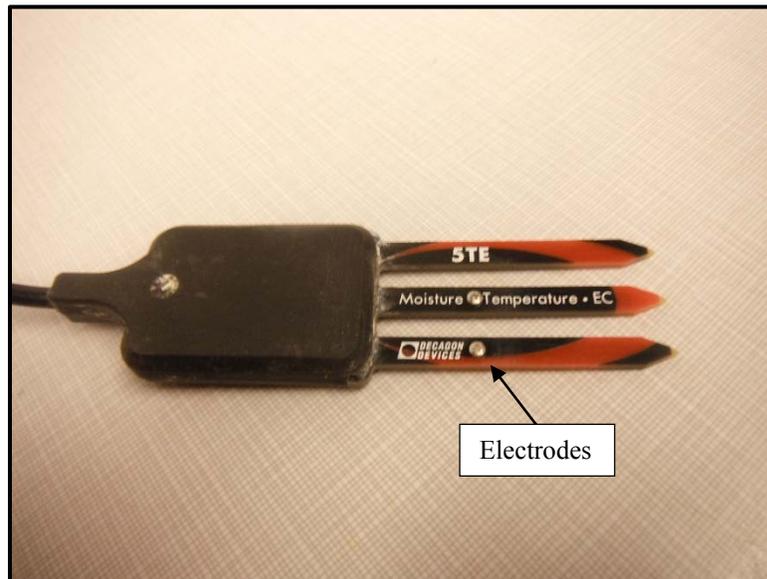
Figure 3.8: Decagon Devices "5TE" Sensor Used to Measure Dielectric Constant, Volumetric Water Content, Soil Temperature, and Bulk Electrical Conductivity

3.2.4 "MPS-2" Soil Moisture Sensor

The magnitude of pressure acting on soil water is theoretically immeasurable; however, matric suction (potential) of a soil is the significant parameter used to describe the energy state of

water. Matric suction is termed the difference in pressure across two fluids and is why porous systems tend to draw in water and repel air (Mitchell and Soga, 2005). Decagon Devices (Decagon, 2012) "MPS-2" (Figure 3.9) sensors provide continuous real-time measurements of the soil's matric potential and soil temperature at McBaine, MO.

The "MPS-2" sensor determines matric suction, or energy state of water, in a soil using an equilibrium technique. The equilibrium method is based on the second law of thermodynamics. The sensors measure the dielectric constant of two ceramic disks with known static pore distributions. Assuming the disks and surrounding soil have equilibrated, the dielectric constant is converted to water content using the generalized equation developed by Topp et al. (1980). Matric suction is then determined from the ceramic disks' known moisture characteristic curve. Limits for the measured matric suction range between -5 kPa and -500 kPa.

Figure 3.9: Decagon Devices "MPS-2" Sensor Used to Measure Matric Suction and Soil Temperature

3.2.5 "ECRN" Low-Resolution Rain Gauge

The primary source of water into an agricultural soil system, other than irrigation events in agricultural fields, is precipitation from rain and snow. A soil gains water through infiltration. Infiltration amounts are governed by soil and plant characteristics, as well as the intensity of a

wetting event (Schwab et al., 1993).   The addition of moisture into a soil has a critical effect on the soil's dielectric constant.

Precipitation from rain events is measured by a single-spoon tipping bucket (Figure 3.10). Precipitation is collected by the funnel and filled into a self-emptying spoon, which automatically tips at 1 mm of precipitation. The summed number of tips by the self-emptying spoon correspond to the amount of precipitation over a predetermined time interval.   The rain gauge is resistant to frost, water, and ultraviolet light; although the gauge does not measure snowfall amounts.

Figure 3.10: Decagon Devices (Decagon, 2012) "ECRN-50 Low-Resolution Rain Gauge" Sensor Used to Measure Precipitation

3.2.6   Davis Cup Anemometer

Wind is indirectly helpful in the evaporation process of moisture in near surface soils. Wind assists by transporting moist vapor above an evaporating soil surface out of the general area. Higher wind speeds move moist air quicker than lower wind speeds. From a dielectric constant perspective, lower wind speeds have relatively slower changes on the soils dielectric constant and higher wind speeds have relatively quicker changes.

Wind speed and direction are measured by hemispherical cups and the anemometer vane, respectively (Figure 3.11). Wind speeds are measured over one minute intervals regardless of the predetermined time intervals. Average wind speeds are determined by measuring the mean average of one minute recordings. Gust wind speeds are determined by measuring the maximum of one minute recordings. The direction of wind is recorded in one minute intervals similar to wind speeds. The wind direction is resolved into "X" and "Y" components; true north equals "Y" component and 90° clockwise equals "X" component (east). The resultant wind direction is determined by a weighted average and measured for each predetermined time interval.

Figure 3.11: Decagon Devices (Decagon, 2012) Davis Cup Anemometer Used to Measure Wind Speed and Direction

3.2.7 PYR Total Solar Radiation

Evaporation and transpiration are governed by the amount of energy available to turn liquid water into vapor (Hillel, 1998). The largest energy source available is the sun. Solar radiation is

received by the soil surface or vegetation and transformed into heat, which in turn transforms liquid water into vapor. Not all solar radiation energy is used for evaporation and transpiration purposes. Solar radiation energy is also consumed by the atmosphere to heat air.

The PYR solar radiation sensor (Figure 3.12) measures the solar irradiance from a field of view of 180° at each predetermined time interval. Solar irradiance is the power per unit area $[\frac{W}{m^2}]$ of solar radiation. The sensors measure solar irradiance by way of a thermopile with a black coating. The black coating absorbs all electromagnetic solar radiation in the spectrum range of 300 nm to 1100 nm. The glass dome serves to block all electromagnetic energy less than 300 nm and greater than 1100 nm from being absorbed. The irradiance absorbed by the black coating is turned into heat, which is then measured by the thermopile.

Figure 3.12: Decagon Devices "PYR Total Solar Radiation" Sensor Used to Measure Solar Irradiance

3.2.8 VP-3 Humidity Temperature

Relative humidity (RH) is the ratio of vapor pressure at a given temperature to saturated vapor pressure at that same air temperature. Air temperature dictates saturated vapor pressure and thus controls the amount of water vapor in the atmosphere. Air temperature and RH are important

meteorological characteristics when evaporation and transpiration are a concern. When meteorological vapor pressure is greater than the vapor pressure in a soil medium evaporative processes are low. The inverse occurs when meteorological vapor pressure is lower than the vapor pressure of a soil.

Air temperature and RH (Figure 3.13) are measured individually by sensor chips. The sensors are calibrated for temperature and RH recordings before being stored by the "EM50" data logger. RH is measured by capacitance of the surrounding air. For the RH sensor to measure correctly it is imperative the humidity sensor be at air temperature. A radiation shield is installed to protect the sensors from solar irradiance and to maximize air flow across the surface. The radiation shield ensures accurate and consistent measurements of air temperature and RH.

Figure 3.13: Decagon Devices "VP-3" Sensor Used to Measure Air Temperature and Relative Humidity

3.3   Laboratory Characterization of McBaine, Missouri Soil

Laboratory testing was conducted to determine properties of soils at one location from the McBaine, MO field site. Samples representative of the soil at depths of 6 in., 12 in., 18 in., and 24 in. below ground surface (BGS) were collected and returned to the University of Missouri Soil

Characterization and Geotechnical Engineering Laboratory for physical testing. Soil properties are implemented into the computer program (WinUnSat-H) to forecast the moisture migration, which is subsequently used in dielectric constant predictive models to forecast the dielectric constant. Characterization of soil properties is also necessary as dielectric constant predictive models include them as variables. Properties determined include grain size distribution, Atterberg limits, dry density, specific density of solids, specific surface area, cation exchange capacity, saturated hydraulic conductivity, and water retention characteristics (soil water characteristic curves). The aforementioned tests were performed using applicable standards; American Society for Testing and Materials (ASTM) (Table 3.3) and United States Department of Agriculture (USDA) National Soil Survey Laboratory.

Table 3.3: ASTM Standards and the Associated Property Determined

Standard	*Property Determined*
(ASTM D2487, 2011)	Grain Size Distribution
(ASTM D4318, 2010)	Atterberg Limits
(ASTM D2216, 2010)	Gravimetric Water Content
ASTM (Cerato and Lutenegger, 2002)	Specific Surface Area
(ASTM D2937, 2011)	Dry Density
(ASTM D584, 2010)	Specific Density of Solids
(ASTM D5084, 2010)	Saturated Hydraulic Conductivity

3.3.1   Grain Size Distributions

Grain size distributions of the McBaine, MO soils were determined by sieve and hydrometer (ASTM D2487) methods. Sieve analyses are performed to determine the distribution of coarser, larger-sized particles, while hydrometers determine the distribution of fine-grained particles. The tests were performed to determine the percent fraction of sand, silt, and clay constituents and were helpful in classifying the soils.

44

3.3.2   Atterberg Limits

Atterberg limits (ASTM D4318) were measured to identify, classify, and describe the McBaine, MO soils.   The results provide a preliminary assessment of the cohesive soil's mechanical properties. The behavior of fine-grained soils can be described when Atterberg limits are measured in conjunction with clay-size fraction, specific surface area, and cation exchange capacity determinations. Soils with lower plasticity indices tend to shrink-swell less than soils with higher plasticity indices.

A cohesive soil's plasticity index is a measure of the range of gravimetric water contents in the plastic state (Equation 3.1).

$$P_I = L_L - P_L$$ **Equation 3.1**

where,

P_I = cohesive soil's plasticity index,

L_L = cohesive soil's liquid limit, and

P_L = cohesive soil's plastic limit

3.3.3   Cation Exchange Capacities

Cation exchange capacities (CEC) of the McBaine, MO soils were determined by the University of Missouri Soil Characterization and Geotechnical Engineering Laboratory following procedures outlined by the USDA National Survey Laboratory (USDA, 2004). Cation exchange capacities are a measure of the soil's ability to attract and exchange cations. Clay minerals have negative charges and to achieve electrical neutrality cations are attracted and held between a soil particles layers. Attracted cations may be exchanged with cations of a differing type. Cations attracted to clay minerals are exchanged in three ways; structure, broken bonds exchanging along the particle edges and non-cleavage surfaces, and replacement of exposed hydrogen hydroxyls by

another cation (Mitchell and Soga, 2005). Cation exchange is helpful in characterizing the physical and chemical processes of the clay portion of soils; however, organic matter also yields increased CEC's due to their negative charge and should be given consideration.

3.3.4 Specific Surface Areas

Specific surface area (SSA) refers to the surface area per unit mass of a soil solid particle. Decreasing particle sizes correspond to increasing surface area when compared at similar mass units (Mitchell and Soga, 1976). Similar to CEC quantities, a clay mineral's specific surface area (SSA) is important in characterizing chemical and physical behavior. Swell potential can be determined by a soil's SSA, with swelling soils such as smectites (particularly montmorillonites) ranging near 800 square meters per gram (m^2/g) and non-expansive kaolin particles ranging near 10 to 40 m^2/g (Cerato and Lutenegger, 2002). A soil's SSA is considered an intrinsic property; water content and other external changes do not affect SSA.

3.3.5 Dry Densities

A soil's dry density is an indication of the mass of solids per total volume, including soil and pore space (Equation 3.2).

$$\rho_b = \frac{M_s}{V_t}$$

Equation 3.2

where,

ρ_b = dry density of soil specimen [$\frac{g}{cm^3}$],

M_s = dry mass of soil specimen [g], and

V_t = bulk volume of soil specimen [cm^3]

The dielectric constant of a saturated soil will decrease with increasing density, while the dielectric constant of a soil with no moisture present will increase with increasing density (Abidin, 2002). The effect dry densities have on a soil's dielectric constant is understood as deionized water

has a dielectric constant of 80, while the dielectric constant of soil minerals are typically between two and five and that of air is around one (Thomas, 1966).

Dry densities of McBaine, MO soils were determined using the drive-cylinder method (ASTM D2937). Cylinders were driven into the soil at their respective depths and transported to the lab. Edges of the cylinder with soil extending past were trimmed to a uniform surface and thus a known volume. Cylinders and soils were weighed and then placed in an oven (110 °C) for gravimetric water content determination according to ASTM D2216.

3.3.6 Specific Density of Solids (Specific Gravity of Solids)

Specific density of solids for McBaine, MO soils were determined by standards employing a pycnometer (ASTM D584). The test is performed to determine the ratio between a soil's unit weight, not including pore spaces, to the unit weight of water at a similar temperature. In geotechnical engineering, the specific density of solids is commonly used for weight-volume calculations. Empirical and semi-empirical predictive dielectric models for soils also incorporate the specific density of solids property.

3.3.7 Soil Water Characteristic Curves

A soil water characteristic curve (SWCC) describes the matric suction and corresponding volumetric water content of a soil (Figure 3.14). At lower volumetric water contents a soil's matric suction will be higher due to remaining moisture being tightly adsorbed by soil particles, while at higher volumetric water contents a soil's matric suction is dominated by capillarity (Lu and Likos, 2004). A SWCC's shape is dependent on soil type with clays typically having higher matric potentials than sands due to smaller pore sizes at similar volumetric water contents. Also shown in Figure 3.14, are the multiple volumetric water contents (θ_1 and θ_2) for a given matric potential

(ψ_1), due to the drying and wetting curves being different. Hysteresis of a SWCC is also common due to wetting and drying events indicated between points A and B.

Soil water characteristic curves for McBaine, MO soils at depths of 6 in., 12 in., 18 in., and 24 in. were determined to compare with field measured retention curves and simulate to water flow in unsaturated soils. Umwelt-Monitoring-Systeme's (UMS) "HYPROP"® was used to measure SWCC's, which is a commercial device optimized to perform the evaporation method (Wind, 1968). A schematic of the "HYPROP" system, which is equipped with two vertically aligned tensiometers is shown as Figure 3.15.
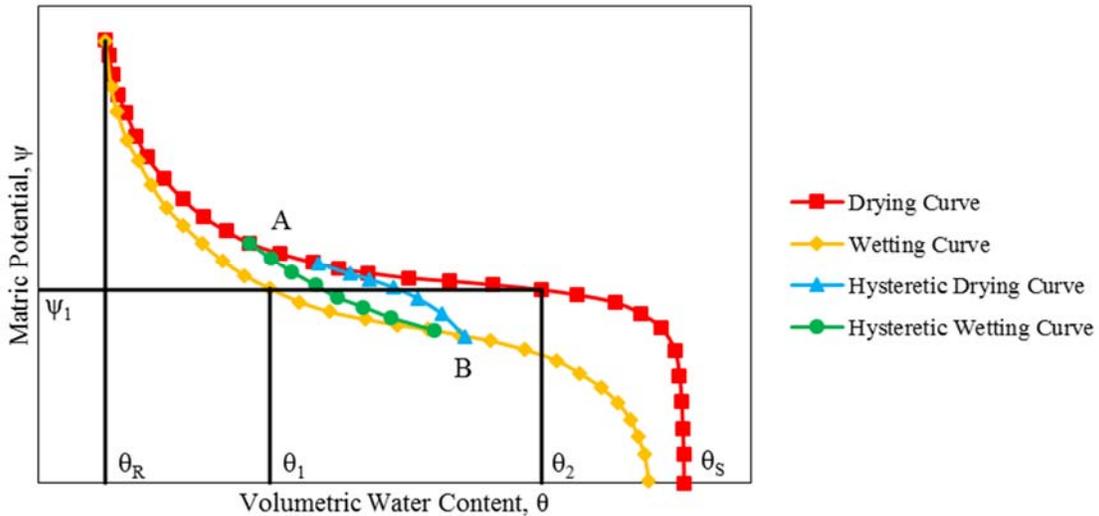
Figure 3.14: Generalized Relationship between Matric Potential and Volumetric Water Content
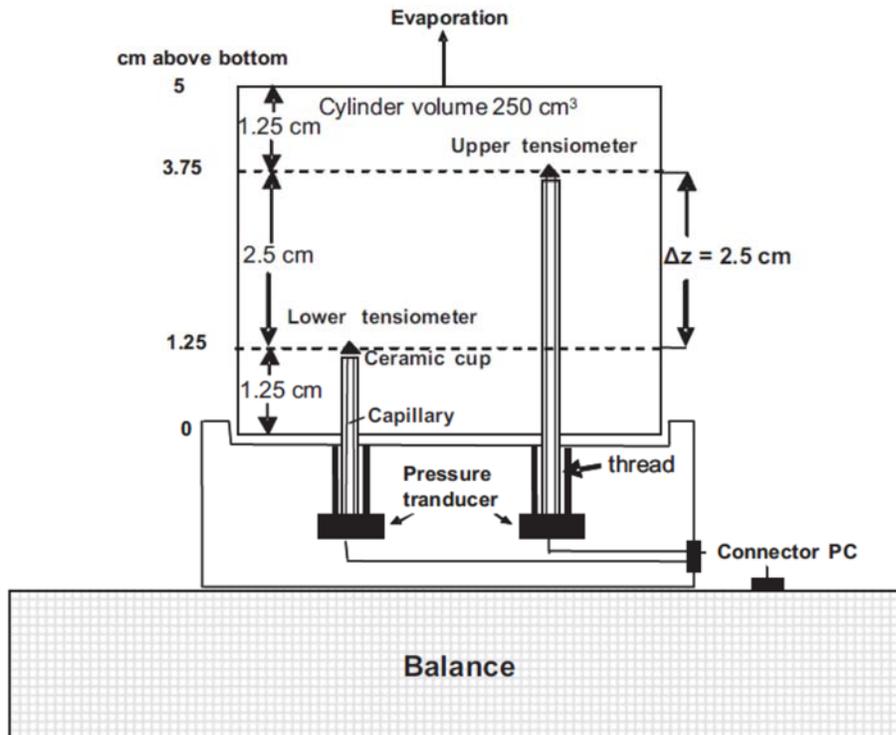
Figure 3.15: Illustration of the "HYPROP" Evaporation-Measurement Device (Schindler et al., 2010)

Soil extracted from McBaine, MO was remolded to field densities into a stainless steel ring (3.98 cm inner diameter x five cm in height). Remolded specimens, sealed at the bottom with a perforated cap, were saturated in a pan of deionized water (Figure 3.16). Pilot holes were drilled in each test specimen (Figure 3.17) and then tensiometers, attached to the device at two different heights, were installed. Specimen surfaces remain open throughout the test to allow moisture loss (Figure 3.18). Suctions at both tensiometers, specimen weight and weight loss from evaporation of moisture were measured at predetermined time intervals.

Figure 3.16: Soil Specimen Saturating in "HYPROP" Sampling Ring

Figure 3.17: Drilling Pilot Holes in "HYPROP" Soil Specimen

Figure 3.18: "HYPROP" Test Specimen and Evaporation - Measurement Process in Progress

Each time interval provides a measured point of water content and matric suction for the SWCC. The "HYPROP" device can measure a maximum suction of 300 kPa before pressure transducers exhibit destructive behavior. This range limits the generated SWCC from showing a complete curve. The importance of having a complete SWCC is great, as many studies have estimated water flow of unsaturated porous media from SWCC's (Lu and Likos, 2004). To generate the complete SWCC, measured data were fit to a closed-form equation developed by van Genuchten (1980) using Excel's® solver feature. To define a SWCC, three parameters were introduced; α, m, n (Equation 3.3). Each parameter is helpful in describing the SWCC and modeling unsaturated water flow.

$$\theta = \left[\frac{1}{1 + \alpha\psi^n}\right]^m$$

Equation 3.3

where,

θ = volumetric water content,

ψ = matric suction for corresponding θ [kPa],

51

α = related to air-entry pressure [kPa] $^{-1}$,

n = related to pore size distribution, and

m = related to overall symmetry of SWCC

3.3.8 Saturated Hydraulic Conductivity

A series of flexible-wall permeability tests (ASTM D5084) was conducted to determine the saturated hydraulic conductivity of McBaine, MO soils. Specimens representative of the McBaine, MO soils at depths of 6 in., 12 in., 18 in., and 24 in. were trimmed to dimensions listed in Table 3.4. Specimen were placed in triaxial cells with porous stones and filter paper separating the ends (Figure 3.19). Each specimen was subjected to a confining pressure of 15 psi. Drainage ends were connected to a pressure panel and subjected to different pressures. Inflow or head water pressures were set to 10 psi, while outflow or tail water pressures were set with a back pressure of 5 psi. The pressure difference of 5 psi across the height of each specimen created hydraulic gradients across each soil specimen, which initiated flow. Confining pressures and inflow and outflow pressures are extremely high for near surface soils, but due to pressure panel fluctuations a difference of 5 psi was deemed a minimum suitable pressure. The higher pressures resulted in higher hydraulic gradients across the length of each specimen (Equation 3.4).
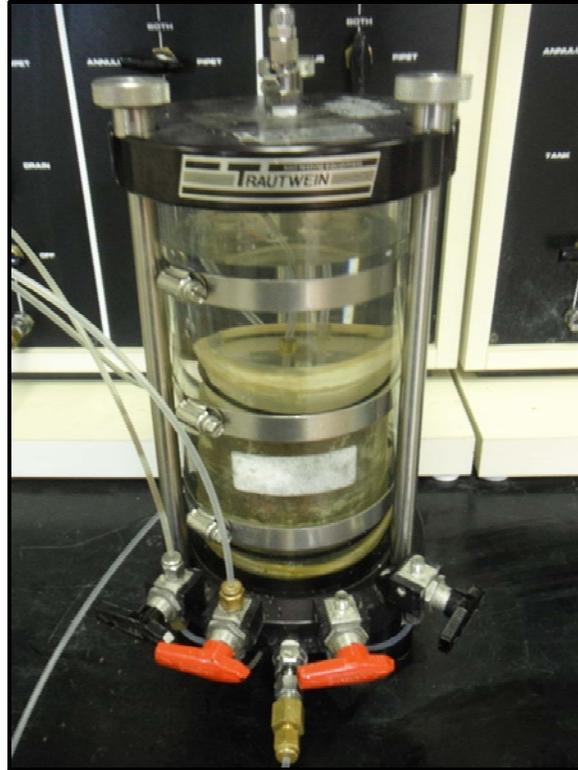
Figure 3.19: Flexible-Wall Permeability Testing of McBaine, MO Soils

Table 3.4: Trimmed Dimensions of Each Soil Specimen for Flexible-Wall Permeability Tests

Depth (in.)	h_{avg} (cm)	diameter (cm)	volume (cm³)
6	4.1	7.6	187
12	6.2	7.6	282
18	4.9	7.6	221
24	6.2	7.6	283

Table 3.5: Hydraulic Gradients for Each Specimen at Their Respective Depth

Depth (in.)	i (unitless)
6	72
12	85
18	57
24	57

Flow was measured into and out of each specimen. When flow reached steady-state conditions, outflow equaling inflow, each specimen was considered saturated. The degree of saturation for each specimen was determined prior to and following each test using applicable

weight-volume relationships (Table 3.6). Saturated hydraulic conductivities were determined using Darcy's Law (Equation 3.4). Determining the saturated hydraulic conductivity is important as a number of empirical relationships employ SWCC fitting parameters with saturated hydraulic conductivity to relate fluid flow of unsaturated soils (Mualem, 1976).

Table 3.6: Pre-Test and Post-Test Degree of Saturation Determination of McBaine, MO Soils

Depth (in.)	*Pre-Test (%)*	*Post-Test (%)*
6	87	103
12	92	105
18	78	105
24	77	96

$$q = kiA \qquad \text{Equation 3.4}$$

where,

q = flow rate through soil specimen $[\frac{L^3}{T}]$,

k = hydraulic conductivity of soil specimen $[\frac{L}{T}]$,

i = hydraulic gradient $[\frac{L}{L}]$, and

A = related to pore size distribution $[L^2]$

3.4 Moisture Migration Modeling

Moisture changes at McBaine, MO were modeled using WinUnsat-H, a Windows-based software of Unsat-H (Fayer, 2000), created at the University of Wisconsin. WinUnsat-H is similar to Unsat-H in the sense it is a one-dimensional computer seepage model which solves a modified Richards' (1931) equation (Equation 3.5) for unsaturated fluid flow using the finite difference method. Water content in WinUnSat-H is dealt with in terms of matric potential, termed head.

$$C(h)\frac{\partial h}{\partial t} = -\frac{\partial}{\partial z}\left[K_L(h)\left(\frac{\partial h}{\partial z}+1\right)\right] - S(z,t) \qquad \text{Equation 3.5}$$

where,

h = head (matric potential) paired to a corresponding volumetric water content [cm],

t = time [hr]

$C(h)$ = chain rule of differentiation for the partial differential equation, $\frac{\partial h}{\partial t}$, and

$S(z,t)$ = sink term for water uptake by plants as a function of time and depth [cm]

The moisture migration model implemented measured meteorological and soil conditions from McBaine, MO during the time period of June 1st, 2013 thru June 30th, 2013. The time period represents common field events where moisture, and consequently dielectric constant, change over time. The computer-based moisture migration model was used in conjunction with predictive dielectric constant models to simulate changes in a near-surface soil's dielectric constant.

3.4.1 Hydrologic Processes

WinUnSat-H simulates the dynamic hydrologic processes: precipitation, infiltration, evaporation, transpiration, and drainage. Each hydrologic process is applied in WinUnSat-H by numerical implementation and in some cases differs from actual behavior.

A soil's infiltration rate is set equal to the precipitation rate during a wetting event. Runoff is indirectly accounted for when the surface node of a soil becomes saturated. Evaporation and transpiration are modeled as potential evapotranspiration (PET). Measured meteorological data input into the Penman (1948) equation and plant water uptake using the equation developed by Feddes et al. (1978) are used to calculate PET. When nodes (soil at a specified depth) dry to a defined matric potential limit as described by the soils SWCC, PET decreases or even ceases. Downward drainage is also dependent on the soil's hydraulic properties determined by its SWCC and saturated hydraulic conductivities.

3.4.2 Boundary Conditions

WinUnSat-H numerically solves water flow the same as UnSat-H, using the finite difference method with a Crank-Nicholson scheme. The Crank-Nicholson scheme solves derivatives at the midpoint of each time step and approximates the modified Richards' (1931) equation in the computer code (Equation 3.6).

$$C_i^{\frac{j-1}{2}} \frac{h_i^j - h_i^{j-1}}{t^j - t^{j-1}} = \frac{-2}{z_{i+1} - z_{i-1}} \left[q_{\frac{i+1}{2}}^{\frac{j-1}{2}} - q_{\frac{i-1}{2}}^{\frac{j-1}{2}} \right] - S_i^{\frac{j-1}{2}} \qquad \text{Equation 3.6}$$

where,

i = subscript denoting the point at a depth, z_i, and

j = subscript denoting the point in time, t_j, an approximation will be made

3.4.3 Boundary and Internal Node Conditions

Boundary and internal node conditions are important to developing an accurate numerical approximation. The upper boundary was denoted as the soil to atmosphere boundary (ground surface) and considered to be node one. The upper boundary was allowed to fluctuate so measured meteorological conditions at the McBaine, MO field site could be simulated realistically. Upper boundaries can be fixed to simulate ponding, but was not done so in these analyses.

The lower boundary was considered the last node and was allowed to change similar to the upper boundary. Flux simulated drainage below the lower boundary depth. The lower boundary can be fixed to simulate an impermeable boundary and/or water table, but was not done in these analyses.

Internal boundary water storage is allowed to change based on the unsaturated hydraulic conductivities and water storages of surrounding internal nodes. Saturated storages below a node create ponding until storages become unsaturated. Unsaturated hydraulic conductivities were determined using van Genuchten's (1980) SWCC parameters and Mualem's (1976) model. Nodal

spacing of boundaries, layer interfaces, and time steps need to be small (0.1 cm) for accurate approximations (Fayer, 2000)

3.4.4   Input Requirements

WinUnSat-H requires a specific set of inputs to successfully perform accurate simulations. Along with necessary boundary and internal conditions, the modeling program must include information concerning soil depth, nodal spacing, material properties, and time steps used.

The analyses used the constitutive relationships developed by van Genuchten (1980) and Mualem (1976) to describe the behavior of McBaine, MO soil properties.   Soil properties necessary to model moisture migration at the McBaine, MO field site in WinUnSat-H are listed in Table 3.7. Measured initial conditions of the soil at the field site are used as simulation starting values. The initial conditions are input at their respective depth in WinUnSat-H as head (matric potential) of a corresponding water content.

Meteorological data are necessary to simulate PET and are input as daily values. The meteorological parameters measured at McBaine, MO and input into WinUnSat-H are listed in Table 3.8. In addition to the parameters listed in Table 3.8, Cloud cover is a parameter that can be input into the computer model, but was not measured at the McBaine, MO field site or used to calculate PET.

Table 3.7: Soil Information Needed for Each Layer to Run WinUnSat-H Simulations

Soil Information
Saturated Water Content (cm^3/cm^3)
Residual Water Content (cm^3/cm^3)
Coefficient of Van Genuchten Function (cm^{-1})
The "n" exponent (unitless)
The "m" symmetry term (unitless)
Saturated Hydraulic Conductivity (cm/hr)
Matric Potential of Soil for Day One (cm of H_2O)

Table 3.8: Daily Meteorological Data Input into WinUnSat-H to Simulate PET

Daily Meteorological Inputs
Maximum Daily Air Temperature (°F)
Minimum Daily Air Temperature (°F)
Average Daily Dew Point Temperature (°F)
Total Daily Solar Radiation (Langleys)
Average Daily Wind Speed (miles per hour)
Daily Precipitation (in.)

3.5   Summary

The soil moisture and meteorological measuring sensors installed at McBaine, MO were presented in this chapter.   The measuring sensors provide 'ground-truth' data for comparison with forecasted dielectric constants of near-surface soils and changes with time as predicted using measured meteorological data.

Background on the tests performed to characterize the McBaine, MO soils in the University of Missouri Soil Characterization and Geotechnical Engineering Laboratory have been presented. Specific procedures used for sample preparation and testing were also presented.

The moisture migration modeling program WinUnsat-H and how it functions were also presented in this chapter. Information key to performing accurate simulations, as well as necessary soil and meteorological inputs were also mentioned.

4 Results

4.1 Introduction

A study was performed to quantify the effectiveness of forecasted dielectric constants in McBaine, Missouri (MO) soils and *in situ* measured dielectric constants Results of measured meteorological and soil conditions at the McBaine, MO field site are presented in this chapter. Laboratory testing used to characterize the behavior of McBaine, MO soils are also presented. The computer program (WinUnSat-H) implemented measured meteorological data and soil properties to forecast soil moisture migration at the McBaine, MO field site. Results of the moisture migration model were used in conjunction with dielectric constant predictive models to forecast the dielectric constant of McBaine, MO soils. *In situ* measurements of the McBaine, MO dielectric constants over time are presented along with forecasted dielectric constants.

4.2 Meteorological and Soil Conditions at McBaine, Missouri

Meteorological and soil conditions measured at McBaine, MO provided 'ground-truth' information for comparison with forecasts of the dielectric constant of the surficial soils. *In situ* soil moisture sensors were placed in the undisturbed sides of a test pit at depths of 6 in., 12 in., 18 in., and 24 in. below ground surface (BGS). Each sensor installed at the McBaine, MO field site measured continuous real-time data during the dates listed in Table 4.1. Results of meteorological and soil conditions measured by the sensors at McBaine, MO are presented.

Table 4.1: Sensors Installed at McBaine, MO Field Site, their Parameters Measured, and Actuation Dates

Sensor Type	Parameter	Date Actuated
ECRN Low-Res Rain Gauge	Precipitation	April 24th, 2012
Davis Cup Anemometer	Wind Speed and Wind Direction	November 12th, 2012
PYR Total Solar Radiation	Solar Irradiance	November 12th, 2012
VP-3 Humidity Temperature	Relative Humidity and Air Temperature	April 24th, 2012
5TE	Dielectric Constant, Soil Temperature, Bulk Electrical Conductivity, and Volumetric Water Content (from Topp et al., 1980)	April 24th, 2012
MPS-2	Matric Potential, Soil Temperature	April 24th, 2012

4.2.1 Dielectric Constant

In situ dielectric constants were measured using Decagon Devices (Decagon, 2012) "5TE" soil moisture sensor. Continuous real-time measurements of the soil's dielectric constant versus depth and over time for McBaine, MO were measured from April 24th, 2012 thru July 11th, 2013 (Figure 4.1). Ranges of the soil's *in situ* dielectric constant at their respective depths are shown in Figure 4.2.
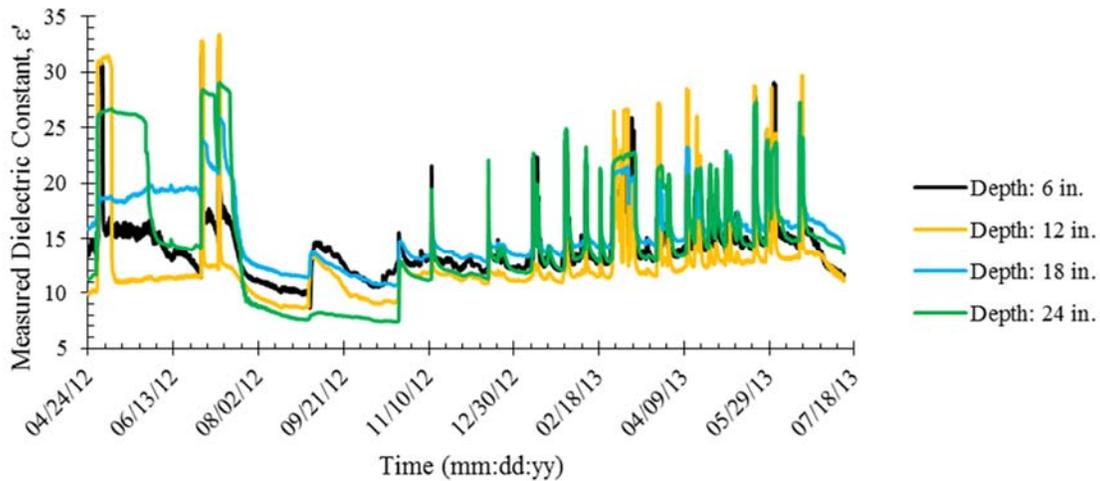
Figure 4.1: Measured Dielectric Constant of McBaine, MO Soils versus Depth and their Changes over the Period of April 24th, 2012 thru July 11th, 2013
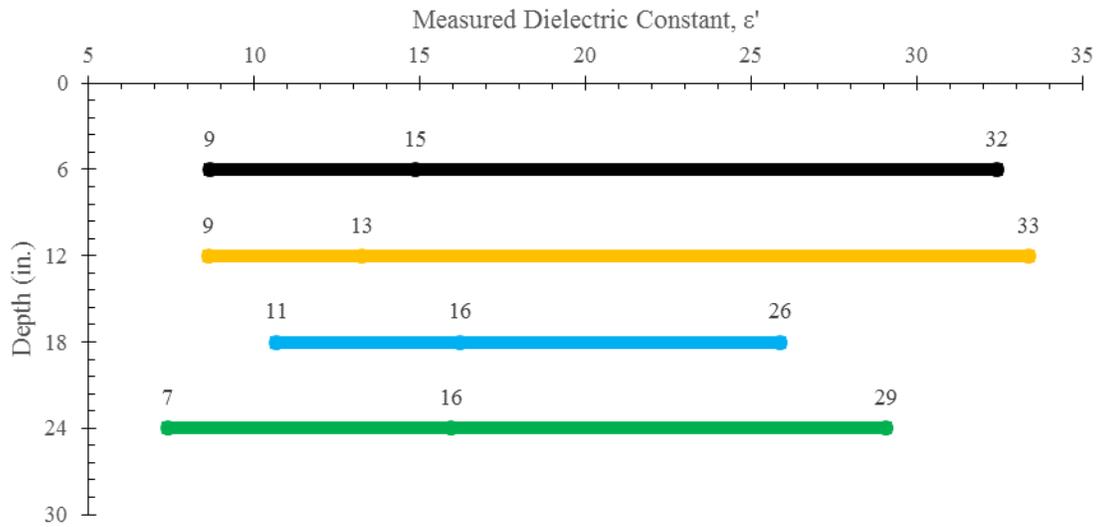
Figure 4.2: Ranges (including Minimum, Average, and Maximum) of Measured Dielectric Constant at McBaine, MO Field Site for their Respective Depths from April 24th, 2012 thru July 11th, 2013

4.2.2 Soil Temperature

In situ soil temperatures were measured using Decagon Devices (Decagon, 2012) "5TE" soil moisture sensor. Continuous real-time measurements of the soil's temperature versus depth and over time for McBaine, MO were measured from April 24th, 2012 thru July 11th, 2013 (Figure 4.3). Ranges of the soils measured temperature at their respective depths are shown in Figure 4.4.
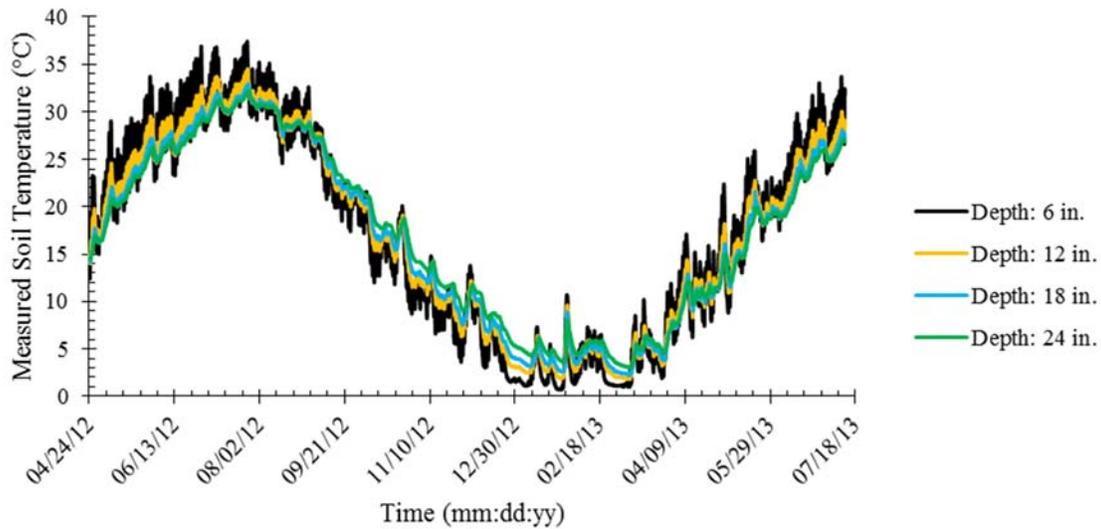
Figure 4.3: Measured Soil Temperature of McBaine, MO Soils versus Depth and their Changes over the Period of April 24th, 2012 thru July 11th, 2013
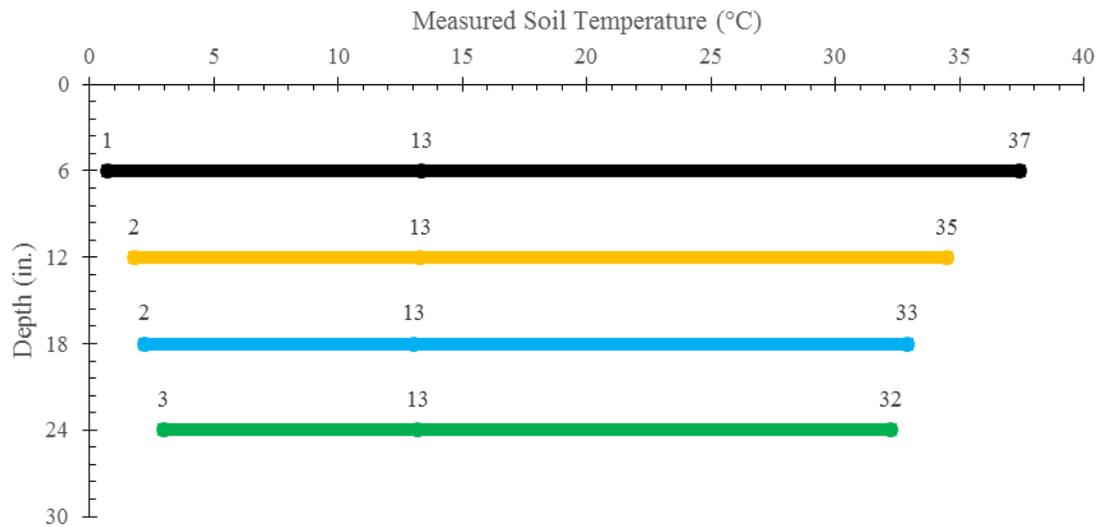
Figure 4.4: Ranges (including Minimum, Average, and Maximum) of Measured Soil Temperature at McBaine, MO Field Site for their Respective Depths from April 24th, 2012 thru July 11th, 2013

4.2.3 Volumetric Water Content from Topp et al. (1980) Model

In situ volumetric water contents were measured using Decagon Devices (Decagon, 2012) "5TE" soil moisture sensor. Continuous real-time measurements of the soil's volumetric water content versus depth and over time for McBaine, MO were measured from April 24th, 2012 thru

July 11th, 2013 (Figure 4.5). Ranges of the soils *in situ* measured volumetric water content at their

respective depths are shown in Figure 4.6.
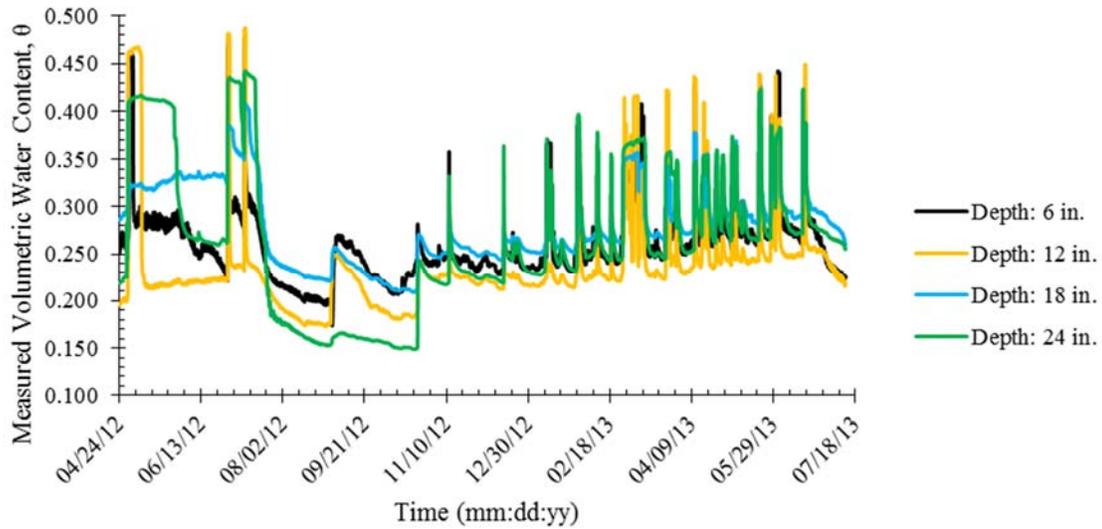
Figure 4.5: Measured Volumetric Water Content of McBaine, MO Soils versus Depth and their Changes over the Period of April 24th, 2012 thru July 11th, 2013
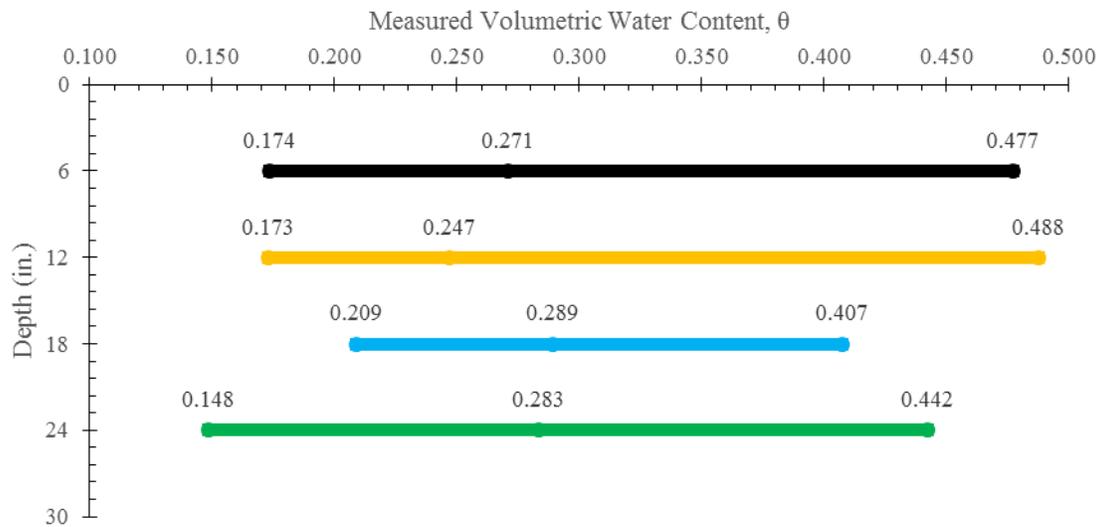
Figure 4.6: Ranges (including Minimum, Average, and Maximum) of Measured Volumetric Water Content at McBaine, MO Field Site for their Respective Depths from April 24th, 2012 thru July 11th, 2013

4.2.4 Matric Potential

In situ soil matric potentials were measured using Decagon Devices (Decagon, 2012) "MPS-2" soil potential sensor. Continuous real-time measurements of the soil's matric potential versus depth and over time for McBaine, MO were measured from April 24th, 2012 thru July 11th, 2013 (Figure 4.7). Ranges of the soils *in situ* measured matric potential at their respective depths are shown in Figure 4.8. The mean matric potential is low for the relative range of measured values at the McBaine, MO field site. Histograms of measured matric potentials at their respective depths are shown in Figure 4.9.
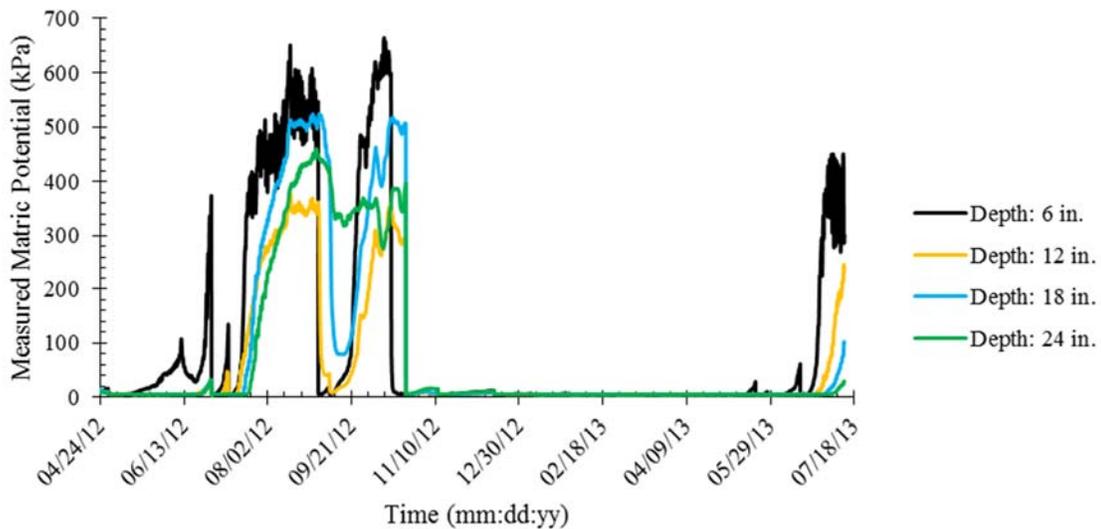
Figure 4.7: Measured Matric Potential of McBaine, MO Soils versus Depth and their Changes over the Period of April 24th, 2012 thru July 11th, 2013
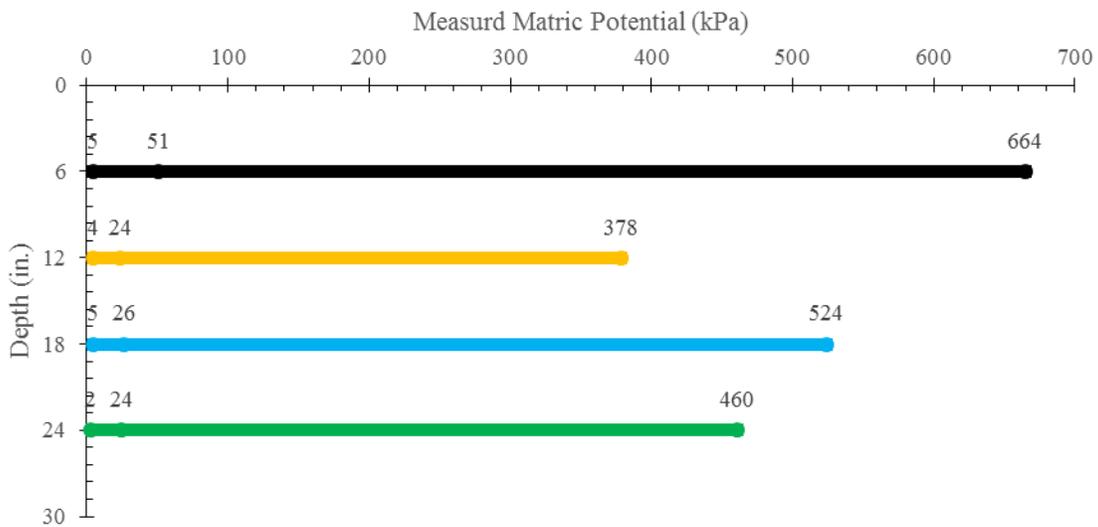
Figure 4.8: Ranges (including Minimum, Average, and Maximum) of Measured Matric Potential at McBaine, MO Field Site for their Respective Depths from April 24th, 2012 thru July 11th, 2013
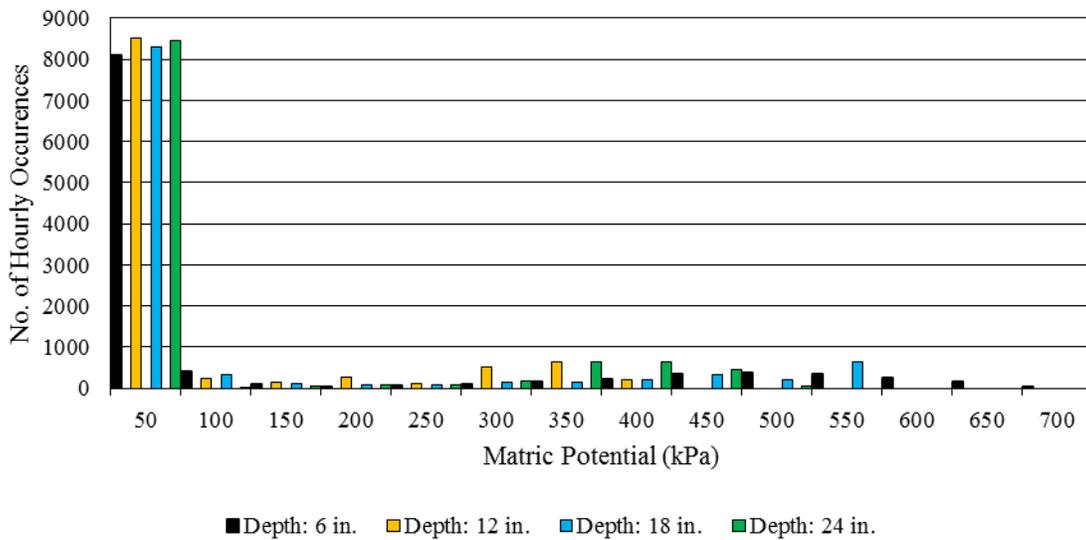
Figure 4.9: Histogram of Measured Matric Potential at the McBaine, MO Field Site at Their Respective Depths

The measured volumetric water contents and corresponding matric potential were used to plot soil water characteristic curves (SWCC's) for each sensor depth (Figure 4.10, Figure 4.11, Figure 4.12, and Figure 4.13, respectively).
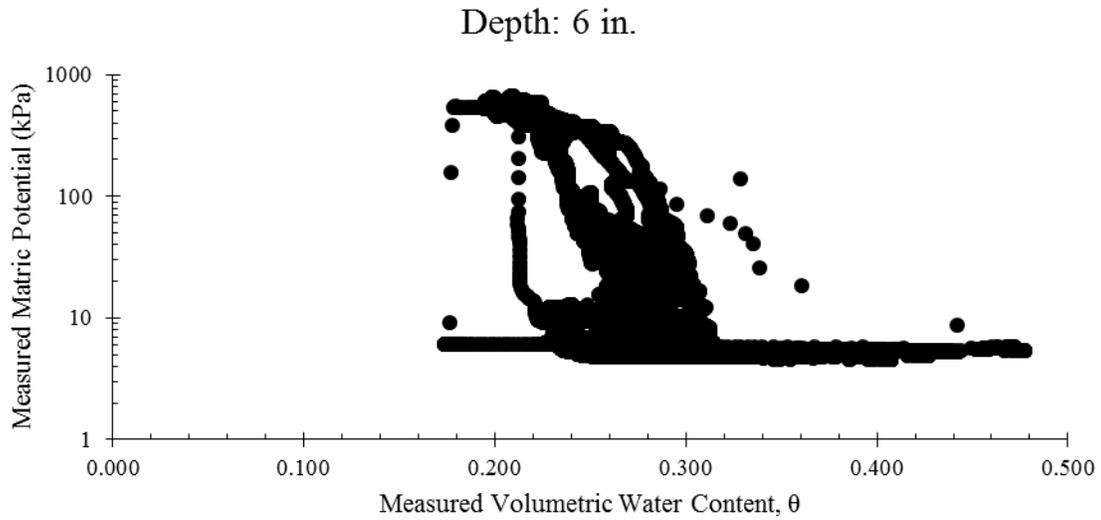
Figure 4.10: Soil Water Characteristic Curve for McBaine, MO Soil at Depth of 6 in. from April 24th, 2012 thru July 11th, 2013
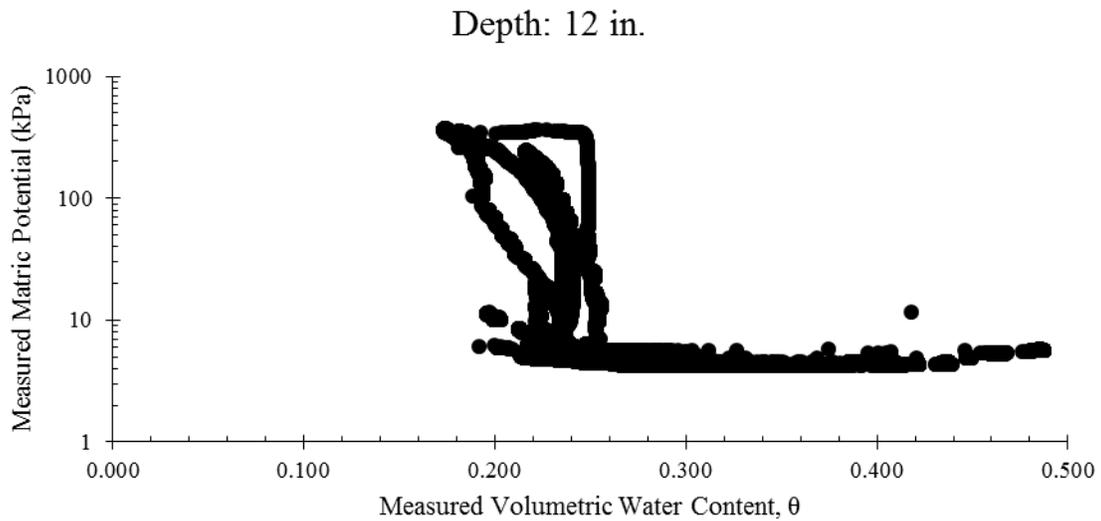
Figure 4.11: Soil Water Characteristic Curve for McBaine, MO Soil at Depth of 12 in. from April 24th, 2012 thru July 11th, 2013

Depth: 18 in.
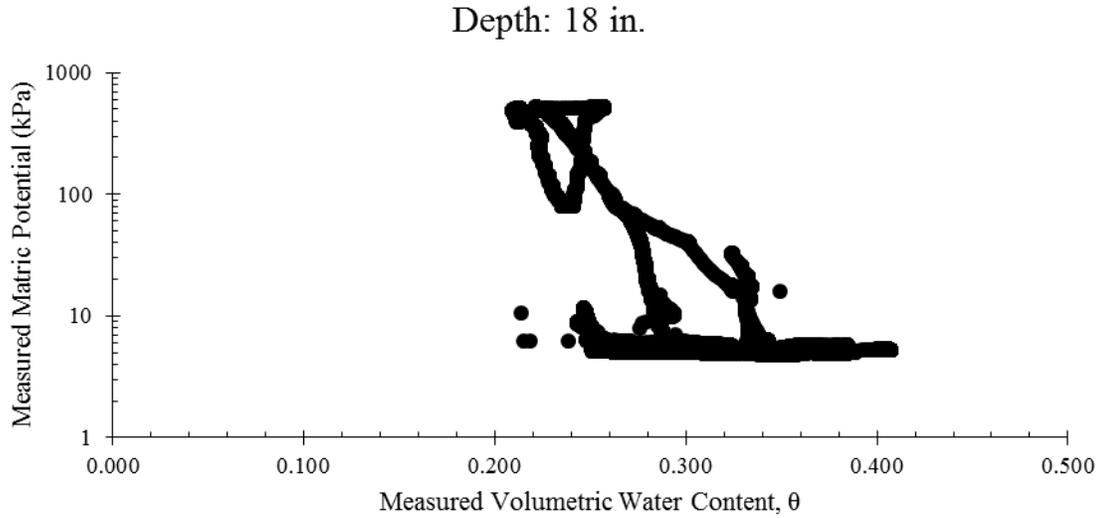
Figure 4.12: Soil Water Characteristic Curve for McBaine, MO Soil at Depth of 18 in. from April 24th, 2012 thru July 11th, 2013

Depth: 24 in.
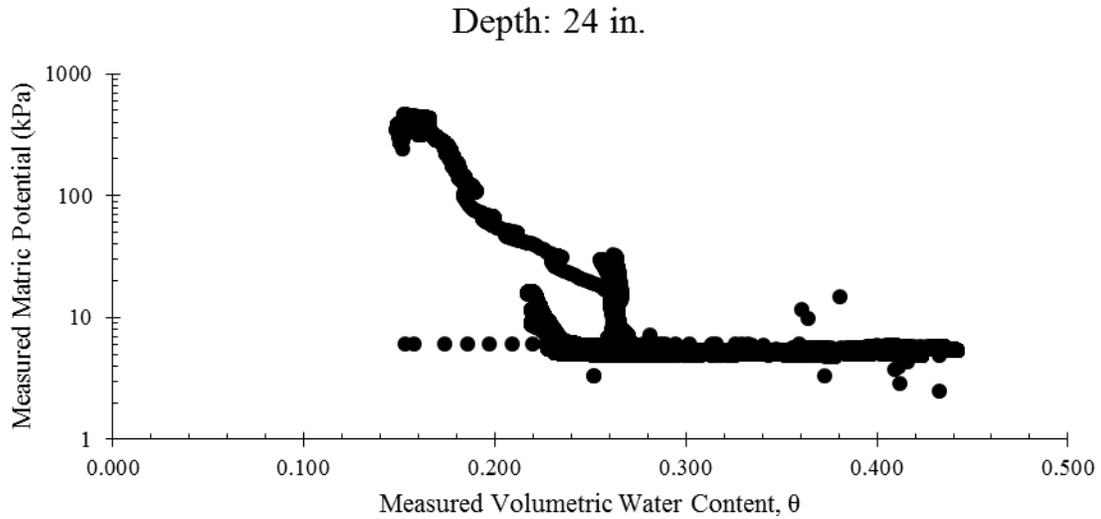
Figure 4.13: Soil Water Characteristic Curve for McBaine, MO Soil at Depth of 24 in. from April 24th, 2012 thru July 11th, 2013

4.2.5   Precipitation

Precipitation was measured using Decagon Devices (Decagon, 2012) "ECRN" Low-Resolution Rain Gauge. Measurements of daily precipitation events for McBaine, MO were

68

recorded from April 24th, 2012 thru July 11th, 2013 (Figure 4.14). Cumulative precipitation over the same time period are shown in Figure 4.15.
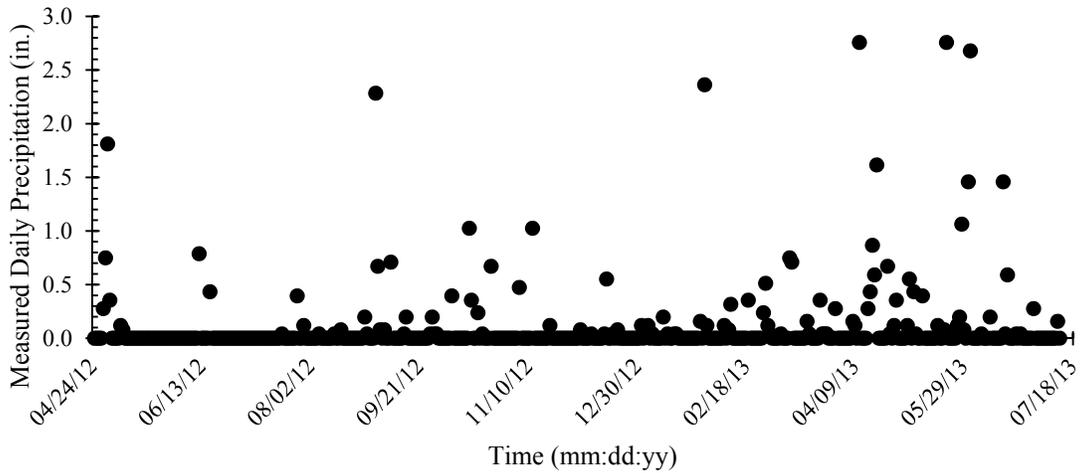
Figure 4.14: Measured Daily Precipitation at the McBaine, MO Field Site over the Period of April 24th, 2012 thru July 11th, 2013
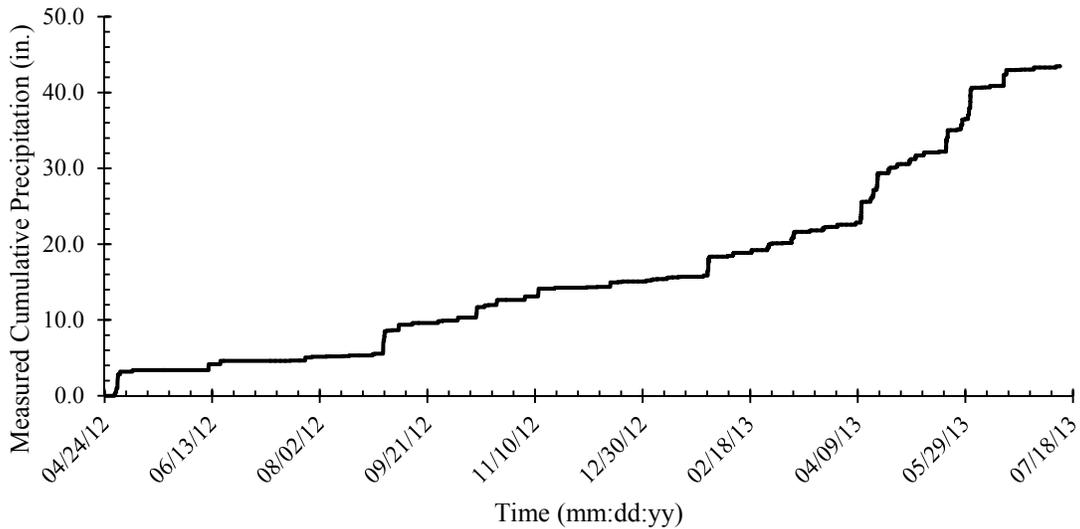
Figure 4.15: Measured Cumulative Precipitation at the McBaine, MO Field Site over the Period of April 24th, 2012 thru July 11th, 2013

4.2.6   Solar Irradiance

Solar Irradiance was measured using Decagon Devices (Decagon, 2012) "PYR" Total Solar Radiation sensor. Continuous real-time measurements of the solar irradiance at McBaine,

MO were measured from November 8th, 2012 thru July 11th, 2013 (Figure 4.16). November 8th, 2012 was the date the "PYR" Total Solar Radiation sensor was installed and became fully operational. Average and maximum daily solar irradiances are shown in Figure 4.17.
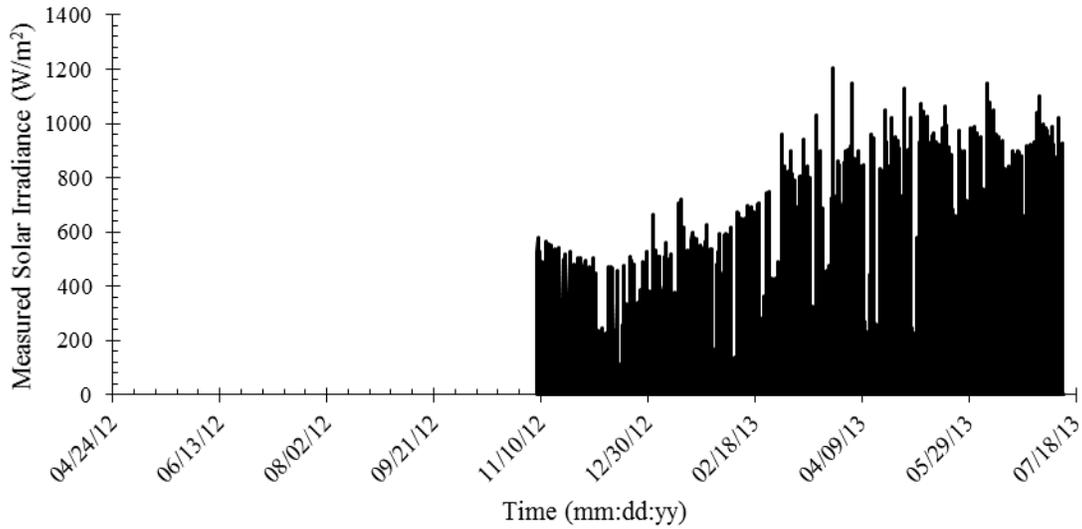
Figure 4.16: Measured Solar Irradiance at the McBaine, MO Field Site over the Period of April 24th, 2012 thru July 11th, 2013
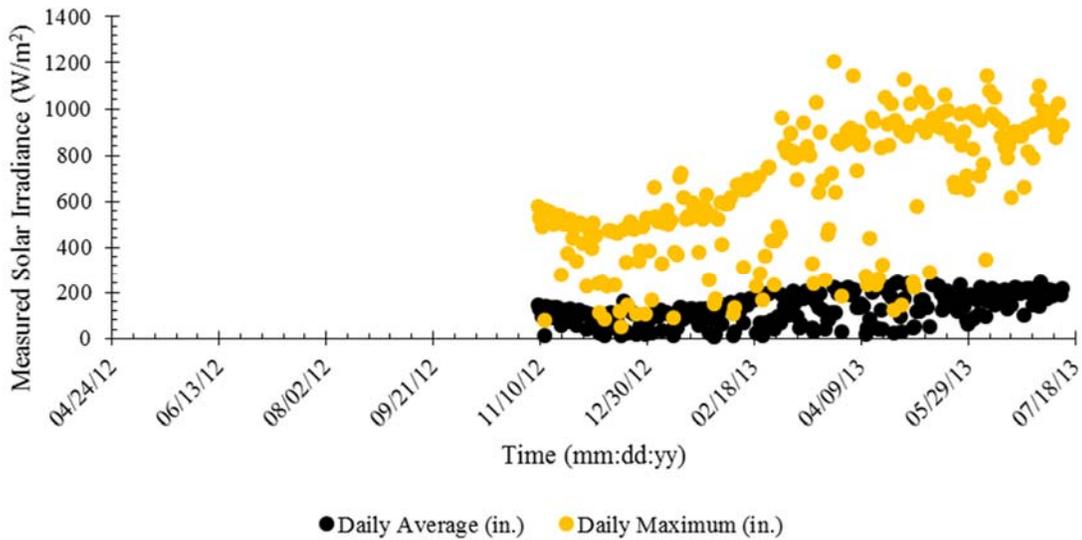
Figure 4.17: Measured Daily Average and Maximum Solar Irradiance at McBaine, MO Field Site over the Period of April 24th, 2012 thru July 11th, 2013

4.2.7 Air Temperature

Air Temperature was measured using Decagon Devices (Decagon, 2012) "VP-3" Humidity Temperature sensor. Continuous real-time measurements of the air temperature at McBaine, MO were measured from April 24th, 2012 thru July 11th, 2013 (Figure 4.18). Minimum, average, and maximum daily air temperatures are shown in Figure 4.19.
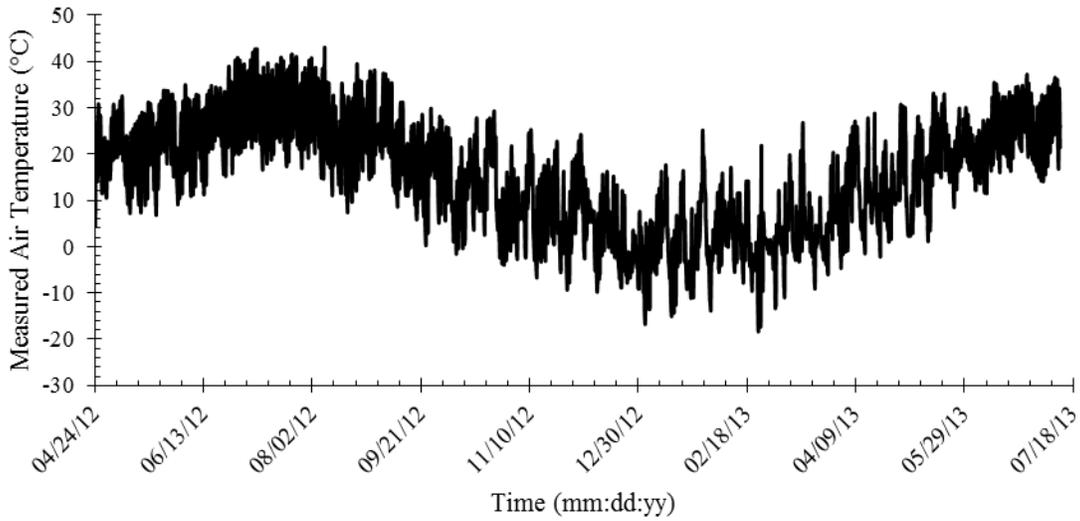
Figure 4.18: Measured Air Temperature at the McBaine, MO Field Site over the Period of April 24th, 2012 thru July 11th, 2013
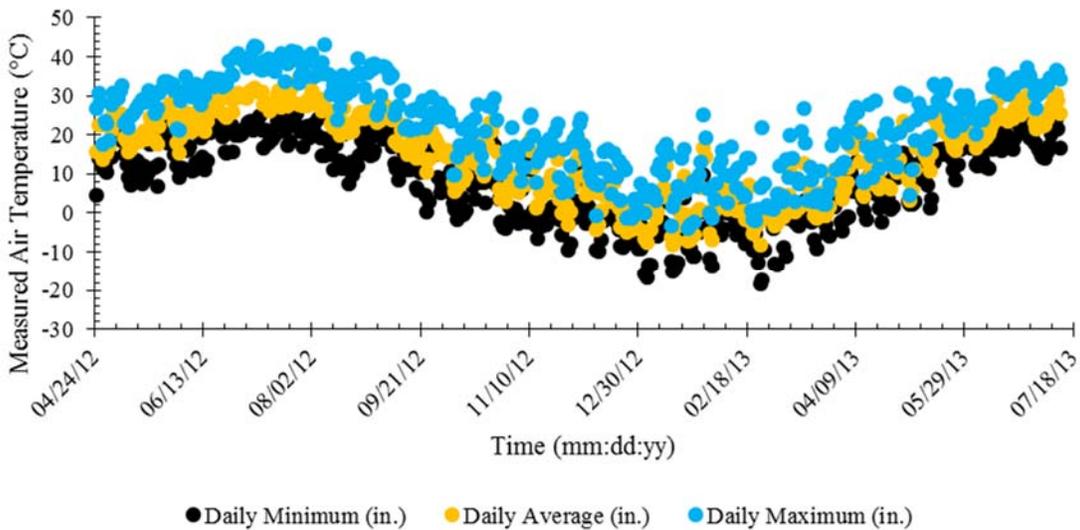
Figure 4.19: Daily Minimum, Average, and Maximum Air Temperature at the McBaine, MO Field Site over the Period of April 24th, 2012 thru July 11th, 2013

71

4.2.8 Relative Humidity

Relative humidity was measured using Decagon Devices (Decagon, 2012) "VP-3" Humidity Temperature sensor. Continuous real-time measurements of relative humidity at McBaine, MO were measured from April 24th, 2012 thru July 11th, 2013 (Figure 4.20). Minimum, average, and maximum daily air temperatures are shown in Figure 4.19.
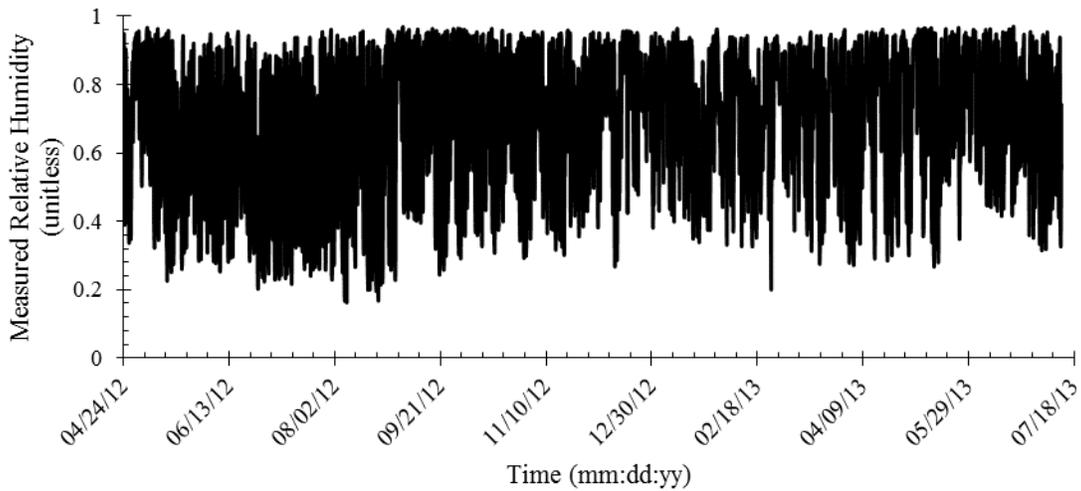
Figure 4.20: Measured Relative Humidity at the McBaine, MO Field Site over the Period of April 24th, 2012 thru July 11th, 2013
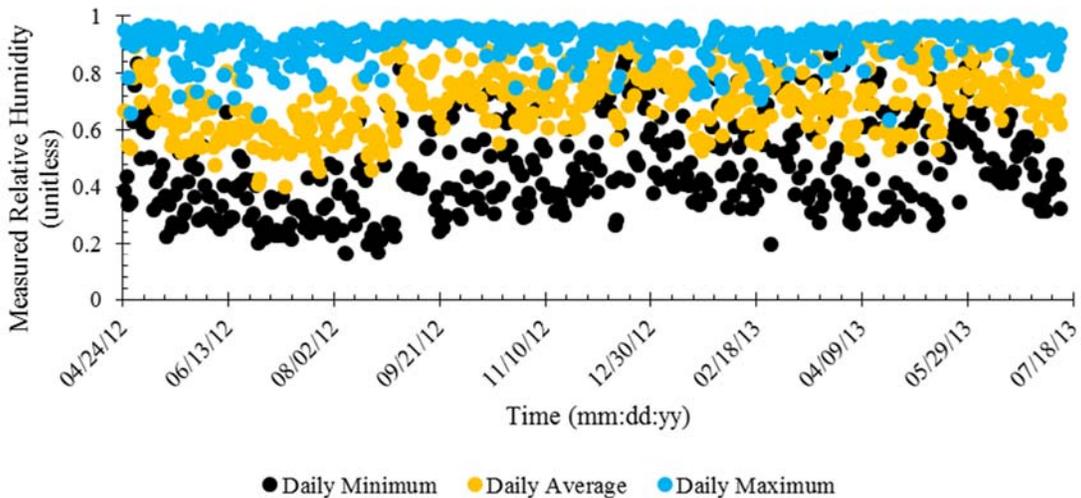
Figure 4.21: Daily Minimum, Average, and Maximum Relative Humidity at the McBaine, MO Field Site over the Period of April 24th, 2012 thru July 11th, 2013

4.2.9   Wind Speed

Wind speeds were measured using Decagon Devices (Decagon, 2012) Davis Cup Anemometer.   Continuous real-time measurements of wind speeds at McBaine, MO were measured from November 8th, 2012 thru July 11th, 2013 (Figure 4.22).   November 8th, 2012 was the date the Davis Cup Anemometer was installed and became fully operational.   Average and maximum daily wind speeds are shown in Figure 4.23.
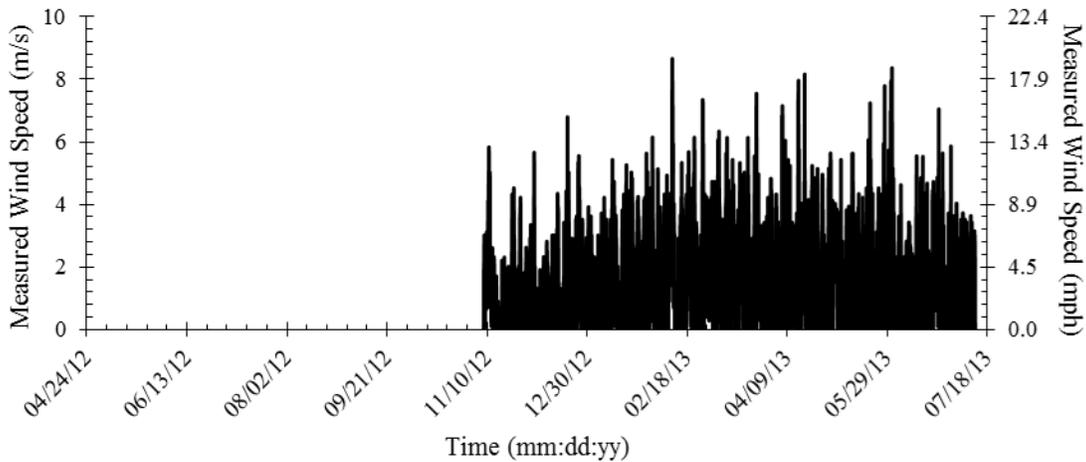
Figure 4.22: Measured Wind Speeds at the McBaine, MO Field Site over the Period of April 24th, 2012 thru July 11th, 2013
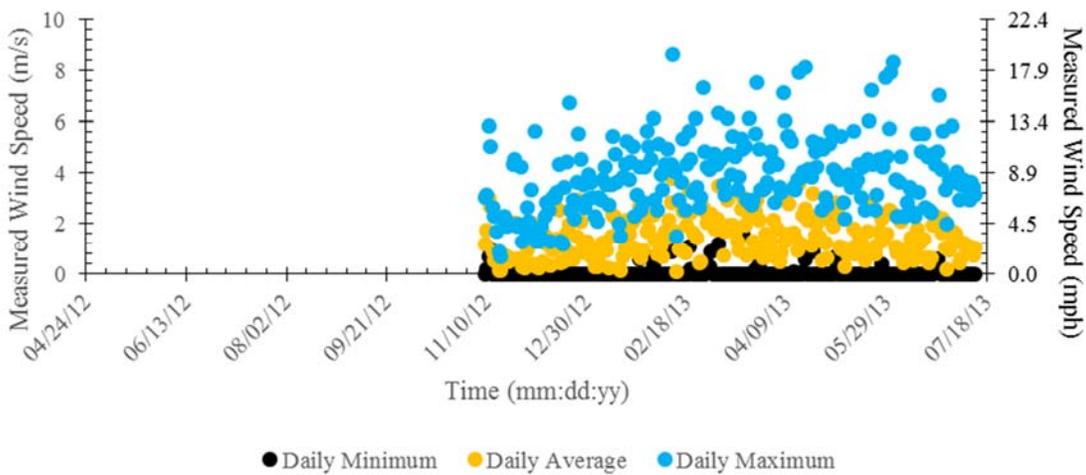
Figure 4.23: Daily Minimum, Average, and Maximum Wind Speeds at the McBaine, MO Field Site over the Period of April 24th, 2012 thru July 11th, 2013

4.3   McBaine, Missouri Soil Characterization

Laboratory testing was conducted to characterize the properties and behavior of soils from the McBaine, MO field site. The soil properties, along with meteorological data, were implemented into the moisture migration computer program (WinUnSat-H) to forecast changes in soil volumetric water content. Characterization of soil properties was also necessary as the dielectric constant predictive models (Chapter 2), which are used in conjunction with results from the moisture migration model, include them as variables to forecast the dielectric constant. Results of the laboratory characterization concerning soil classification and soil behavior are shown in Table 4.2 and Table 4.3, respectively.

Table 4.2: Soil Classification Results for McBaine, MO Soils

	Grain-Size Fraction			*Atterberg Limits*			*Classification*	
Depth (in.)	Sand (2 mm to 0.05 mm)	Silt (0.05 mm to 2 μm)	Clay (< 2 μm)	LL (%)	PL (%)	PI (%)	USCS	USDA
6	31	43	26	42	22	20	CL	Loam
12	6	37	57	73	28	45	CH	Clay
18	29	43	28	40	20	20	CL	Clay Loam
24	61	23	16	21	16	5	CL-ML	Sandy Loam

Table 4.3: Soil Behavior Characterization Results for McBaine, MO Soils

Depth (in.)	*Cation Exchange Capacity* (meq/100g)	*Specific Surface Area* (m^2/g)	*Density of Solids* (g/cm^3)
6	60	174	2.70
12	57	217	2.72
18	40	183	2.70
24	23	129	2.66

4.3.1 Grain Sizes

Grain-size distributions of soil from the test site near McBaine, MO at depths of 6 in., 12 in., 18 in., and 24 in. are shown in Figure 4.24. United States Department of Agriculture (USDA) (USDA, 2004) considers soil particles with a diameter between 0.05 mm to 2.0 mm to be "sand", between 0.002 mm to 0.05 mm to be "silt", and less than 0.002 mm to be "clay". The McBaine, MO soils can be classified as described in the USDA Textural Triangle shown in Figure 4.25 and listed in Table 4.2.
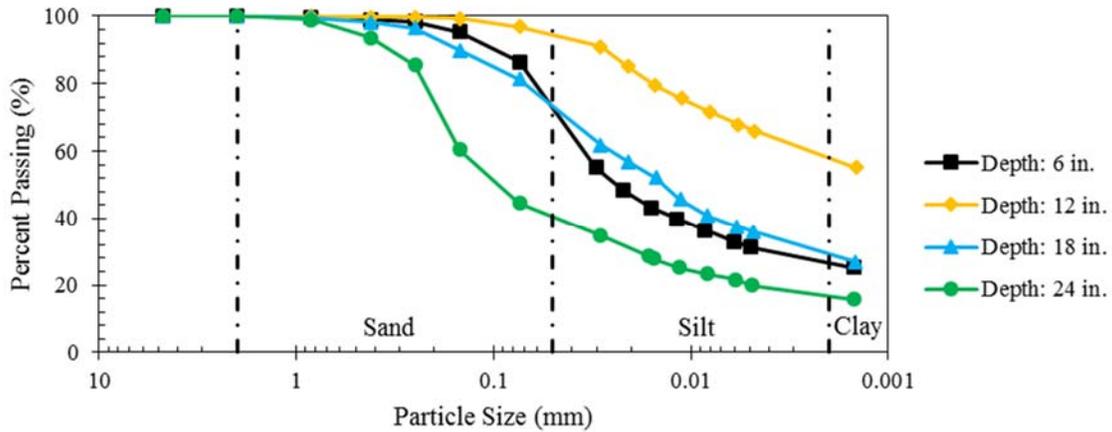
Figure 4.24: Grain-Size Distributions of Soil from McBaine, MO Test Site
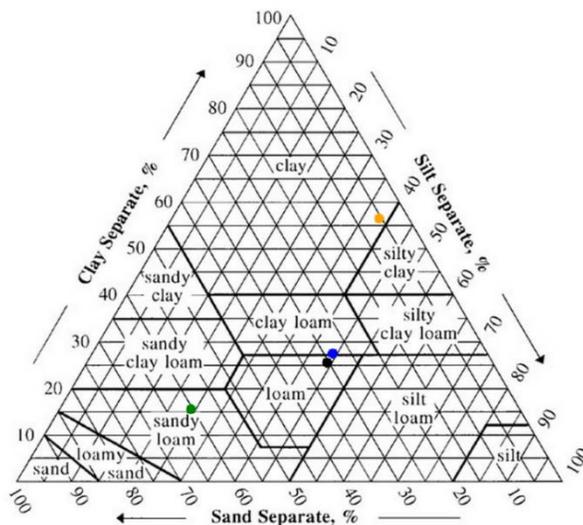
Figure 4.25: USDA Textural Triangle for the McBaine, MO Soils (USDA)

4.3.2 Atterberg Limits

Atterberg limits for the McBaine, MO soil from depths of 6 in., 12 in., 18 in., and 24 in. are shown on the Unified Soil Classification System (USCS) plasticity chart in Figure 4.26. Soils used in this procedure passed a #40 Sieve (0.42 mm).
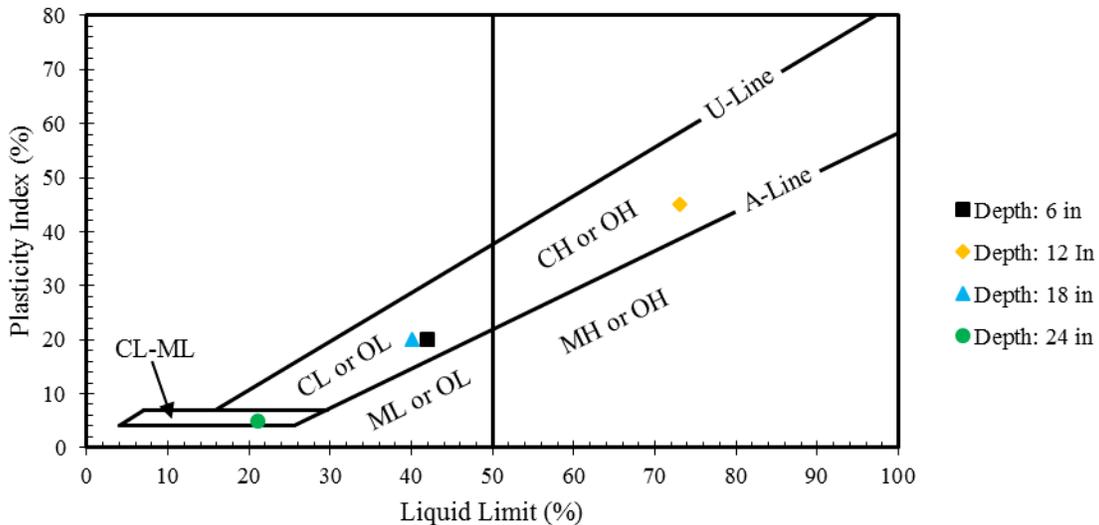
Figure 4.26: Atterberg Limits of McBaine, MO Soils at Their Respective Depths

where,

M = silt,

C = clay,

O = organic,

L = low plasticity (shrink-swell), and

H = high plasticity

4.3.3 Dry Density

Dry densities (dry unit weight) of McBaine, MO soils representative of depths at 6 in., 12 in., 18 in., and 24 in. are shown Figure 4.27 and listed in Table 4.4. The minimum, average, and maximum dry densities for McBaine, MO soils at their respective depths are listed in Table 4.5.
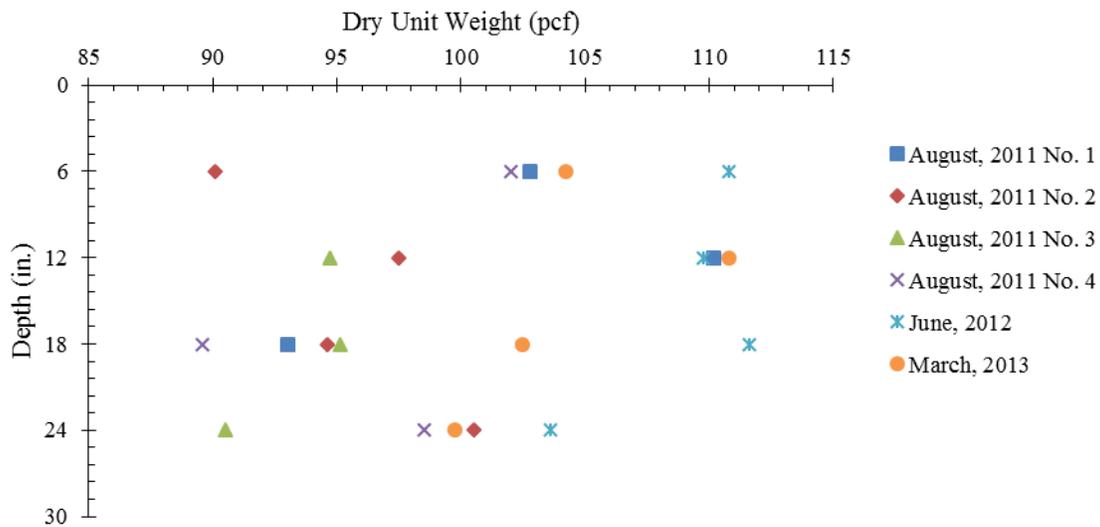
Figure 4.27: Dry Densities versus Depth of McBaine, MO Soils from Three Different Sampling Dates

Table 4.4: Dry Densities of McBaine, MO Soils from Three Different Sampling Dates.

Depth (in.)	August, 2011 No. 1	August, 2011 No. 2	August, 2011 No. 3	August, 2011 No. 4	June, 2012	March, 2013
6	103	90	No Sample	102	111	104
12	110	98	95	No Sample	110	111
18	93	95	95	90	112	102
24	No Sample	101	91	99	104	100

Table 4.5: Minimum, Average, and Maximum Dry Densities Measured at McBaine, MO

Depth (in.)	Minimum (pcf)	Average (pcf)	Maximum (pcf)
6	90	102	111
12	95	105	111
18	90	98	112
24	91	96	104

4.3.4   Soil Water Characteristic Curves

The drying portion of the SWCC's measured in the laboratory on soil extracted from McBaine, MO at depths of 6 in., 12 in., 18 in., and 24 in. are shown in Figure 4.28, Figure 4.29,

Figure 4.30, and Figure 4.31, respectively. Each figure includes measured data from the "HYPROP" device, as well as the fit closed-form equation developed by van Genuchten (1980). van Genuchten (1980) fitting parameters (Chapter 2) used to describe the measured McBaine, MO SWCC's are listed in Table 4.6.
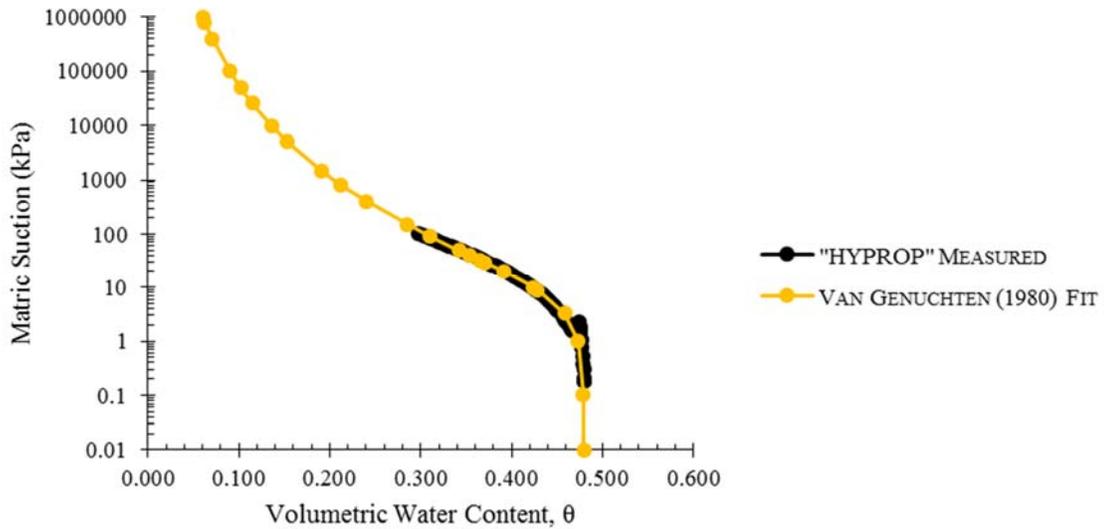
Figure 4.28: Laboratory Measured and van Genuchten (1980) Fit SWCC for McBaine, MO Soils at a Depth of 6 in.
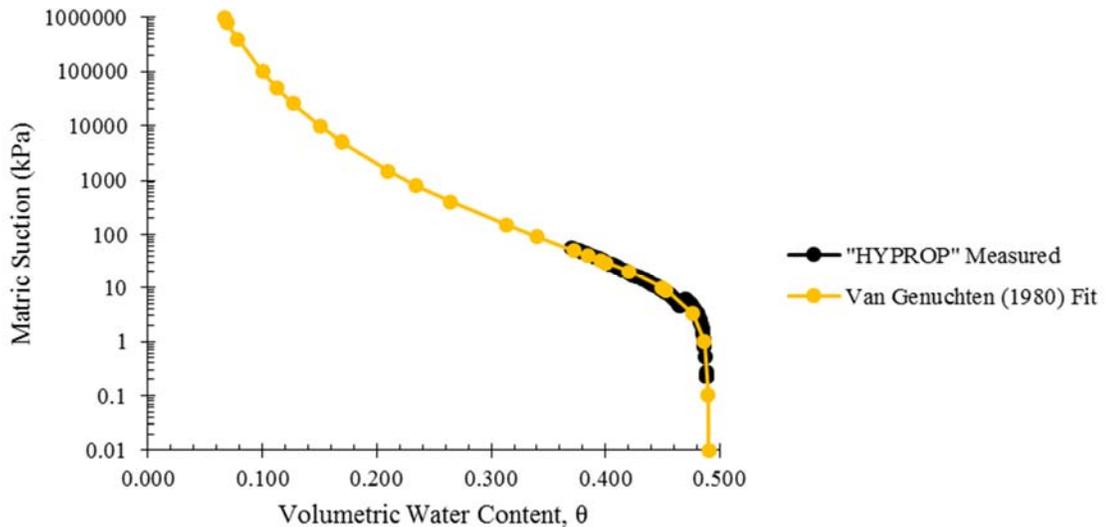
Figure 4.29: Laboratory Measured and van Genuchten (1980) Fit SWCC for McBaine, MO Soils at a Depth of 12 in.
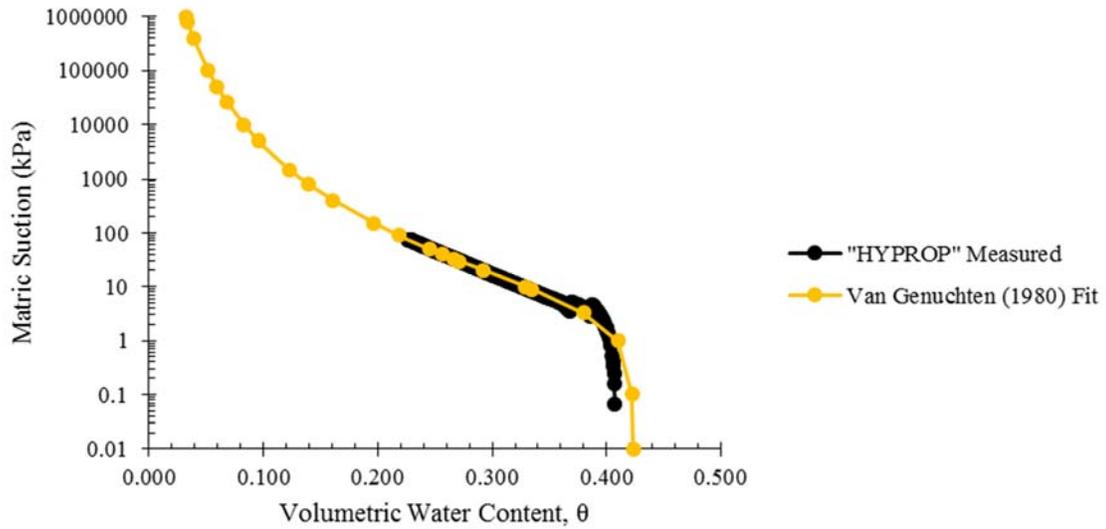
Figure 4.30: Laboratory Measured and van Genuchten (1980) Fit SWCC for McBaine, MO Soils at a Depth of 18 in.
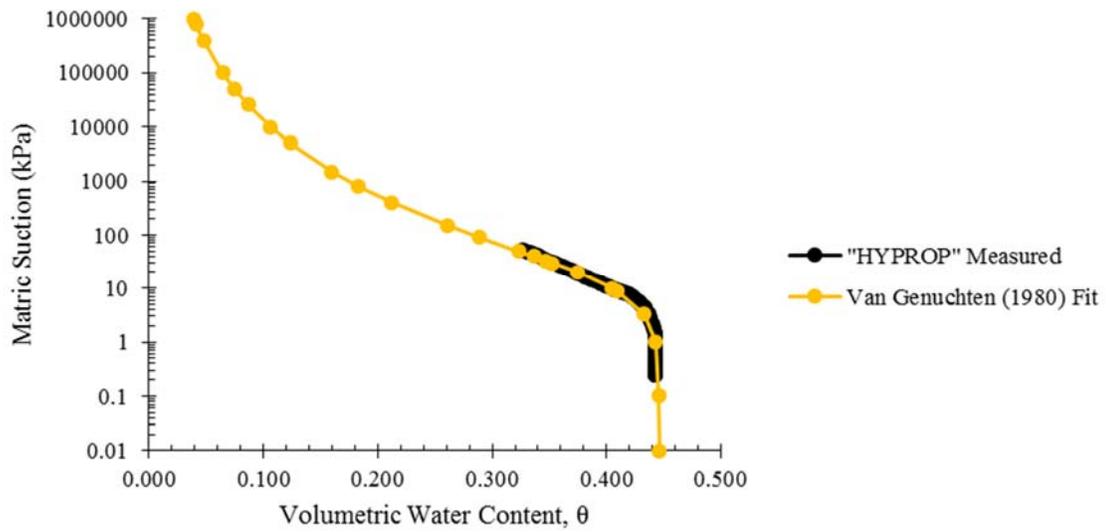
Figure 4.31: Laboratory Measured and van Genuchten (1980) Fit SWCC for McBaine, MO Soils at a Depth of 24 in.

Table 4.6: van Genuchten (1980) fitting parameters from the Laboratory Measured McBaine, MO SWCC's

Depth (in.)	α (cm⁻¹)	n (unitless)	m (unitless)	θ_s (unitless)	θ_r (unitless)
6	0.12	1.18	0.15	0.479	0.000
12	0.08	1.18	0.15	0.490	0.000
18	0.27	1.21	0.17	0.423	0.000
24	0.08	1.22	0.18	0.446	0.000

4.3.5 Saturated Hydraulic Conductivity

Undisturbed soil samples were collected from the McBaine, MO field site at depths of 6 in., 12 in., 18 in., and 24 inches. Their hydraulic conductivities were measured in the University of Missouri Geotechnical Engineering Laboratory (ASTM D5084). Measurements of the normalized flow through each specimen versus the number of pore volumes are shown in Figure 4.32. A pore volume is defined as the volume of voids in a test specimen. Summed pore volumes describe the number of times the soil water has been flushed or drained. Each specimen was considered saturated when the normalized discharges $\left(\frac{Q_{out}}{Q_{in}}\right)$ were between 0.75 and 1.25. Hydraulic conductivity values at their respective depth and corresponding number of pore volumes of flow are shown in Figure 4.33. As the specimens became saturated, hydraulic conductivities become constant.
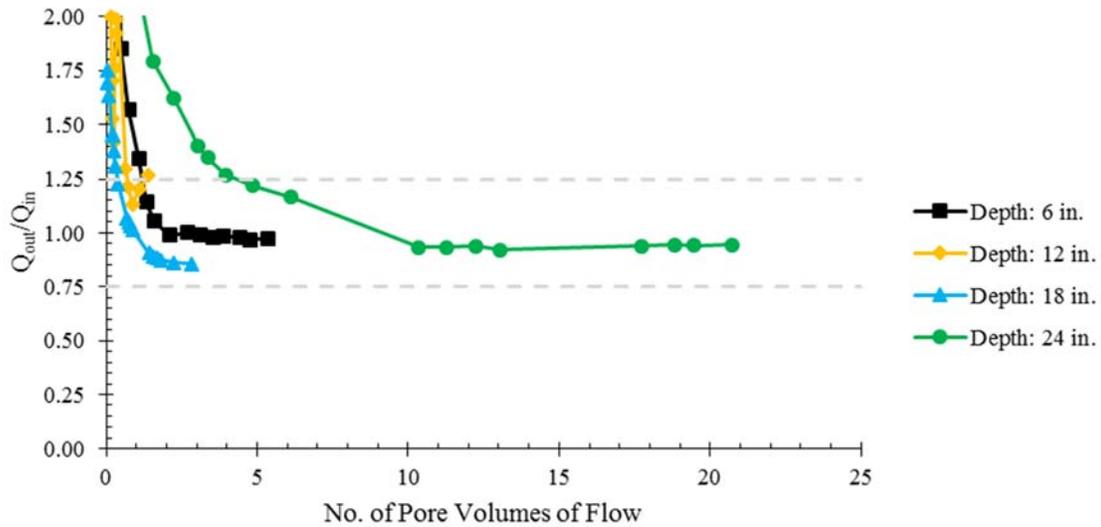
Figure 4.32: Normalized Discharge versus the Number of Pore Volumes of Flow Describing Saturation of Test Specimen's
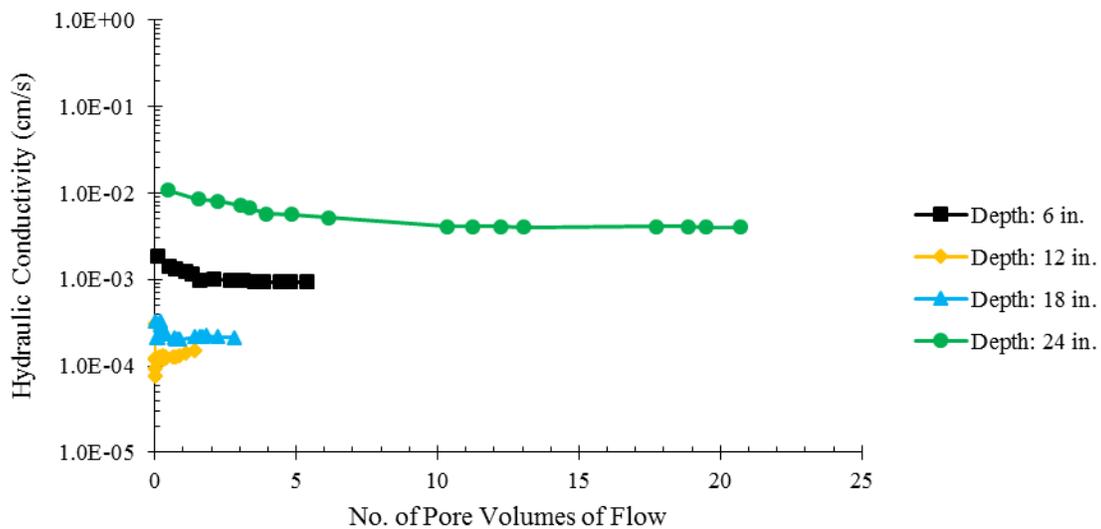
Figure 4.33: Hydraulic Conductivity versus the Number of Pore Volumes of Flow for McBaine, MO Test Specimen's

4.4 Moisture Migration Modeling

Moisture changes over time in McBaine, MO soils using the computer seepage program (WinUnSat-H) are presented. Measured meteorological conditions and soil properties were implemented into WinUnSat-H to predict future soil moisture conditions over time. Predicted

moisture changes of the McBaine, MO field site were used in conjunction with dielectric constant models, to forecast the dielectric constant as a function of depth and time. The forecasted dielectric constants are then compared with measured dielectric constants at McBaine, MO to assess their agreement.

The moisture migration model used measured meteorological and soil conditions from McBaine, MO over a specific time period. The time period covered the end of the spring season and the beginning of the summer season; June 1st, 2013 thru June 30th, 2013. The time period represented common field events where moisture, and subsequently dielectric constant, change over time.

4.4.1   Simulation Inputs

Moisture migration modeling using WinUnSat-H required three distinct inputs to describe the McBaine, MO field site. The number of soil layers, their properties and thicknesses were used to provide boundary conditions for the model. Recorded meteorological conditions were used to model the period of June 1st, 2013 thru June 30th, 2013. Conditions measured at the McBaine, MO field site on June 1st, 2013 were used as the model's starting point. The initial conditions provided a common starting point between measured and forecasted soil volumetric water contents.

Four soil layers were modeled to represent the McBaine, MO soils. The layers were based on visual inspection from test pits and the results of the soil characterization program. The soil characterization and installed soil moisture sensors represented properties and conditions at the field site, respectively, at depths below ground surface of 6 in., 12 in., 18 in., and 24 inches. Layer interfaces were modeled to occur at the vertical midpoint between the installed soil sensors (Table 4.7). Nodes representing a corresponding depth of the modeled subsurface are shown in Figure

4.34. The node spacing was smaller (0.1 cm) at boundaries, and larger in the middle of layers (2.5 cm) (Figure 4.34).

Table 4.7: Soil Materials and Their Corresponding Thicknesses to Represent the McBaine, MO Field Site

Layer	Depth (in.)	Thickness (in.)
Soil No. 1	0 to 9	9
Soil No. 2	9 to 15	6
Soil No. 3	15 to 21	6
Soil No. 4	21 to 30	9
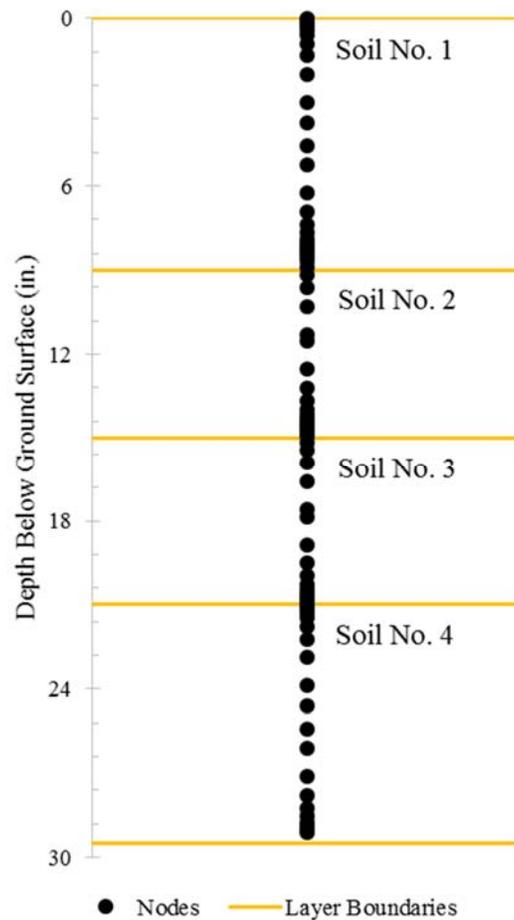
Figure 4.34: Node Placement and their Corresponding Depths Below Ground Surface of the McBaine, MO Field Site Subsurface

The moisture migration model employed van Genuchten's (1980) fitting parameters to describe the McBaine, MO soils relationship between matric potential and volumetric water content (SWCC). The fitting parameters were used in conjunction with Mualem's (1976) unsaturated hydraulic conductivity model to determine the changes in moisture as the soil drains (and wets). Table 4.8 shows the soil properties used to model the McBaine, MO field site.

Table 4.8: Soil Properties used to Model Moisture Changes at the McBaine, MO Field Site

Layer	*Soil No. 1*	*Soil No. 2*	*Soil No. 3*	*Soil No. 4*
Saturated Water Content (cm^3/cm^3)	0.368	0.352	0.389	0.403
Residual Water Content (cm^3/cm^3)	0.000	0.000	0.000	0.000
Coefficient of Van Genuchten Function (cm^{-1})	0.12	0.10	0.26	0.10
"n" Exponent (unitless)	1.25	1.23	1.23	1.35
"m" Exponent (unitless)	0.20	0.19	0.19	0.26
Saturated Hydraulic Conductivity (cm/s)	9.7E-04	1.5E-04	2.1E-04	3.8E-03

The meteorological conditions input into the model were measured at the McBaine, MO field site. The installed sensors recorded measurements on five minute intervals, and were converted to daily values to be input in WinUnSat-H. Precipitation and solar irradiance were input as cumulative sums throughout the day. Wind speed and dew point temperature were input as daily averages. The lowest and highest temperature readings at an interval were input as the minimum and maximum temperatures. Meteorological conditions measured at the McBaine, MO field site and used in the model are shown in Table 4.9.

Table 4.9: Meteorological Data Measured at McBaine, MO Field Site and Used in Moisture Migration Simulations

Date (mm/dd/yy)	Max Daily Temp (°F)	Min Daily Temp (°F)	Dew Point Temp (°F)	Solar Radiation (Langleys)	Wind Speed (mph)	Precipitation (in.)
06/01/13	75	63	61	348	2.5	0
06/02/13	68	54	55	219	1.8	0
06/03/13	75	54	54	463	2.2	0
06/04/13	77	57	59	375	4.7	0
06/05/13	75	56	61	200	0.9	0.04
06/06/13	81	61	59	340	1.5	0
06/07/13	80	53	55	390	1.7	0
06/08/13	81	53	57	444	2.5	0
06/09/13	81	64	62	298	3.2	0.20
06/10/13	90	61	63	431	1.2	0
06/11/13	96	64	68	390	1.9	0
06/12/13	95	70	72	361	4.0	0
06/13/13	91	66	64	430	2.7	0
06/14/13	88	61	64	434	2.9	0
06/15/13	90	68	69	264	3.1	1.46
06/16/13	90	69	71	312	1.5	0.04
06/17/13	86	67	69	295	1.5	0.59
06/18/13	92	63	66	409	1.0	0
06/19/13	91	61	65	465	1.4	0
06/20/13	90	66	69	454	4.3	0
06/21/13	94	74	73	402	5.1	0.04
06/22/13	94	76	74	433	5.0	0.0
06/23/13	92	70	70	209	5.0	0.04
06/24/13	95	69	73	447	3.6	0
06/25/13	93	77	73	413	4.9	0
06/26/13	99	74	72	448	2.3	0
06/27/13	96	67	71	297	0.4	0
06/28/13	92	68	66	429	2.1	0
06/29/13	86	64	62	382	3.5	0.28
06/30/13	80	64	63	291	3.8	0

Dielectric constants measured at the McBaine, MO field site on June 1st, 2013 are shown in Figure 4.35. Initial volumetric water contents at the McBaine, MO field site were determined using two of the predictive models previously mentioned as they are included as variables; Topp et al. (1980) and Peplinski et al. (1995). It should be noted, the initial dielectric constant for June 1st, 2013 is what was measured at the McBaine, MO field site.   Back calculated volumetric water contents using the Topp et al. (1980) model from measured dielectric constants at the McBaine, MO field site are shown in Figure 4.36. Back calculated volumetric water contents using the Peplinski et al. (1995) model from measured dielectric constants at the McBaine, MO field site are shown in Figure 4.37. The back calculated volumetric water contents are used in the moisture migration model to forecast the changes in moisture due to wetting and draining. The forecasted volumetric water contents are entered back into dielectric constant predictive models (Topp et al., 1980, Peplinski et al., 1995) to forecast the McBaine, MO soil's dielectric constant.
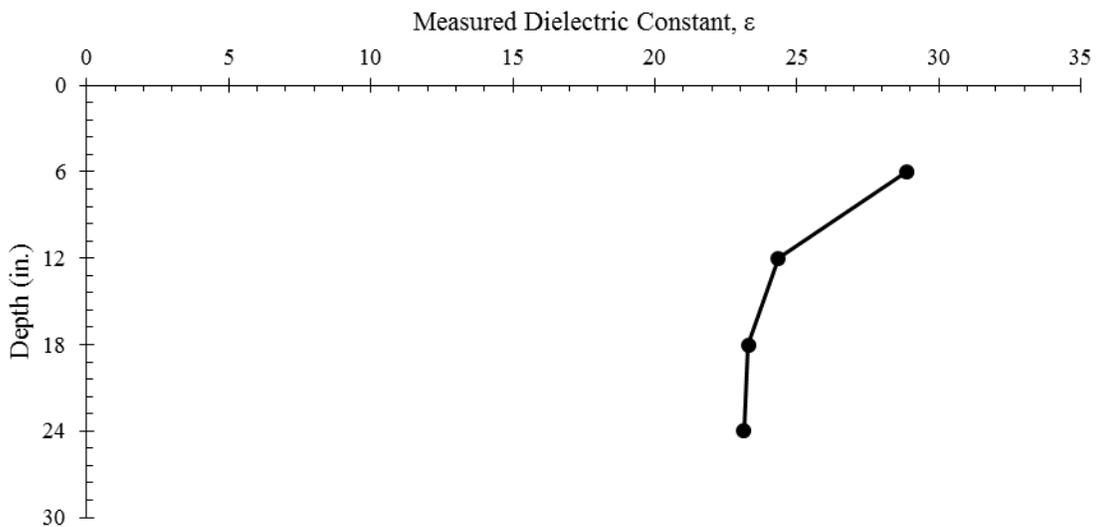
Figure 4.35: Initial Conditions of Measured Dielectric Constant versus Depth at McBaine, MO Field Site on June 1st, 2013
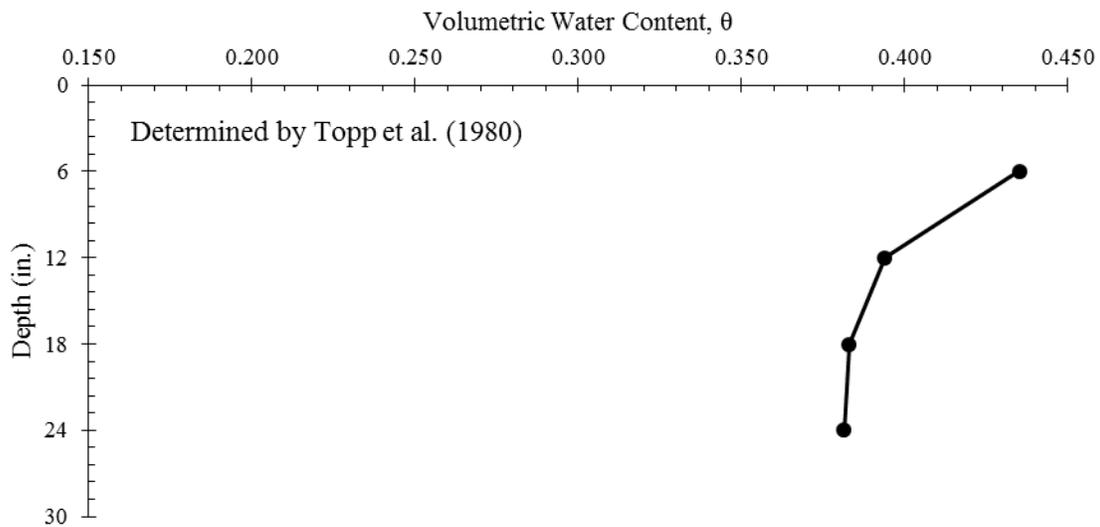
Figure 4.36: Initial Conditions of Back Calculated Volumetric Water Content using the Topp et al. (1980) Model versus Depth at McBaine, MO Field Site on June 1st, 2013
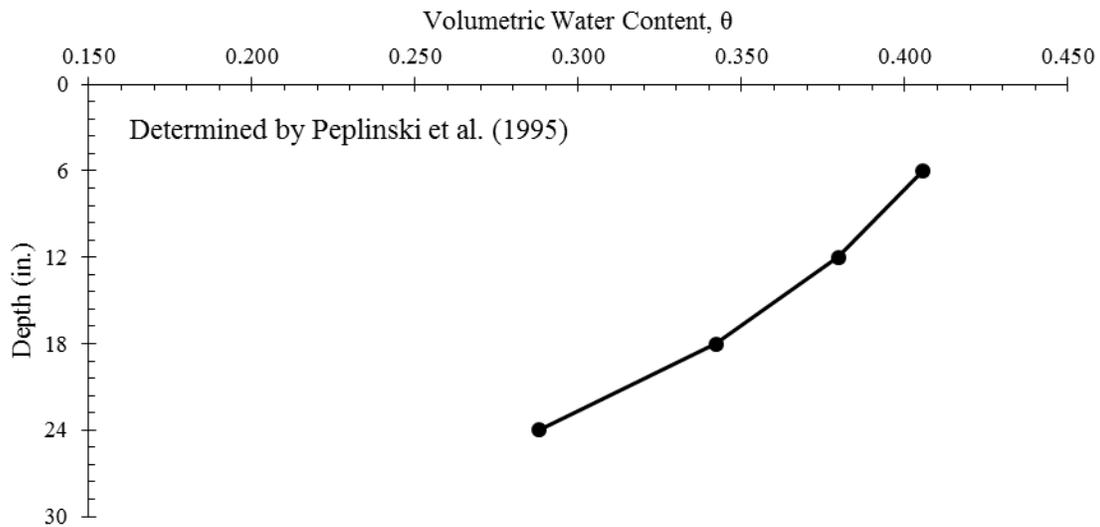
Figure 4.37: Initial Conditions of Back Calculated Volumetric Water Content using the Peplinski et al. (1995) Model versus Depth at McBaine, MO Field Site on June 1st, 2013

4.4.2 Simulation Outputs

The first simulation started from back calculated volumetric water contents using measured dielectric constants on June 1st, 2013. Forecasted volumetric water contents using moisture conditions back calculated from the Topp et al. (1980) model are shown in Figure 4.38.

Volumetric water contents are output as end of day values (WinUnSat-H only outputs end of day values). The Topp et al. (1980) model was used to calculate dielectric constants from the forecasted volumetric water contents (Figure 4.39).
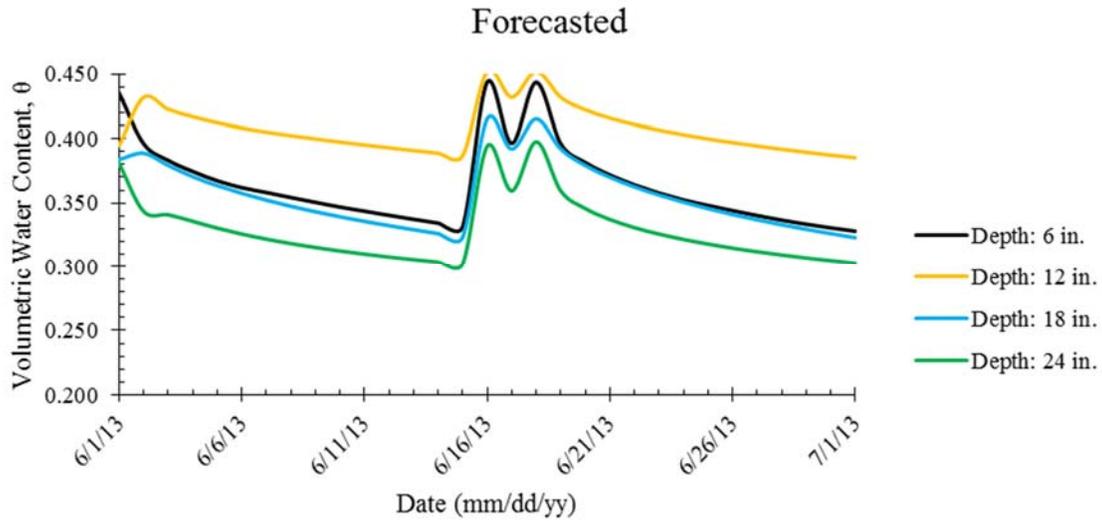
Figure 4.38: Forecasted Volumetric Water Contents for the McBaine, MO Field Site using Initial Conditions Determined by the Topp et al. (1980) Model from June 1st, 2013 thru June 30th, 2013
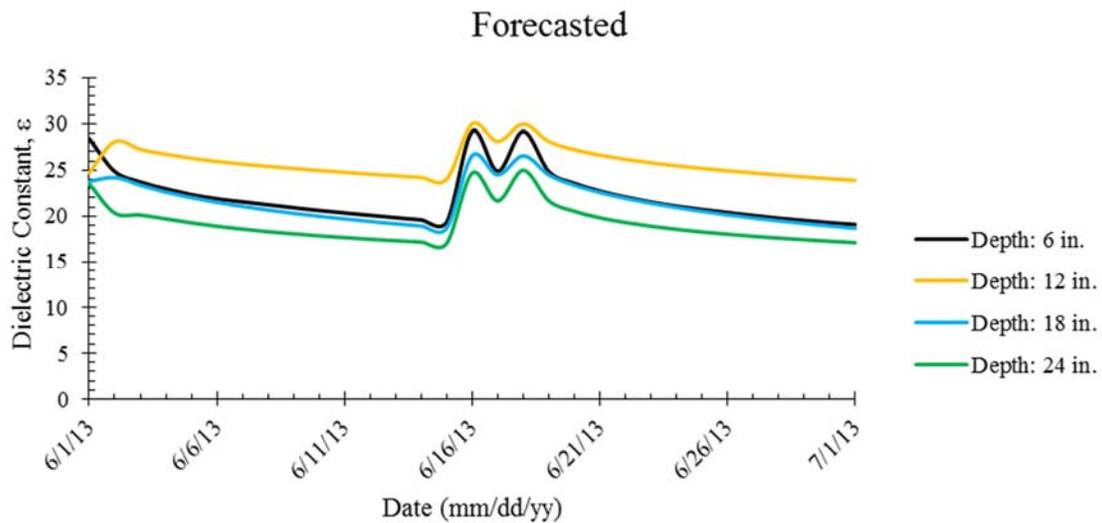
Figure 4.39: Forecasted Dielectric Constants for the McBaine, MO Field Site using the Topp et al. (1980) Model from June 1st, 2013 thru June 30th, 2013

The second simulation started from back calculated volumetric water contents using measured dielectric constants on June 1st, 2013, from the Peplinski et al. (1995) model. Forecasted volumetric water contents using moisture conditions back calculated from the Peplinski et al. (1995) model are shown in Figure 4.40. The Peplinski et al. (1995) model was then used to calculate dielectric constants from the forecasted volumetric water contents (Figure 4.41).
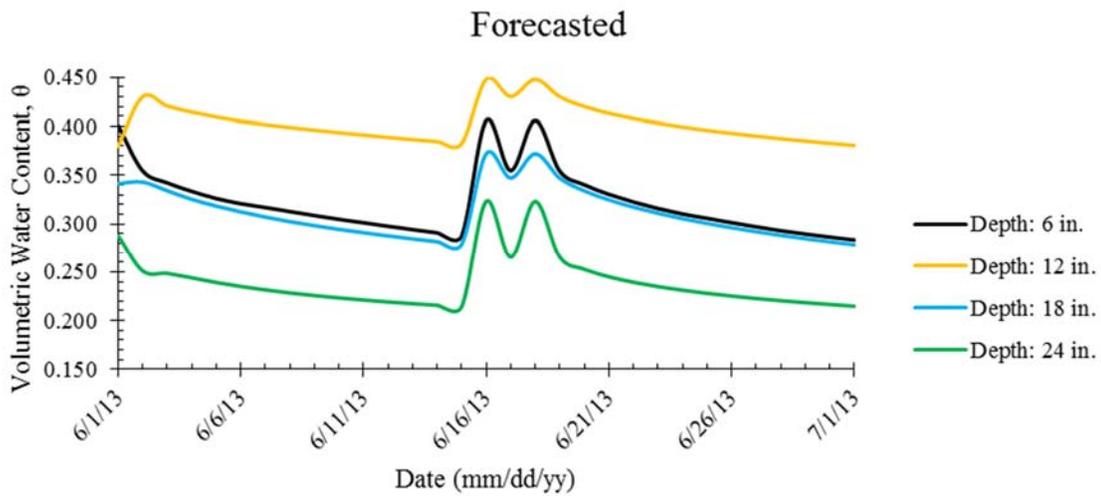
Figure 4.40: Forecasted Volumetric Water Contents for the McBaine, MO Field Site using Initial Conditions Determined by the Peplinski et al. (1995) Model from June 1st, 2013 thru June 30th, 2013
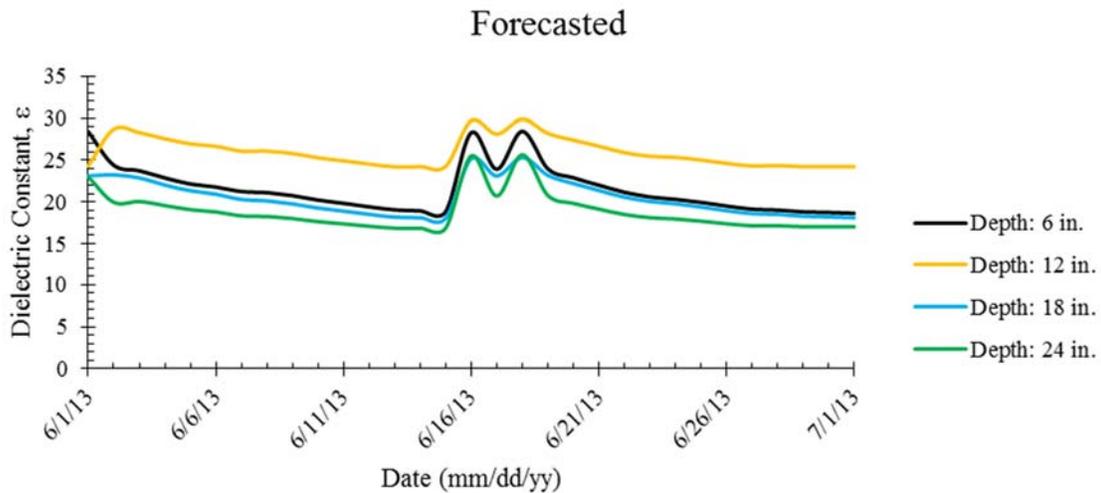
Figure 4.41: Forecasted Dielectric Constants for the McBaine, MO Field Site using the Peplinski et al. (1995) Model from June 1st, 2013 thru June 30th, 2013

4.4.3   Forecasted vs. Measured Dielectric Constant (Topp et al., 1980)

In situ measurements of dielectric constants at the McBaine, MO field site are compared with forecasted dielectric constants of the soil using the measured meteorological and soil property data. The *in situ* measured dielectric constants from the time period of June 1st, 2013 thru June 30th, 2013 are shown in Figure 4.42. Forecasted dielectric constants using the Topp et al. (1980) predictive model are shown in Figure 4.43.
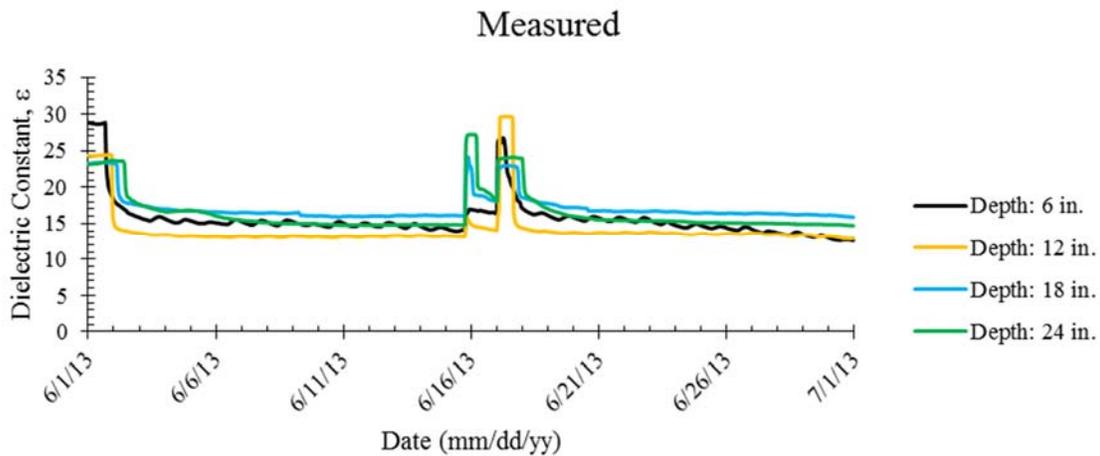
Figure 4.42: Measured Dielectric Constants at the McBaine, MO Field Site over the Time Period of June 1st, 2013 thru June 30th, 2013
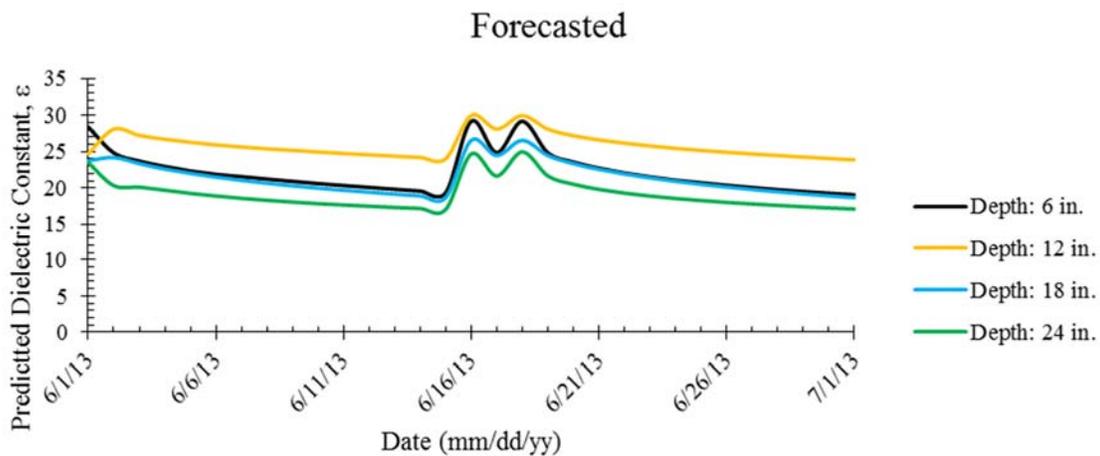
Figure 4.43: Forecasted Dielectric Constants for the McBaine, MO Field Site using the Topp et al. (1980) Model from June 1st, 2013 thru June 30th, 2013

Forecasted (Topp et al., 1980) and measured dielectric constants for the McBaine, MO field site at depths of 6 in., 12 in., 18 in., and 24 in. are shown in Figure 4.44, Figure 4.45, Figure 4.46, and Figure 4.47, respectively. McBaine, MO soil's volumetric water contents predicted from WinUnSat-H were used in Topp et al.'s (1980) predictive model to forecast the dielectric constant.
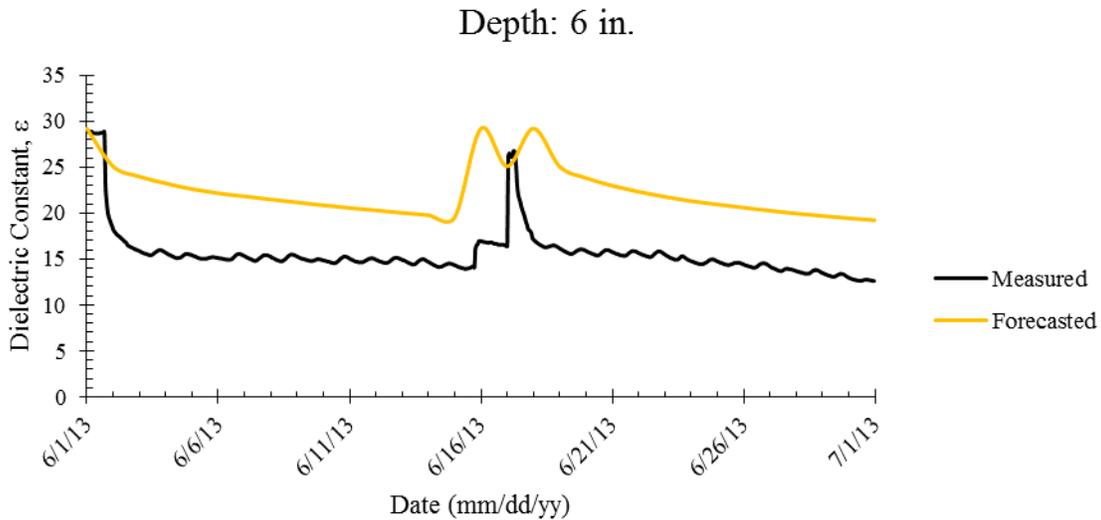
Figure 4.44: Forecasted (Topp et al., 1980) and Measured Dielectric Constants at a Depth of 6 in. at the McBaine, MO Field Site over the Time Period of June 1st, 2013 thru June 30th, 2013
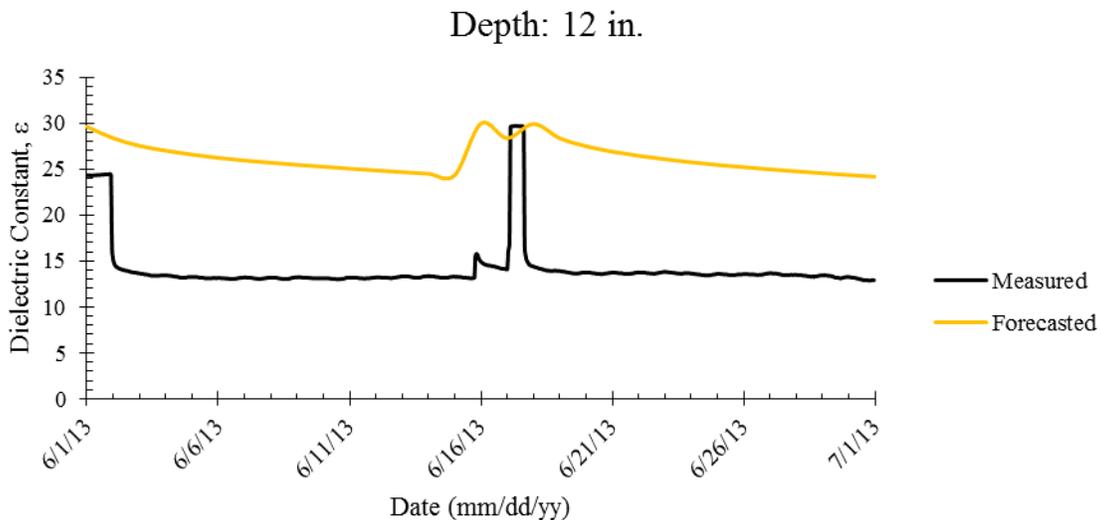
Figure 4.45: Forecasted (Topp et al., 1980) and Measured Dielectric Constants at a Depth of 12 in. at the McBaine, MO Field Site over the Time Period of June 1st, 2013 thru June 30th, 2013

91

Depth: 18 in.
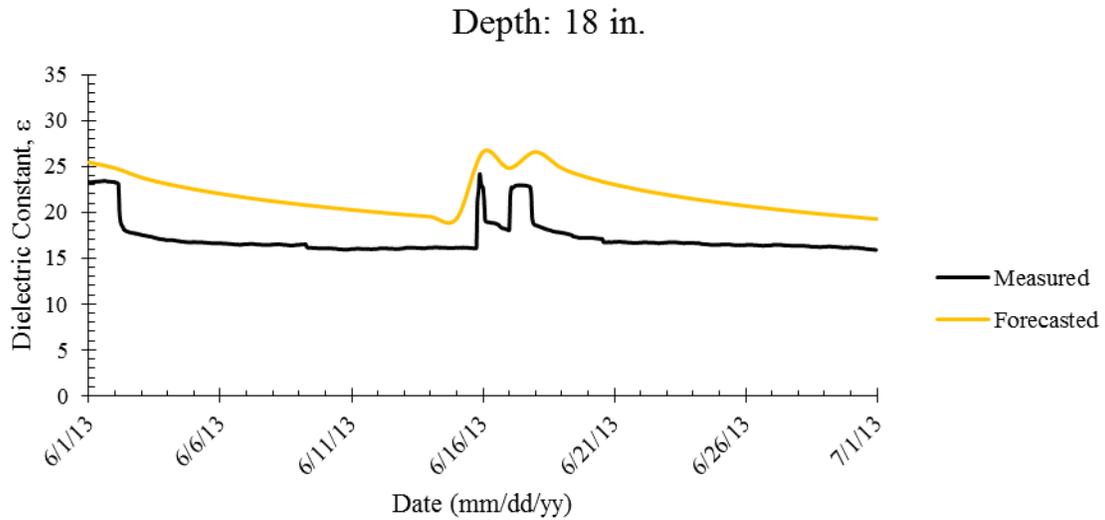
Figure 4.46: Forecasted (Topp et al., 1980) and Measured Dielectric Constants at a Depth of 18 in. at the McBaine, MO Field Site over the Time Period of June 1st, 2013 thru June 30th, 2013

Depth: 24 in.
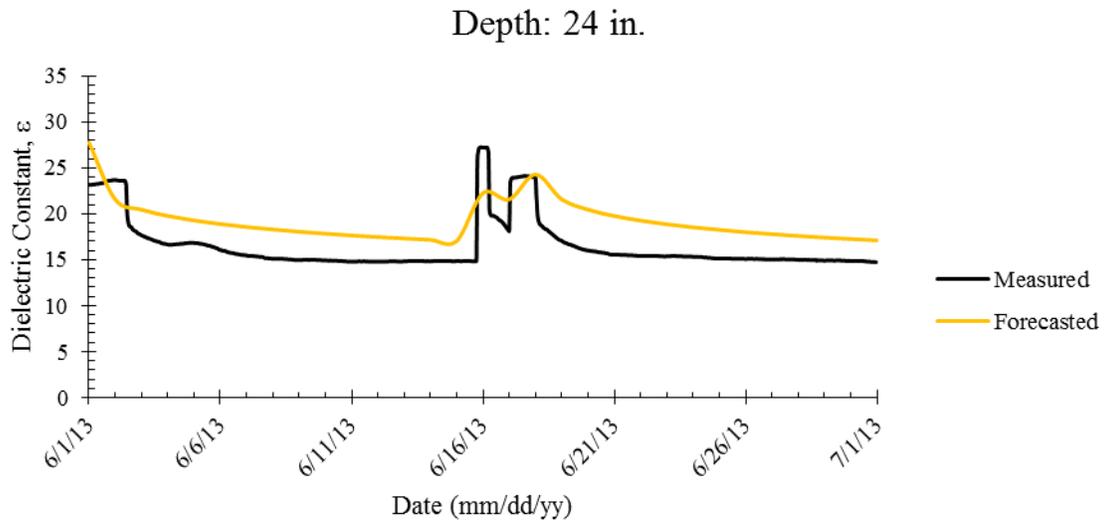
Figure 4.47: Forecasted (Topp et al., 1980) and Measured Dielectric Constants at a Depth of 24 in. at the McBaine, MO Field Site over the Time Period of June 1st, 2013 thru June 30th, 2013

4.4.4   Forecasted vs. Measured Dielectric Constant (Peplinski et al., 1995)

The *in situ* measured dielectric constants from the time period of June 1st, 2013 through June 30th, 2013 are shown in Figure 4.48. Forecasted dielectric constants using the Peplinski et al. (1995) predictive model are shown in Figure 4.49.
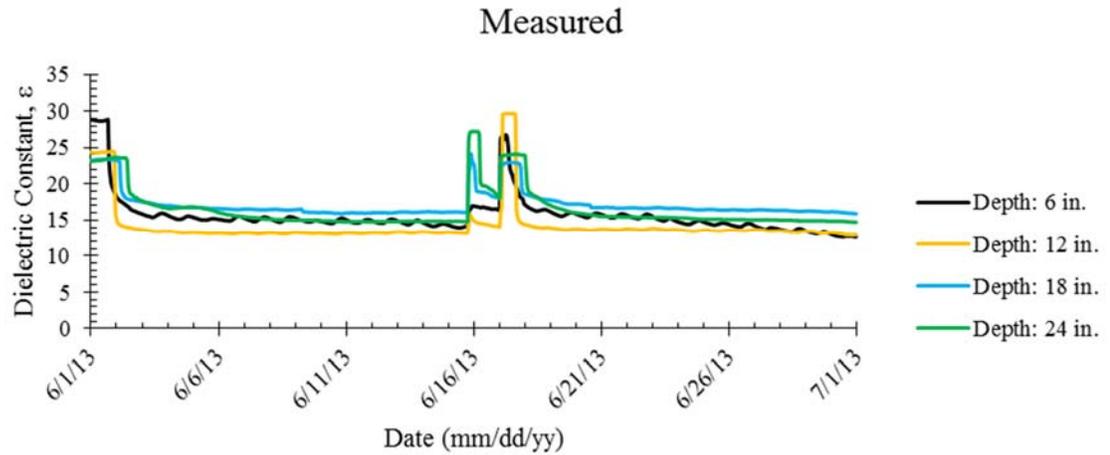
Figure 4.48: Measured Dielectric Constants at the McBaine, MO Field Site over the Time Period of June 1st, 2013 thru June 30th, 2013
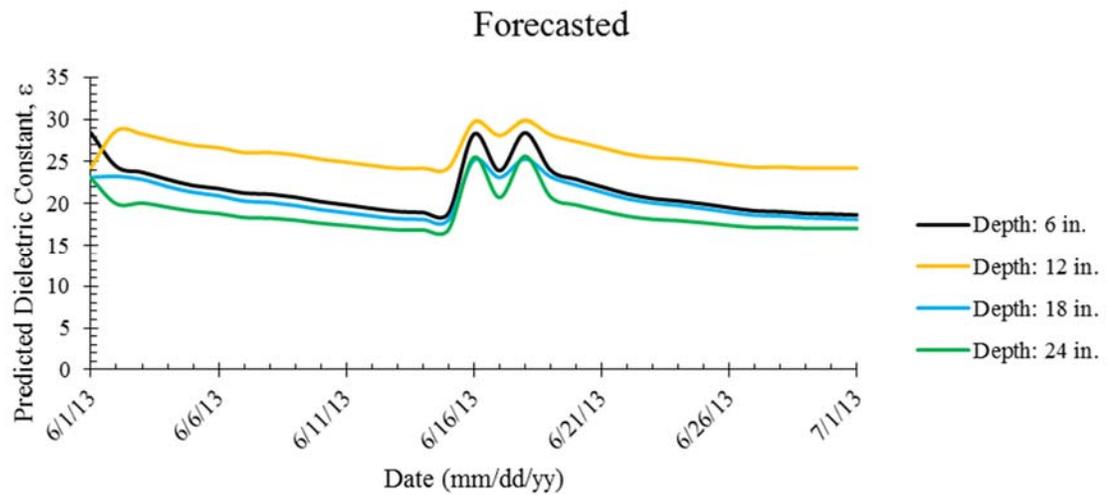
Figure 4.49: Forecasted Dielectric Constants for the McBaine, MO Field Site using the Peplinski et al. (1995) Model from June 1st, 2013 thru June 30th, 2013

Forecasted (Peplinski et al., 1995) and measured dielectric constants at depths of 6 in., 12 in., 18 in., and 24 in. are shown in Figure 4.50, Figure 4.51, Figure 4.52, and Figure 4.53, respectively. McBaine, MO soil's volumetric water contents predicted from WinUnSat-H were used in Peplinski et al.'s (1995) predictive model to forecast the dielectric constant.

93

Depth: 6 in.
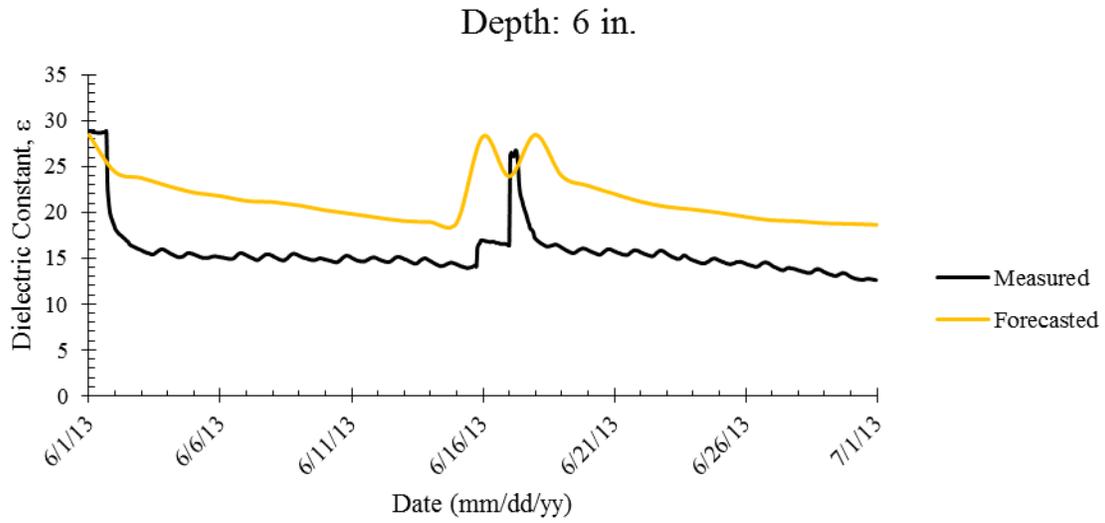
Figure 4.50: Forecasted (Peplinski et al., 1995) and Measured Dielectric Constants at a Depth of 6 in. at the McBaine, MO Field Site over the Time Period of June 1st, 2013 thru June 30th, 2013

Depth: 12 in.
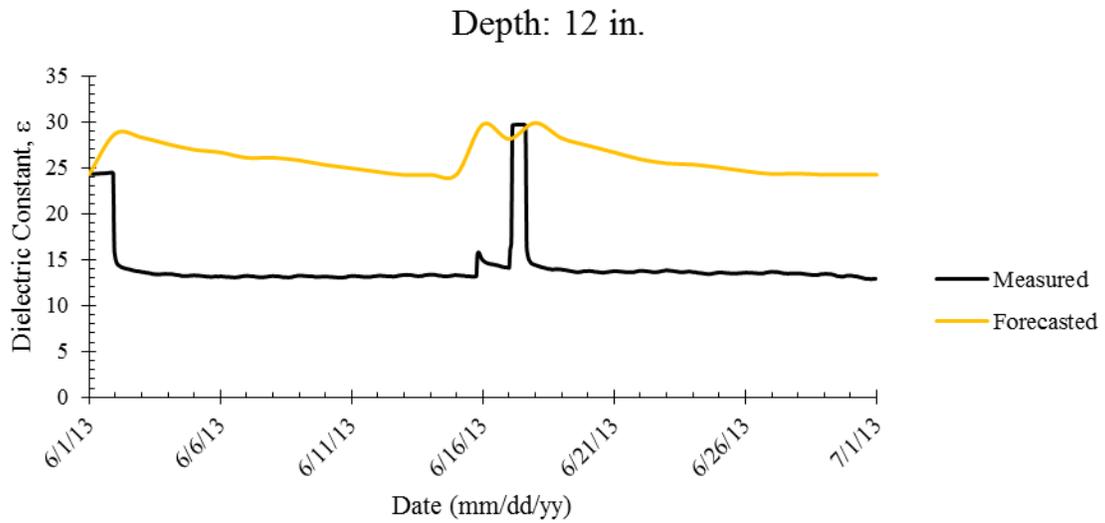
Figure 4.51: Forecasted (Peplinski et al., 1995) and Measured Dielectric Constants at a Depth of 12 in. at the McBaine, MO Field Site over the Time Period of June 1st, 2013 thru June 30th, 2013

Depth: 18 in.
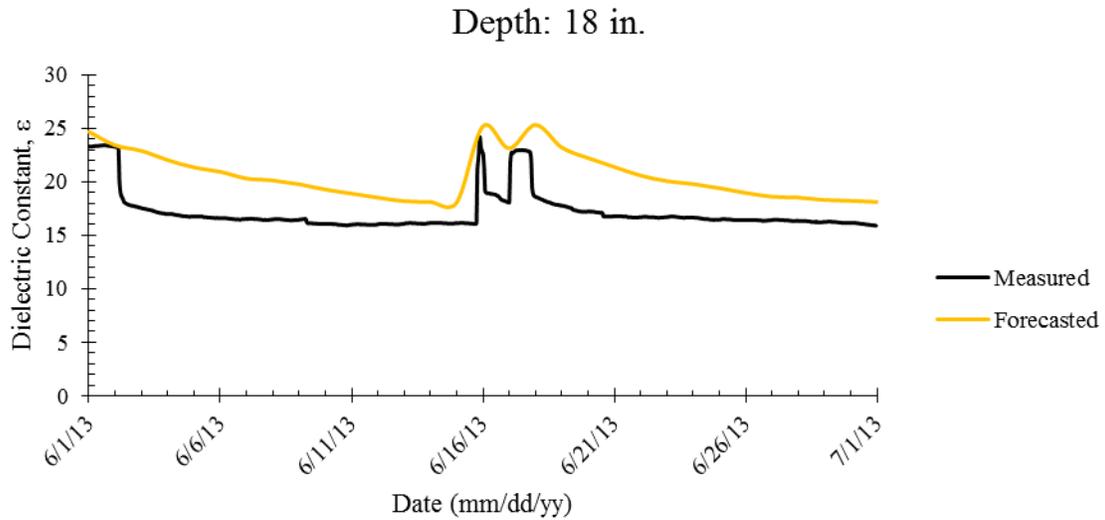
Figure 4.52: Forecasted (Peplinski et al., 1995) and Measured Dielectric Constants at a Depth of 18 in. at the McBaine, MO Field Site over the Time Period of June 1st, 2013 thru June 30th, 2013

Depth: 24 in.
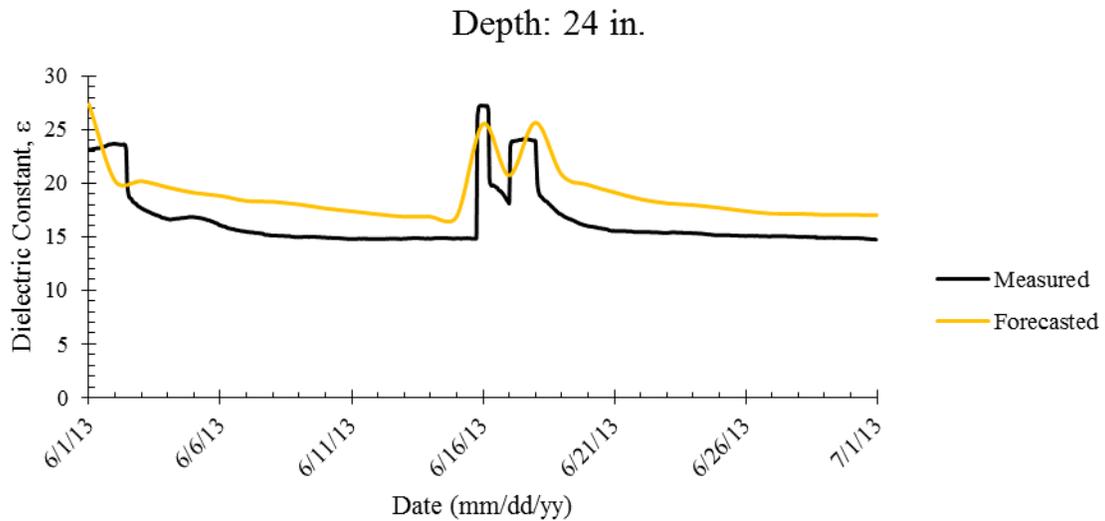
Figure 4.53: Forecasted (Peplinski et al., 1995) and Measured Dielectric Constants at a Depth of 24 in. at the McBaine, MO Field Site over the Time Period of June 1st, 2013 thru June 30th, 2013

4.5 Summary

The results to assess the agreement between forecasted and measured dielectric constants of McBaine, Missouri (MO) soils based on meteorological data and *in situ* measured dielectric constants were presented. Results of measured meteorological and soil conditions at the McBaine,

95

MO field site were presented. Laboratory testing used to characterize the behavior of McBaine, MO soils was also presented. The measured meteorological data and soil properties were used in WinUnSat-H to forecast changes in soil moisture as a function of time. Results of the moisture migration model were used in conjunction with two dielectric constant predictive models to forecast the dielectric constant of McBaine, MO soils. *In situ* measurements of the McBaine, MO dielectric constants were presented together with the forecasted dielectric constants.

5 Discussion

5.1 Introduction

The measured and forecasted dielectric constants of McBaine, Missouri (MO) soils were different. In this chapter, the differences are evaluated in light of measured and observed conditions. The measured meteorological conditions, soil properties, and moisture migration modeling played a role in the creating those differences. The effectiveness of the dielectric constant predictive models are discussed

5.2 Forecasted vs. Measured Dielectric Constants of McBaine, Missouri Soil

Forecasted dielectric constants were determined using dielectric constant predictive models (Topp et al., 1980, Peplinski et al., 1995) in conjunction with the volumetric water contents predicted using WinUnSat-H. Forecasted volumetric water contents were determined from volumetric water contents measured at the McBaine, MO field site using "5TE" soil moisture sensors. Recall, the "5TE" sensors actually measure the soil's dielectric constants and use the Topp et al. (1980) predictive model to determine volumetric water contents. The initial volumetric water contents and subsequent meteorological conditions were input into WinUnSat-H to forecast volumetric water content versus depth over the time period of June 1st, 2013 thru June 30th, 2013. The forecasted volumetric water contents were then substituted into the predictive models (Topp et al., 1980, Peplinski et al., 1995) to forecast dielectric constants for that same period of time.

The measured dielectric constants are shown in Figure 5.1. The forecasted dielectric constants using the Topp et al. (1980) and Peplinski et al. (1995) empirical models are shown in Figure 5.2 and Figure 5.3, respectively. Differences between measured and forecasted dielectric constants using the Topp et al. (1980) and Peplinski et al. (1995) empirical models are shown in Figure 5.4 and Figure 5.5, respectively. Differences between the forecasted and measured dielectric constants were typically less than 10 with the exception of the soil at a depth of 12 in. (highest clay content, 57 percent). The soil at a depth of 12 in. had differences in dielectric constant ranging from 10 to 15. The soil at a depth of 24 in. (highest sand content, 61 percent) showed the best agreement between forecasted and measured dielectric constant; typically a difference less than five. The percentage differences between forecasted and measured dielectric constants at each soil depth, listed in Table 5.1, show that the soil with less than 50 percent sand content had widely varying differences.
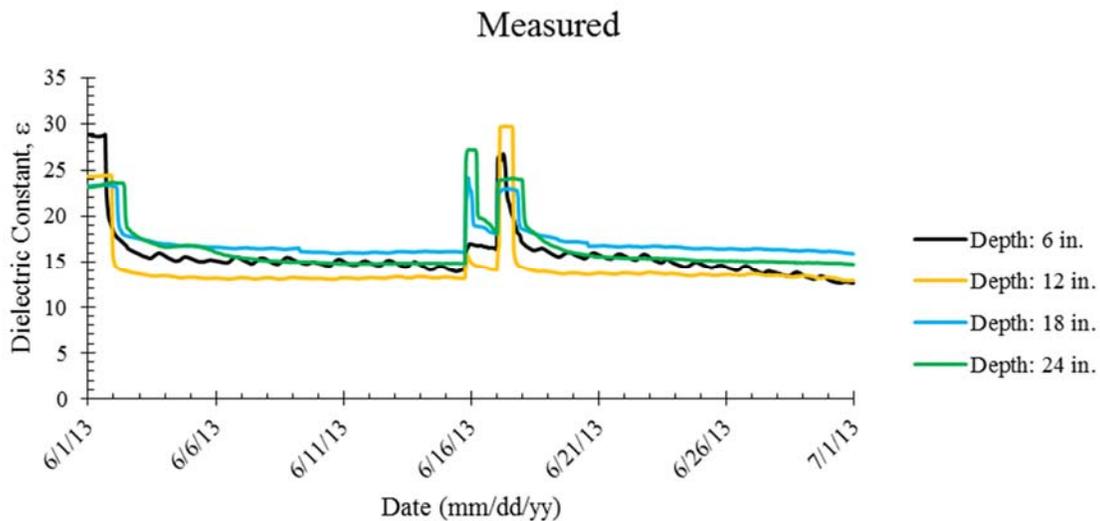
Figure 5.1: Measured Dielectric Constants at the McBaine, MO Field Site over the Time Period of June 1st, 2013 thru June 30th, 2013
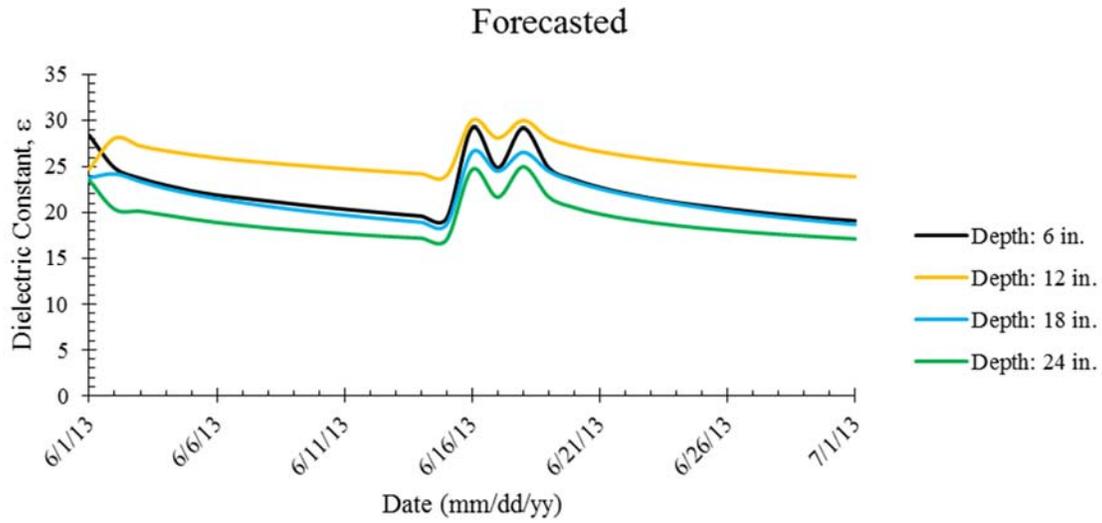
Figure 5.2: Forecasted Dielectric Constants for the McBaine, MO Field Site using the Topp et al. (1980) Model from June 1st, 2013 thru June 30th, 2013
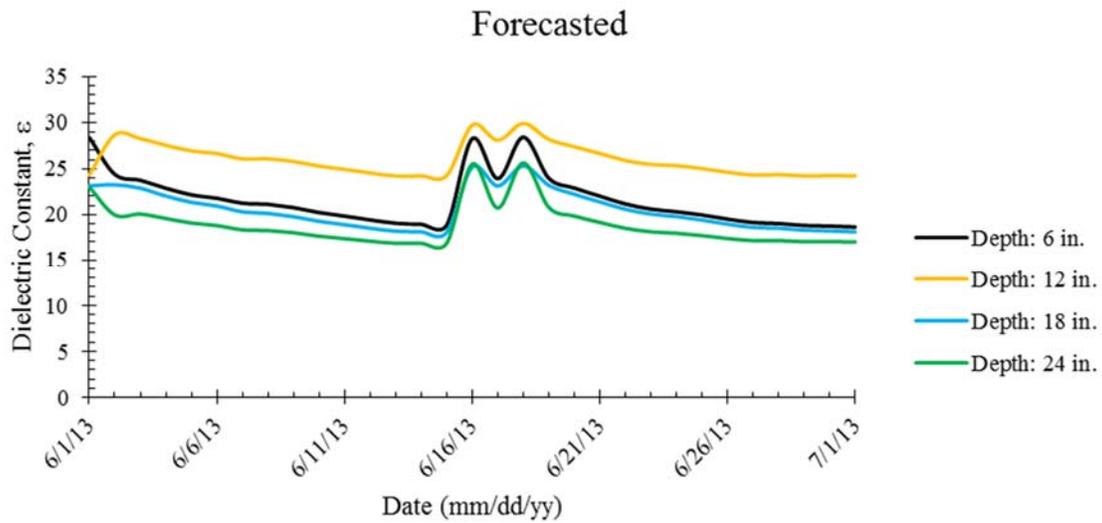
Figure 5.3: Forecasted Dielectric Constants for the McBaine, MO Field Site using the Peplinski et al. (1995) Model from June 1st, 2013 thru June 30th, 2013
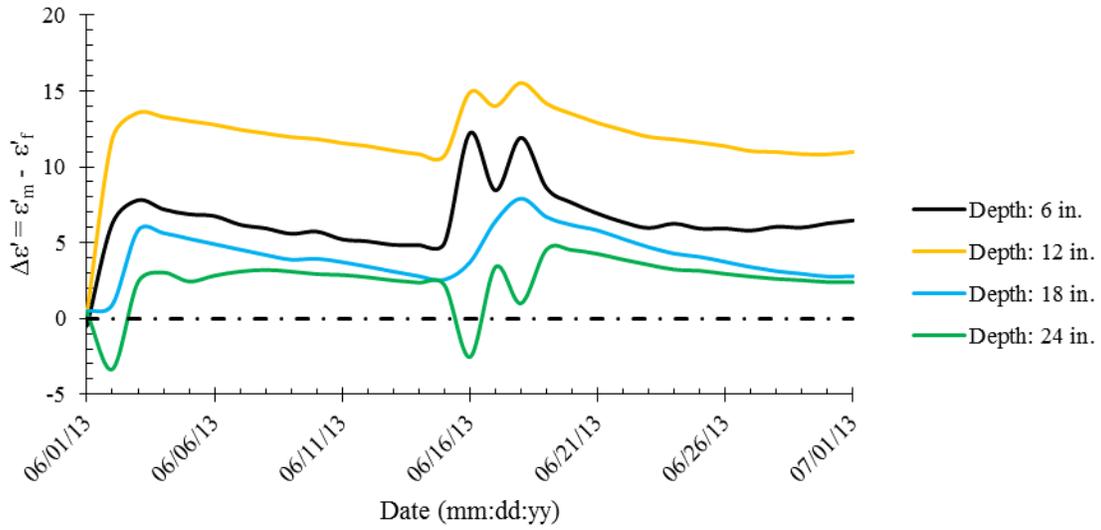
Figure 5.4: Difference between Measured and Forecasted Dielectric Constants (Topp et al., 1980) using Laboratory Measured Saturated Hydraulic Conductivity
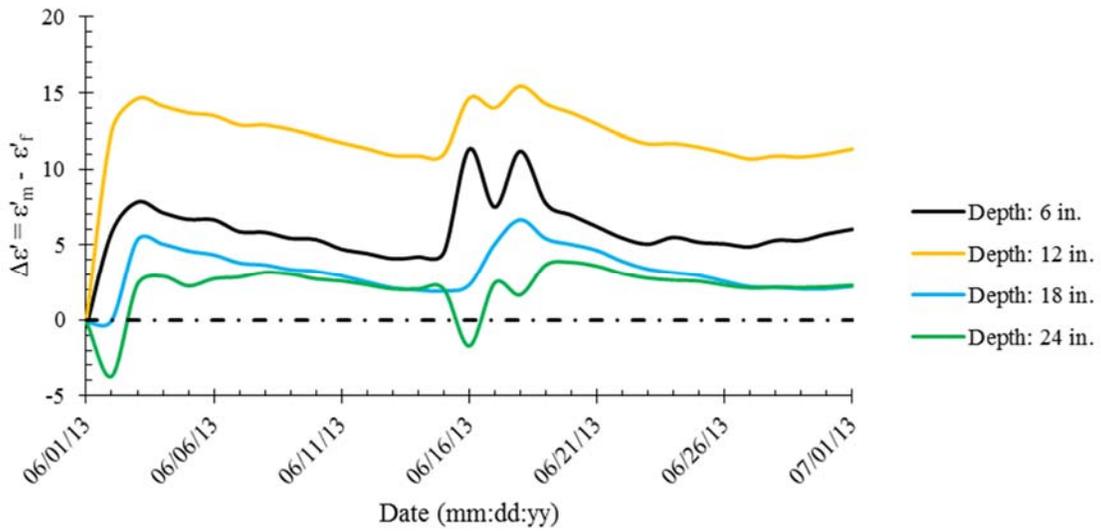
Figure 5.5: Difference between Measured and Forecasted Dielectric Constants (Peplinski et al. (1995)) using Laboratory Measured Saturated Hydraulic Conductivity

100

Forecasted dielectric constants using the Topp et al. (1980) and Peplinski et al. (1995) predictive models were each compared to measured McBaine, MO field site dielectric constants at their respective depths (Figure 5.6, Figure 5.7, Figure 5.8, and Figure 5.9). A one to one linear relationship indicates agreement between the forecasted and measured dielectric constants. Comparisons serve the purpose of showing the effectiveness of the forecasted dielectric constants.

Table 5.1: Percentage Differences between Forecasted (Topp et al., 1980 and Peplinski et al., 1995) and Measured Dielectric Constants of the McBaine, MO Field Site

Depth (in.)	Percentage Differences (%)	Clay-size Percent (%)	Sand-size Percent (%)
6	20 to 80	26	31
12	80 to 100	57	6
18	20 to 80	28	29
24	0 to 20	16	61
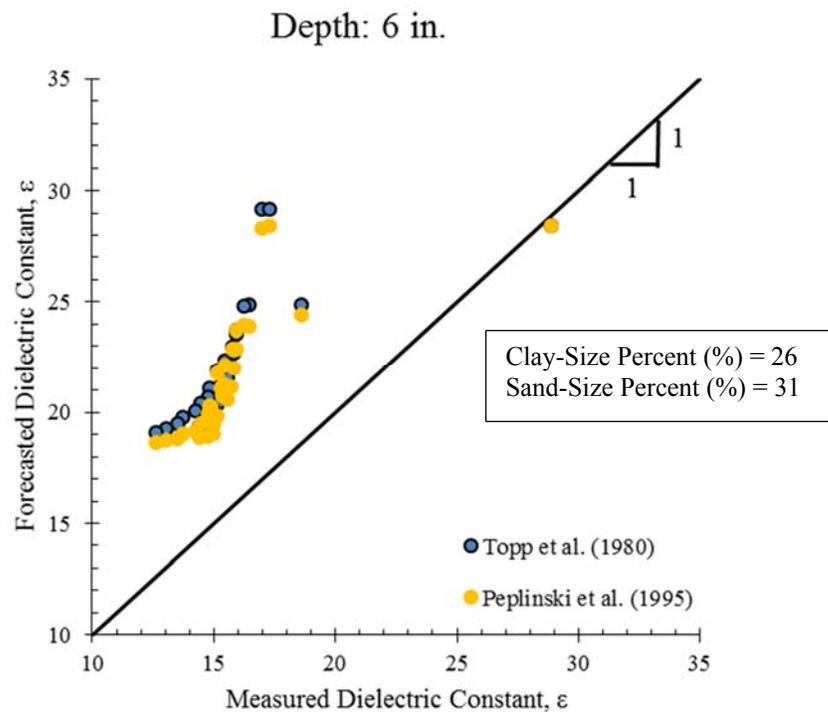
Figure 5.6: Forecasted versus Measured Dielectric Constants of McBaine, MO Field Site at a Depth of 6 in.
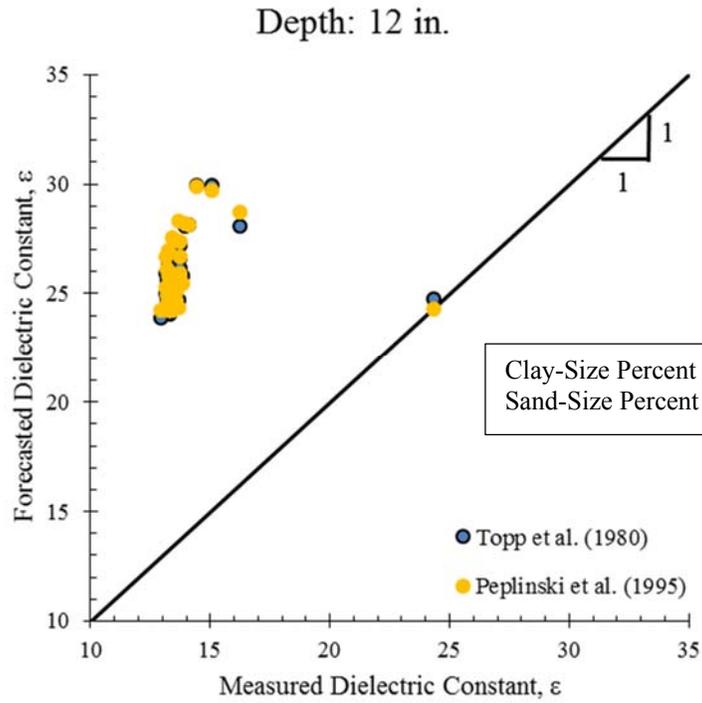
Figure 5.7: Forecasted versus Measured Dielectric Constants of McBaine, MO Field Site at a Depth of 12 in.
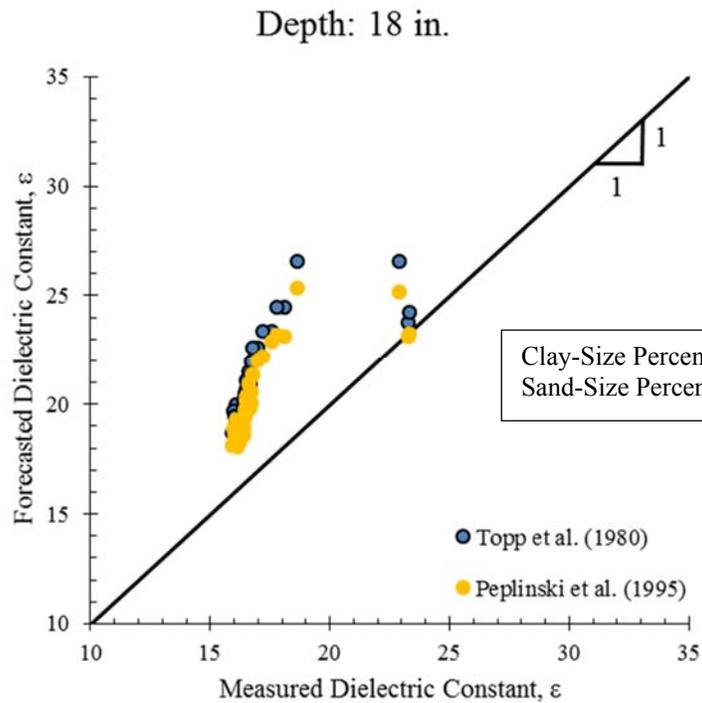
Figure 5.8: Forecasted versus Measured Dielectric Constants of McBaine, MO Field Site at a Depth of 18 in.
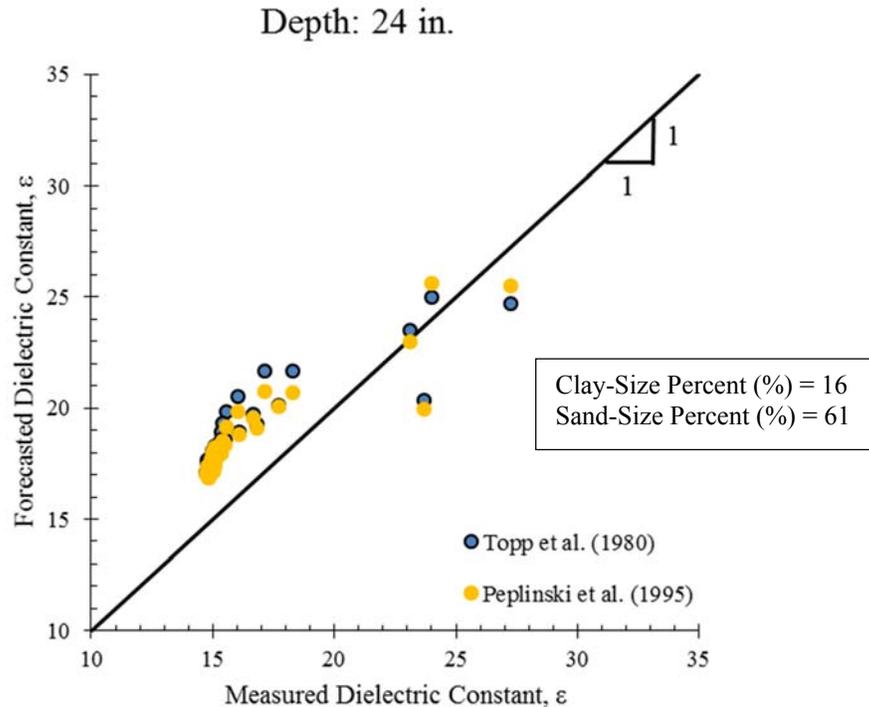
Figure 5.9: Forecasted versus Measured Dielectric Constants of McBaine, MO Field Site at a Depth of 24 in.

The comparisons show forecasted dielectric constants using the Topp et al. (1980) and Peplinski et al. (1995) predictive model were consistently higher than measured dielectric constants. Observations indicated the forecasted dielectric constants using Peplinski et al.'s (1995) predictive model had marginally better agreement with measured dielectric constants than forecasted dielectric constants using Topp et al.'s (1980) model. The observations between the forecasted versus measured dielectric constants comparisons confirmed the soil with the highest amount of clay (12 in. depth) had the poorest agreement and sand (24 in. depth) had the best agreement.

Changes of dielectric constants due to diurnal fluctuations in volumetric water contents were not accounted for in the moisture modeling program (WinUnSat-H). The forecasted dielectric constants do not show diurnal fluctuations because WinUnSat-H produced outputs as daily values. Figure 5.10, Figure 5.11, Figure 5.12, and Figure 5.13 show the forecasted and

measured dielectric constant at their respective depth for June 22nd, 2013. Measured dielectric constants at McBaine, MO do exhibit diurnal fluctuations. The figures show daily fluctuations in measured dielectric constants the magnitude of which decreases as depth increases. Diurnal variations in the measured dielectric constant may have played a small part in the differences between forecasted and measured dielectric constants. In all cases the diurnal change in dielectric constant was less than one (less than five percent).
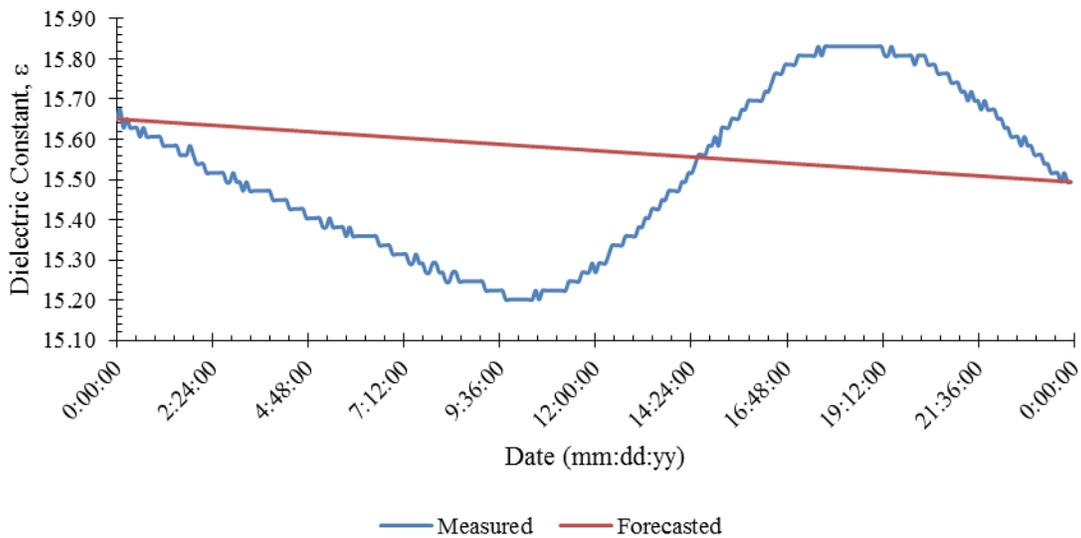
Figure 5.10: Daily Diurnal Fluctuations Seen by Measured Dielectric Constants but not Forecasted Dielectric Constants on June 22nd, 2013 at a depth of 6 in.
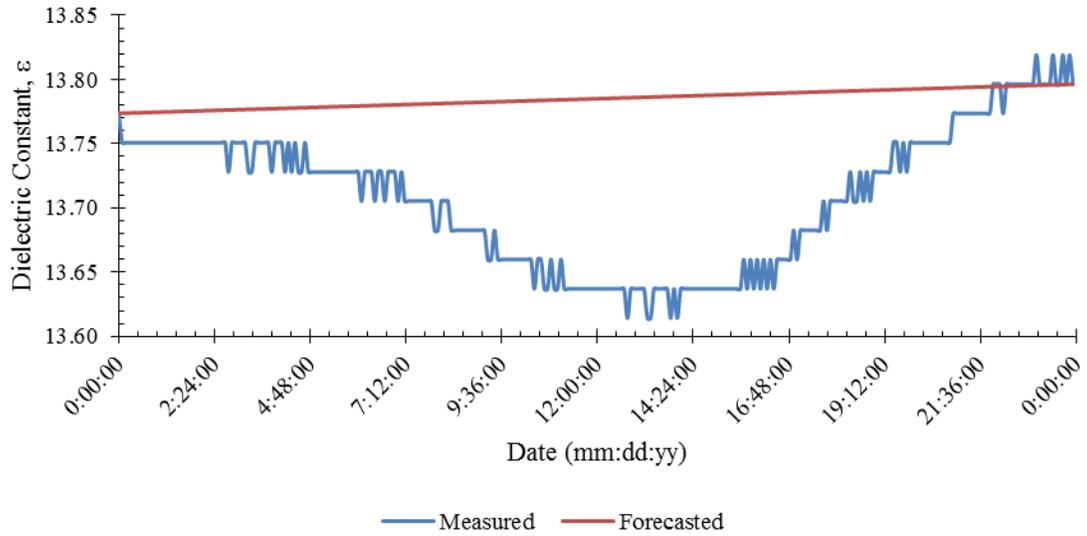
Figure 5.11: Daily Diurnal Fluctuations Seen by Measured Dielectric Constants but not Forecasted Dielectric Constants on June 22nd, 2013 at a depth of 12 in.
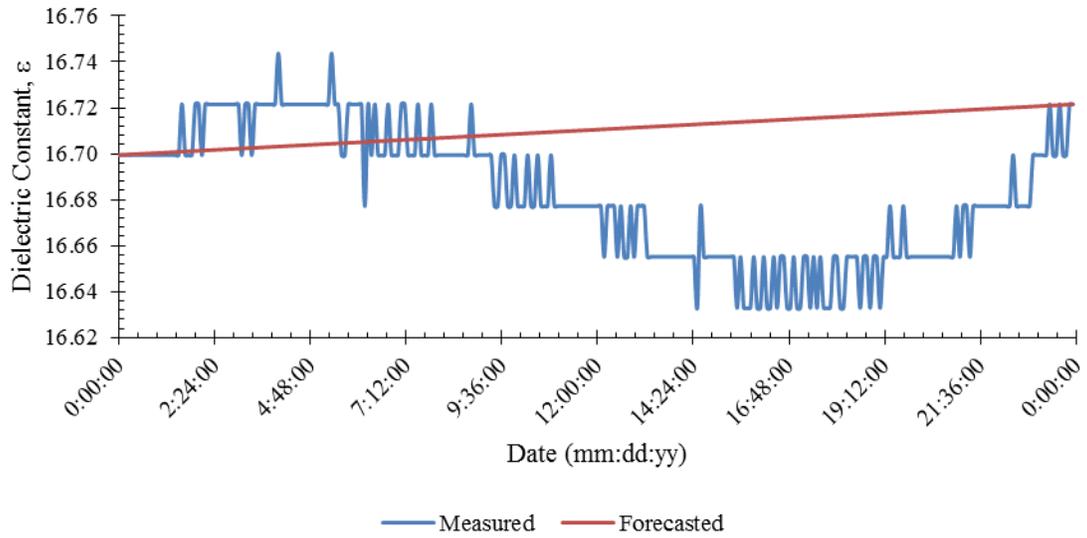
Figure 5.12: Daily Diurnal Fluctuations Seen by Measured Dielectric Constants but not Forecasted Dielectric Constants on June 22nd, 2013 at a depth of 18 in.
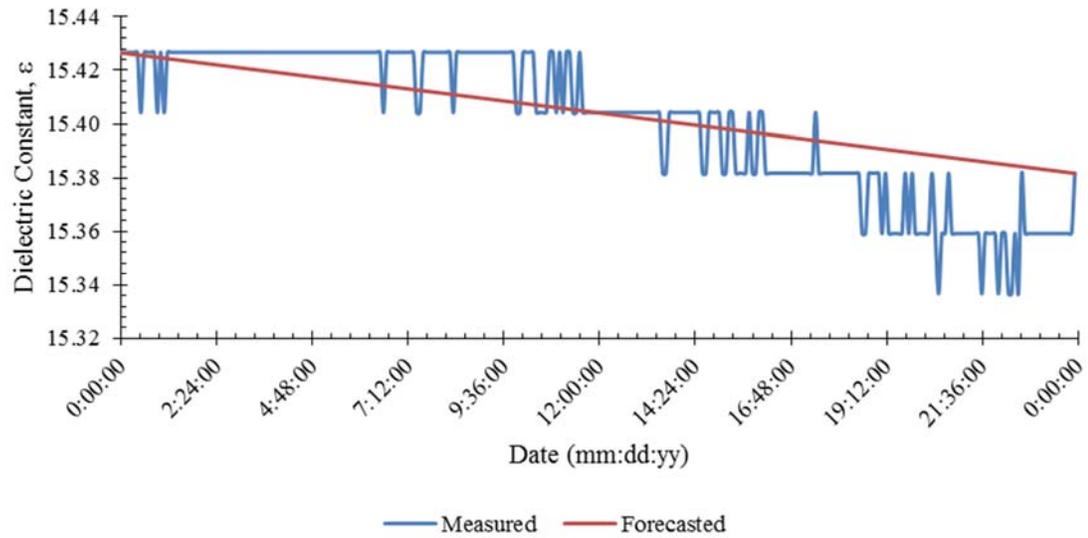
Figure 5.13: Daily Diurnal Fluctuations Seen by Measured Dielectric Constants but not Forecasted Dielectric Constants on June 22nd, 2013 at a depth of 24 in.

Measured dielectric constants at the McBaine, MO field site were recorded at a higher sampling rate (5-minute intervals) compared to the forecasted values (daily) from WinUnSat-H. The smaller time intervals (5-minute) in measured dielectric constants showed more defined values during the precipitation events that occurred on June 15th, 2013 and June 16th, 2013 (Figure 5.14, Figure 5.15, Figure 5.16, Figure 5.17). The forecasted dielectric constants showed a time lag with respect to the measured values; however, forecasted values followed a similar trend of increasing or decreasing as exhibited in the measured values.
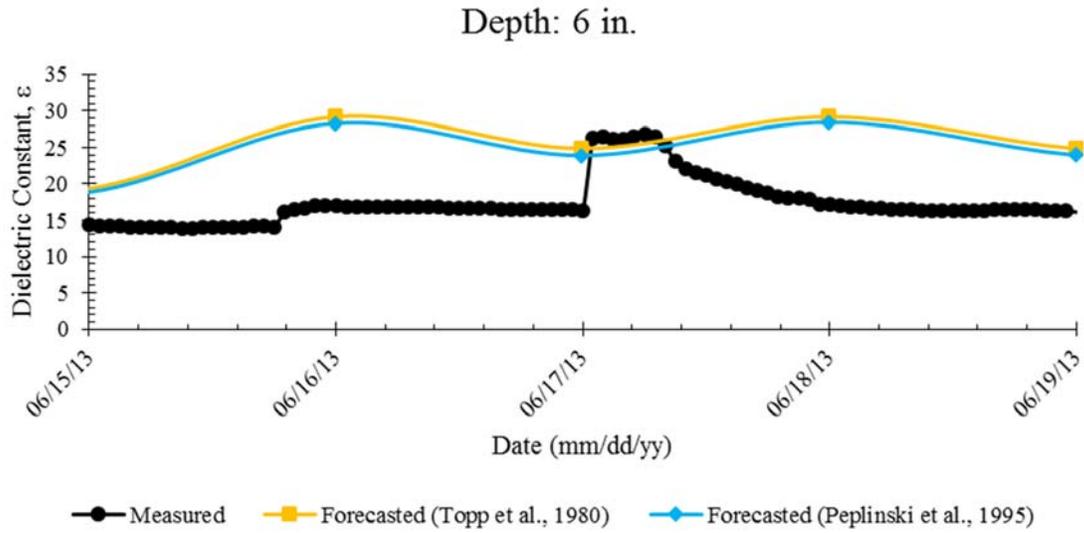
Figure 5.14: Measured (5-minute intervals) and Forecasted (daily) Dielectric Constants of the McBaine, MO Field Site at a Depth of 6 in.
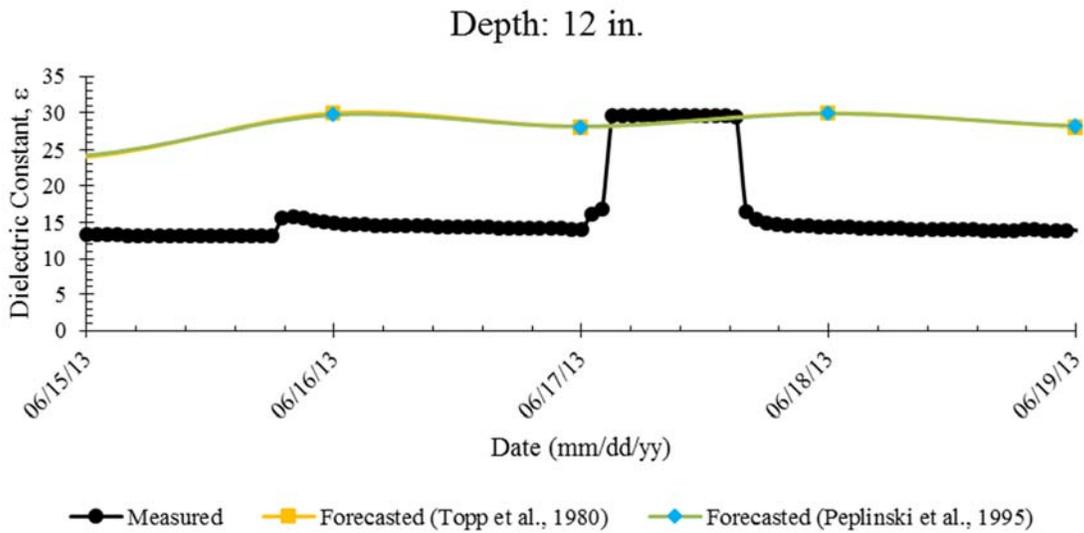
Figure 5.15: Measured (5-minute intervals) and Forecasted (daily) Dielectric Constants of the McBaine, MO Field Site at a Depth of 12 in.

Depth: 18 in.
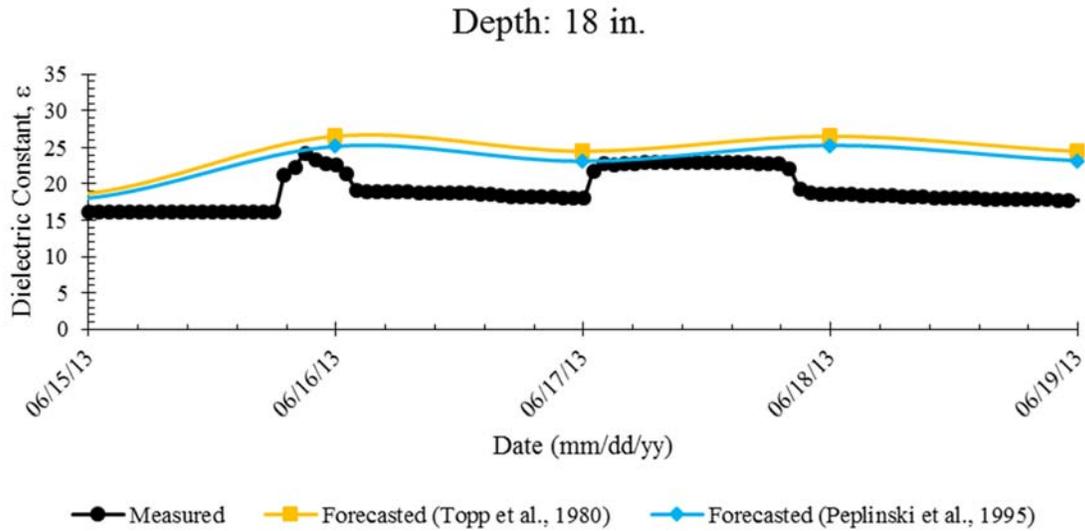
Figure 5.16: Measured (5-minute intervals) and Forecasted (daily) Dielectric Constants of the McBaine, MO Field Site at a Depth of 18 in.

Depth: 24 in.
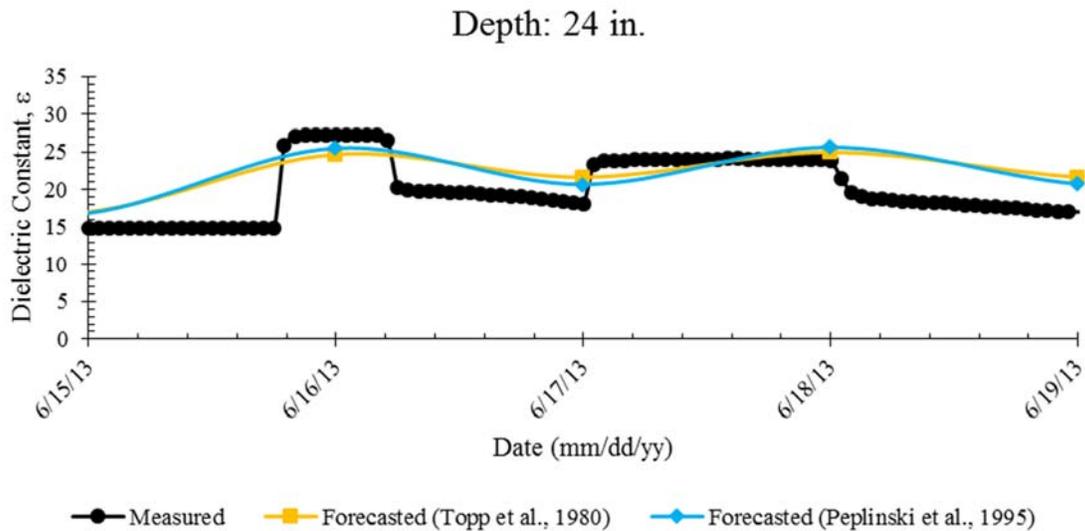
Figure 5.17: Measured (5-minute intervals) and Forecasted (daily) Dielectric Constants of the McBaine, MO Field Site at a Depth of 24 in.

The magnitude of increase by forecasted and measured dielectric constants also differed. The magnitude difference between forecasted and measured dielectric constants were indicated by the precipitation event on June 15th, 2013. The total measured precipitation for June 15th, 2013 was 1.5 in., but 0.94 inches fell during a one-hour time frame, which is considered a high intensity

108

event in this geographical region. High-intensity precipitation events produce greater runoff and less infiltration of water into the soil subsurface (Hillel, 1998). Measured volumetric water contents, and dielectric constants, at a depth of 6 in. showed decreased infiltration due to the high-intensity rainfall over the one-hour time frame on June 15th, 2013 (Table 5.2). Forecasted volumetric water contents, and dielectric constants, at a depth of 6 in. did not exhibit lower infiltration due to the high-intensity rainfall on June 15th, 2013 (Table 5.2). On June 15th, 2013 the measured dielectric constants at a depth of 6 in. increased from 14 to 17 (21 percent increase), while the forecasted dielectric constant at a depth of 6 in. increased from 19 to 28 (47 percent increase) using the Topp et al. (1980) model and 19 to 29 (51 percent increase) using the Peplinski et al. (1995) model (Figure 5.14).

Table 5.2: Increases of Measured and Forecasted Dielectric Constants due to a High-Intensity Precipitation Event at McBaine, MO Field Site

Depth (in.)	Measured ε' (Field)	Forecasted ε' (Topp et al., 1980)	Forecasted ε' (Peplinski et al., 1995)
6	14 to 17 (21 percent)	19 to 28 (50 percent)	19 to 29 (51 percent)
12	13 to 16 (23 percent)	24 to 30 (22 percent)	24 to 30 (25 percent)
18	16 to 24 (50 percent)	18 to 25 (39 percent)	19 to 27 (42 percent)
24	15 to 27 (80 percent)	17 to 26 (51 percent)	17 to 25 (45 percent)

Measured dielectric constants at a depth of 12 in. increased from 13 to 16 (23 percent increase), while the forecasted dielectric constant at a depth of 12 in. increased from 24 to 30 (22 percent increase) using both the Topp et al. (1980) model and Peplinski et al. (1995) model (Figure 5.15). Measured dielectric constants at a depth of 18 in. increased from 16 to 24 (50 percent increase), while the forecasted dielectric constant at a depth of 18 in. increased from 18 to 25 (39 percent increase) using the Topp et al. (1980) model and 19 to 27 (42 percent increase) using the Peplinski et al. (1995) model (Figure 5.16). Measured dielectric constants at a depth of 24 in.

increased from 15 to 27 (50 percent increase), while the forecasted dielectric constant at a depth of 24 in. increased from 17 to 26 (51 percent increase) using the Topp et al. (1980) model and 17 to 25 (45 percent increase) using the Peplinski et al. (1995) model (Figure 5.17).

Following the June 15th, 2013 precipitation event, measured dielectric constants decreased quicker compared to the decrease by forecasted dielectric constants (Table 5.3). After the soil's initial decrease in dielectric constants, shown in the figures, differences between forecasted and measured dielectric constants remained consistent (Table 5.3). The differences between forecasted and measured dielectric constants, following the precipitation event on June 15th, 2013, indicate measured volumetric water contents reached their field capacities quicker than forecasted volumetric water contents as shown in Figure 5.14, Figure 5.15, Figure 5.16, and Figure 5.17. Field capacity is the volumetric water content of soil after gravity drainage ceases (Hillel, 1998).

Table 5.3: Initial Decreases of Measured and Forecasted Dielectric Constants Following a Precipitation Event at McBaine, MO Field Site

| Depth (in.) | *After Precipitation (06/17/2013 to 06/19/2013)* | | |
	Measured ε' (Field)	*Forecasted ε' (Topp et al., 1980)*	*Forecasted ε' (Peplinski et al., 1995)*
6	27 to 16 (40 percent)	29 to 24 (19 percent)	28 to 23 (20 percent)
12	30 to 14 (51 percent)	30 to 27 (9 percent)	30 to 27 (8 percent)
18	23 to 18 (21 percent)	27 to 23 (12 percent)	25 to 22 (12 percent)
24	24 to 18 (25 percent)	25 to 21 (18 percent)	26 to 20 (23 percent)

Table 5.4: Decreases of Measured and Forecasted Dielectric Constants Following Initial Decreases After Precipitation Event at McBaine, MO Field Site

| Depth (in.) | *After Initial Decrease (06/19/2013 to 06/30/2013)* | | |
	Measured ε' (Field)	*Forecasted ε' (Topp et al., 1980)*	*Forecasted ε' (Peplinski et al., 1995)*
6	16 to 13 (21 percent)	24 to 19 (19 percent)	23 to 19 (19 percent)
12	14 to 13 (11 percent)	27 to 24 (12 percent)	27 to 24 (12 percent)
18	18 to 16 (12 percent)	23 to 19 (20 percent)	22 to 18 (19 percent)
24	18 to 15 (18 percent)	21 to 17 (17 percent)	20 to 17 (14 percent)

5.3   McBaine, Missouri Soil Properties and Site Characterization

Visual classification of three test pits (Figure 5.18) excavated to 30 in. below ground surface (BGS) indicated the majority of soil particles were fine-grained (less than 0.05 mm) to a depth of 18 in. BGS. Below a depth of 18 in., the soil's sand content noticeably increased; 61 percent versus less than 30 percent for overlying soil. Test pit excavation was performed by way of a hand shovel and provided the opportunity to see the stiff, blocky structure of the fine-grained soil (Figure 5.19). Grain-size analyses indicated soils at the McBaine, MO field site contained 26 to 56 percent by dry mass of clay-size fraction at depths of 6 in., 12 in., and 18 inches. The sand content increased to 61 percent by dry mass at a depth of 24 in. (Table 5.5).
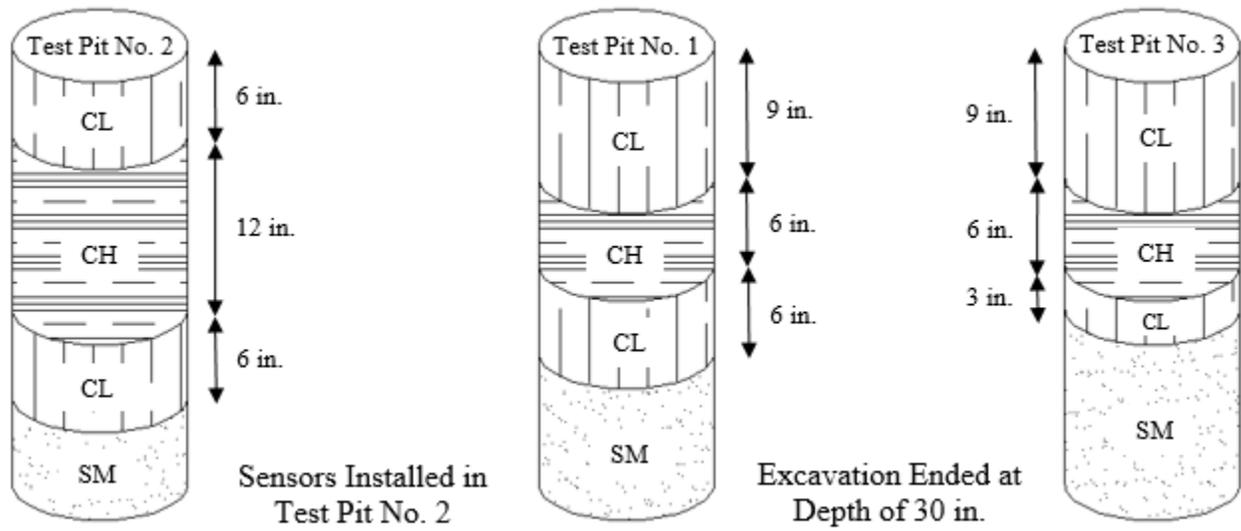
Figure 5.18: Excavated Test Pits at McBaine, MO Field Site and their USCS Soil Classification versus Depth

Figure 5.19: Blocky Soil Structure from Test Pit No. 2 of McBaine, MO Soil at a depth of 6 in.

Table 5.5: Percentage of Grain-Size by Dry Mass for Soil Constituents of McBaine, MO Soils at their Respective Depths

Depth (in.)	Sand (2 mm to 0.05 mm)	Silt (0.05 mm to 2μm)	Clay (≤ 2μm)
6	31	43	26
12	6	37	57
18	29	43	28
24	61	23	16

McBaine, MO field site soils passing a No. 40 Sieve were tested for Atterberg limits, cation exchange capacities (CEC), specific surface area's (SSA's) (Table 5.6). The three aforementioned tests are used to indicate expected clay behavior. With the No. 40 sieve having opening sizes of 0.42 mm, silts and finer sands are allowed to be tested along with clay constituents. Allowing silts and finer sands to be tested along with clays for Atterberg limits, CEC's and SSA's yields different (typically lower) results than if the soil was entirely clay; due to each soil's different characteristics.

The CEC's representative of McBaine, MO soils ranged from 23 meq/100g being the lowest at a depth of 24 in. and 60 meq/100g being the highest at a depth of 6 inches (Table 5.6). The SSA's representative of McBaine, MO soils ranged from 110 m^2/g being the lowest at a depth of 6 in. and 217 m^2/g being the highest at a depth of 12 inches (Table 5.6). Atterberg limits revealed a high plasticity (LL = 73 percent) clay layer at a depth of 12 in. BGS. Atterberg limits indicated clays of lower plasticity (LL = 40 percent) at a depth of 6 in. and 18 in. BGS. The Atterberg limits performed on McBaine, MO soil at a depth of 24 in. BGS revealed low plasticity (LL = 21 percent). The lower plasticity of the soil at a depth of 24 in. correlates with the higher sand content (61 percent by dry mass). The grain-size analyses, Atterberg limits, CEC's, and SSA's performed on the McBaine, MO soils indicated the high presence of clay from the soil surface to a depth of 18

in. BGS (Mitchell and Soga, 1976, Cerato and Lutenegger, 2002). At a depth of 12 in. the measured CEC's and SSA's showed agreement with the Atterberg limits results; their values were consistent with high plasticity clays and soils with higher clay content (Mitchell and Soga, 1976). However, the CEC's at a depth of 6 in. and 18 in. indicate organic content when compared to the other tests performed to the soil at a depth of 12 inches. This is indicated by the slight alkalinity and organic roots present in the Darwin soils. (NRCS, USDA, 2013). The increased sand content at a depth of 24 in. BGS resulted in lower CEC's and SSA's. The hydraulic conductivity of soil at a depth of 6 in., 12 in., and 18 in. were lower than that of the soil at a depth of 24 inches (Table 5.6). Lower hydraulic conductivities are representative of fine-grained soils, and often soils with high clay content.

Table 5.6: Soil Behavior Characterization Results of McBaine, MO Soils at their Respective Depths

Depth (in.)	Atterberg Limits		Cation Exchange Capacity	Specific Surface Area	Saturated Hydraulic Conductivity
-	LL (%)	PI (%)	(meq/100g)	(m^2/g)	(cm/s)
6	42	20	60	174	9.7E-04
12	73	45	57	217	1.5E-04
18	40	20	40	183	2.1E-04
24	21	5	23	129	3.8E-03

The differences between forecasted and measured dielectric constants (Figure 5.4 and Figure 5.5) mainly occur in the McBaine, MO soils with the higher clay content (6 in., 12 in., and 18 in.). The largest difference occurs at a depth of 12 in. where the clay content, SSA, and CEC are highest (Table 5.6). The smallest differences reside at a depth of 24 in. where the clay content is lowest and sand content is highest (Table 5.5).

5.3.1 Geomorphology of McBaine, Missouri Field Site

McBaine, MO, residing in the Missouri River floodplain, has undergone numerous floods throughout its history. Most recently in 1993, the Missouri River levee system in McBaine, MO failed; first due to underseepage, and then by overtopping (Dr. John J. Bowers, personal correspondence, August 15th, 2013). The inflow of river water into the McBaine, MO field site through the breached levee, transported and deposited sand particles on the existing surface. Soil transportation increases with decreasing settling velocities; clay-size fractions have lower settling velocities, followed increasingly by silts and sands (Schwab et al., 1993). Deposition of soil particles increases as particle sizes increase; sand-size fractions deposit first, followed by silts and clays (Schwab et al., 1993). The visual observations and laboratory testing performed for this project show the smaller particle sizes (layers with high clay and silt content) at depths of 6 in., 12 in., and 18 in. were deposited following the deposition of sand particles, which are at a depth of 24 inches. (Dr. R. David Hammer, personal communication, August 23rd, 2013).

5.3.2 Dry Densities

The dry densities calculated from the McBaine, MO soils indicated a wide range of values from soil samples taken at different times (Figure 5.20). The minimum dry densities calculated were around 90 pcf for depths at 6 in., 18 in., and 24 in., BGS, while the soil at a depth of 12 in., BGS had a minimum dry density of around 95 pcf (Table 5.7). The maximum dry densities calculated were around 110 pcf for depths at 6 in., 12 in., and 18 in., BGS, while the soil at a depth of 24 in., BGS had a maximum dry density of around 104 pcf (Table 5.7). The mean average of dry densities calculated was around 100 pcf for each respective depth (Table 5.7). The highest dry densities were determined from the March and June sampling dates (Figure 5.20).
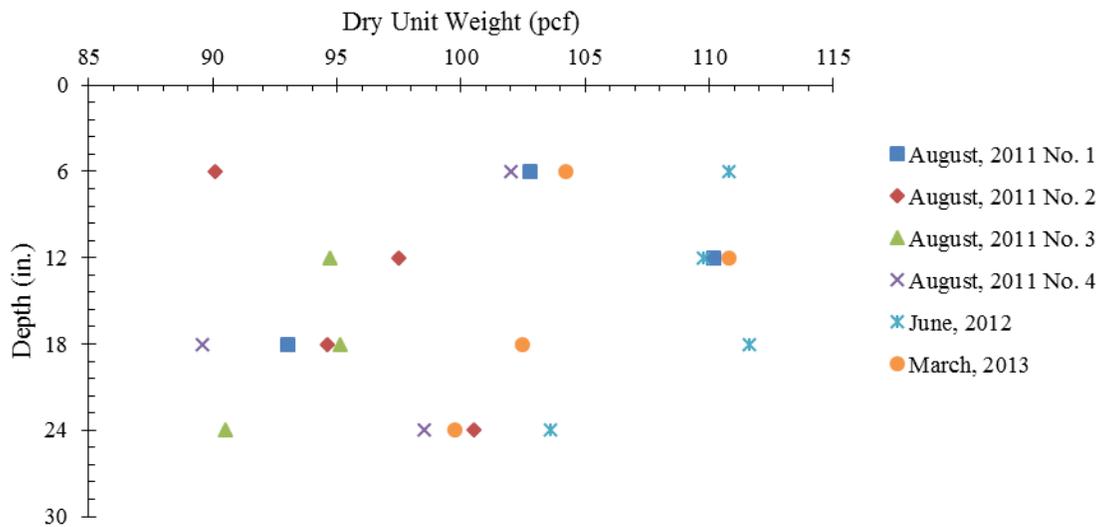
Figure 5.20: Calculated Dry Densities versus Depth of McBaine, MO Soils at Three Different Dates

The soil at a depth of 6 in. has a moderate LL (40 percent) and is subject to large changes in volumetric water content from meteorological events. The moderate LL and meteorological effects are indicative of the variation in dry densities between 90 pcf to 111 pcf at a depth of 6 inches. The soil at a depth of 12 in. has the highest LL (73 percent) and variation in dry densities were between 95 pcf to 111 pcf. The moderate LL at a depth of 18 in. indicates the variation in dry densities between 90 pcf to 112 pcf. The soil at a depth of 24 in. had the lowest LL (21 percent), as well as the lowest variation in dry densities between 91 pcf to 104 pcf. The soil at a depth of 24 in. has the highest sand content (61 percent by dry mass).

Table 5.7: Minimum, Averaged, and Maximum Calculated Densities of McBaine, MO Soils

Depth (in.)	Minimum γ_d (pcf)	Average γ_d (pcf)	Maximum γ_d (pcf)
6	90	102	111
12	95	105	111
18	90	98	112
24	91	99	104

The maximum dry densities were measured on samples extracted from the McBaine, MO field site during June of 2012 during a period of drought; 1.8 in. of precipitation was recorded in the months of May 2012 and June 2012 combined. Drought reduces soil moisture, even to no moisture, which tends to make the soil shrink (especially with high clay content and high PI) and pore sizes to increase. Aside from experimental error and spatial variation, the minimum and other calculated dry densities extracted from the McBaine, MO field site were taken following times of precipitation. The moisture from precipitation tends to fill pore spaces and cause soils (especially with high clay content) to swell. The water and air filling more volume decreases dry densities when compared to soil particles entirely filling an identical volume; due to water (62.4 pcf) and air (0 pcf) having lower unit weights than soil minerals. The soil depths with higher clay content (6 in., 12 in., and 18 in.) exhibited higher maximum dry densities than the soil depth with higher sand content. The soil depths with higher clay content and PI also showed a wider range of dry densities.

The dry densities have an effect on a soil's pore space and it is evident that with the relatively wide range of dry densities, there is a relatively wide range of void ratio and porosities (Table 5.8 and Table 5.9, respectively). Hillel (1982) noted the highly variable pore spaces in clayey soils due to their tendency to shrink, swell, and crack. The wide range of pore space over a given time period increases the uncertainty of forecasted volumetric water contents, and subsequently dielectric constants, for a soil.

Table 5.8: Minimum, Averaged, and Maximum Calculated Void Ratios of McBaine, MO Soils

Depth (in.)	Minimum e (unitless)	Average e (unitless)	Maximum e (unitless)
6	0.52	0.65	0.87
12	0.53	0.62	0.79
18	0.51	0.72	0.88
24	0.60	0.68	0.83

Table 5.9: Minimum, Averaged, and Maximum Calculated Porosities of McBaine, MO Soils

Depth (in.)	Minimum n (unitless)	Average n (unitless)	Maximum n (unitless)
6	0.47	0.39	0.34
12	0.44	0.38	0.35
18	0.47	0.42	0.34
24	0.45	0.41	0.38

5.3.3 Field vs. Laboratory Measured Soil Water Characteristic Curves

The soil water characteristic curves (SWCC) measured at the McBaine, MO field site and in the laboratory provide a general understanding of the soil behavior. Three generalized drying portions of the SWCC representative of a sand, loam and clay are shown in Figure 5.21 (Lu and Likos, 2004). The general shapes of each curve reflects the influence of grain-size, density, and clay content, among others.
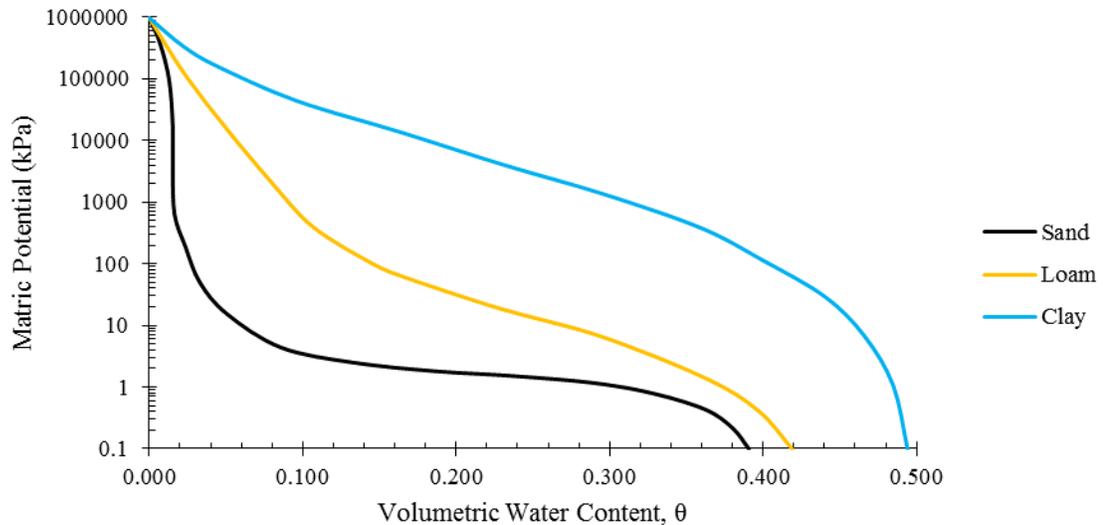
Figure 5.21: Generalized Drying Portion of Soil Water Characteristic Curve for Sand, Loam, and Clay (Lu and Likos, 2004)

The van Genuchten (1980) equation fit to the drying portion of laboratory measured SWCC's for four layers of McBaine, MO soils are shown in Figure 5.22. The van Genuchten (1980) fitting parameters are listed in Table 5.10. Each SWCC indicates the McBaine, MO soils behave similar to the loam and clay type curves shown in Figure 5.21. The McBaine, MO soil at a depth of 24 in. contained 61 percent sand and 16 percent clay-size fraction, but the shape of the van Genuchten (1980) equation fit to the laboratory measured SWCC indicated "clayey" behavior. However, the SWCC on the soil from a depth of 24 in. did show a flatter horizontal characteristic curve in the capillarity regime as determined by McQueen and Miller's (1974) conceptual model shown in Figure 5.23. The McBaine, MO soil at a depth of 12 in. contained 57 percent clay-size fraction, the highest clay content of the four depths measured. The effect of the larger clay-size fraction is illustrated on the normalized (each curve is plotted from the saturated volumetric water content of the soil at a depth of 24 in., 0.400) SWCC by the larger capacity for water adsorption (Figure 5.24). Each SWCC was placed at the volumetric water content determined for the soil at a depth of 24 in. so that each started at an identical saturated volumetric water content. The high

119

capacity for water adsorption is due to clay particles having charged surfaces and higher specific surface areas, indicated by their CEC and SSA's (Lu and Likos, 2004). The McBaine, MO soils at depths of 6 in. and 18 in. have clay contents of 26 percent and 28 percent by grain-size fraction, respectively. The SWCC's measured for depths of 6 in. and 18 in. indicated higher capacity for water adsorption than the SWCC for the soil at a depth of 24 in., but lower than the SWCC for the soil at a depth of 12 inches (Figure 5.24). Adsorption of moisture is higher in the soils with high clay content (depth of 12 in.) due to both the clay's charged particle surfaces and their smaller pore sizes (Hillel, 1998).

Table 5.10: Equation Fitting Parameters for van Genuchten (1980) Equation Fit to Laboratory Measured Drying Portion of Soil Water Characteristic Curve for McBaine, MO Soil at their Respective Depths

Depth (in.)	6	12	18	24
Saturated Water Content (cm^3/cm^3)	0.368	0.352	0.389	0.403
Residual Water Content (cm^3/cm^3)	0.000	0.000	0.000	0.000
"α" (cm^{-1})	0.12	0.10	0.26	0.10
"n" Exponent (unitless)	1.25	1.23	1.23	1.35
"m" Exponent (unitless)	0.20	0.19	0.19	0.26
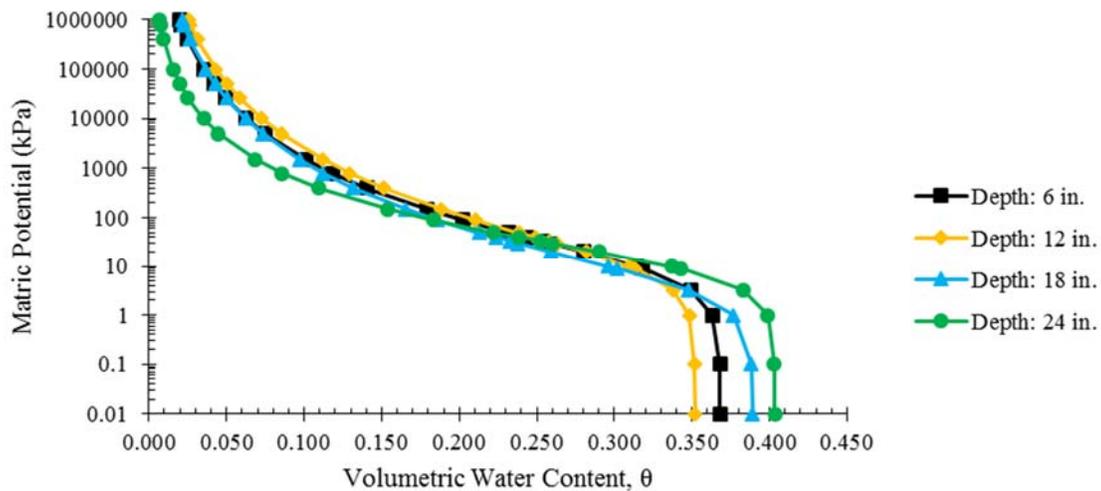
Figure 5.22: van Genuchten (1980) Equation Fit to Laboratory Measured Drying Portion of Soil Water Characteristic Curves for McBaine, MO Soil at their Respective Depths

120
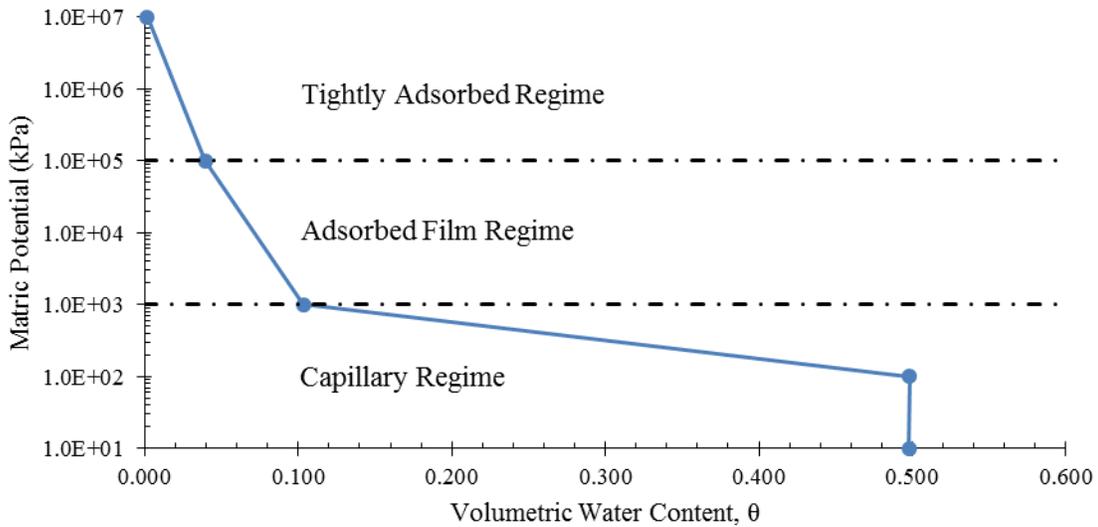
Figure 5.23: Conceptual Behavior of Drying Portion of Soil Water Characteristic Curve as determined by McQueen and Miller (1974)
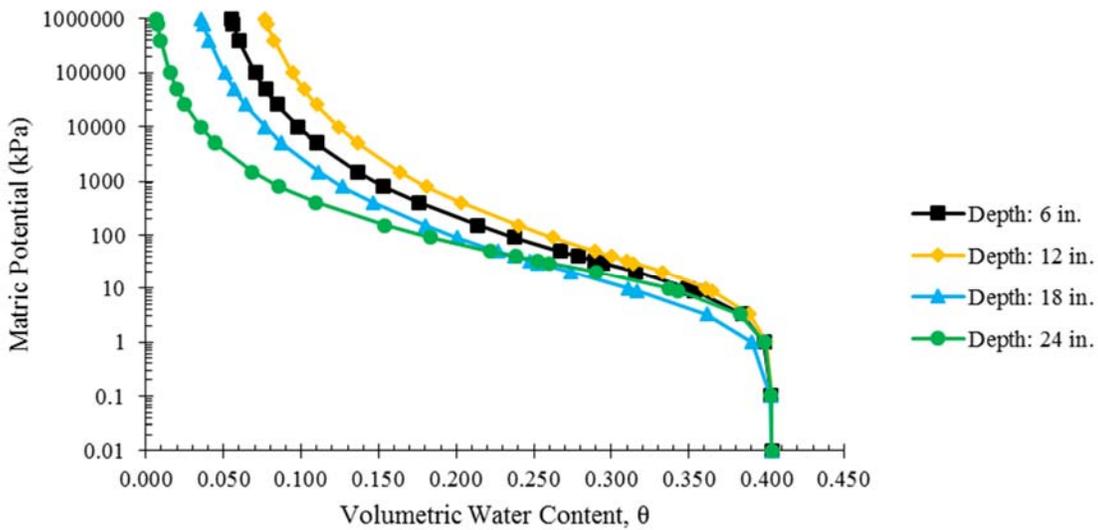
Figure 5.24: Normalized van Genuchten (1980) Equation Fit to Laboratory Measured Drying Portion of Soil Water Characteristic Curves for McBaine, MO Soil at their Respective Depths. The Normalized Curves each Begin at a Volumetric Water Content of 0.40

The laboratory measured SWCC's on remolded McBaine, MO soil presented the opportunity to compare with field measured SWCC's for the same soil. The laboratory SWCC's measured the drying curve for McBaine, MO soils. Field measured SWCC's show the hysteretic behavior when soils are subjected to periods of wetting and drying. The laboratory measured

121

SWCC's are compared with the field measured SWCC's at their respective depths in Figure 5.25, Figure 5.26, Figure 5.27, and Figure 5.28. The comparison of the laboratory and field SWCC's show agreement with each other for the drying portion of the curve. The laboratory measured curves represent an "upper bound" of matric potential for a corresponding volumetric water content. Disagreement between the curves were likely due to the remolded specimens having porosities slightly different from the field conditions. Remolding specimens for the lab preparation tends to destroy the bond between particles exhibited in field specimens, which results in remolded specimens having different porosities than field specimens.
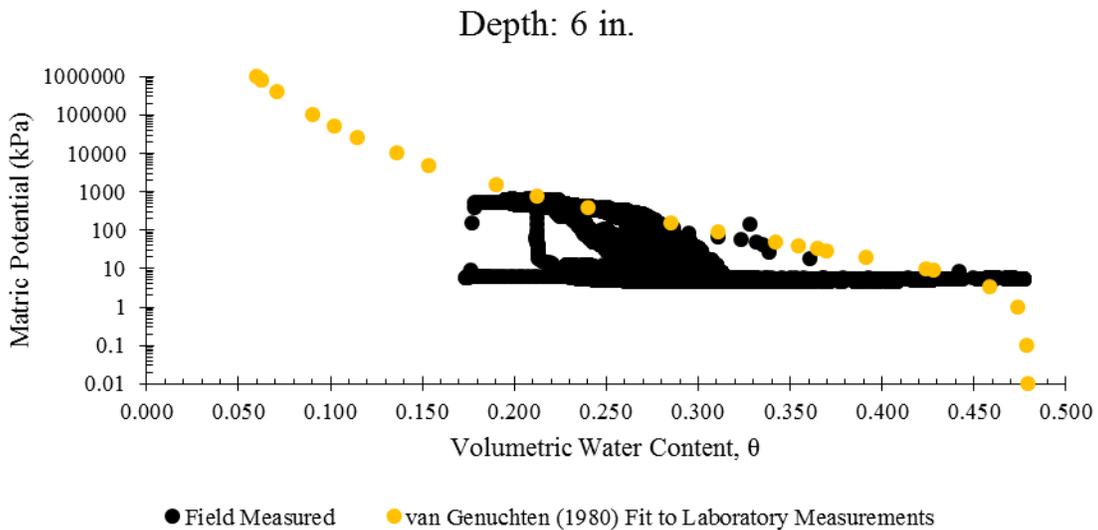
Figure 5.25: Field SWCC and van Genuchten (1980) Fit to Drying Portion of Laboratory Measured SWCC for McBaine, MO Soil at a Depth of 6 in.
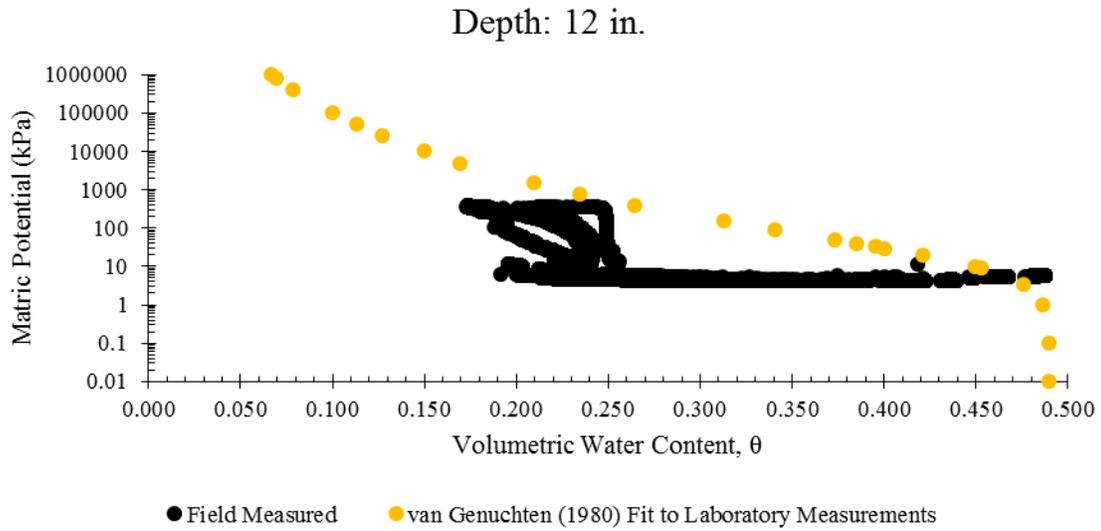
Figure 5.26: Field SWCC and van Genuchten (1980) Fit to Drying Portion of Laboratory Measured SWCC for McBaine, MO Soil at a Depth of 12 in.
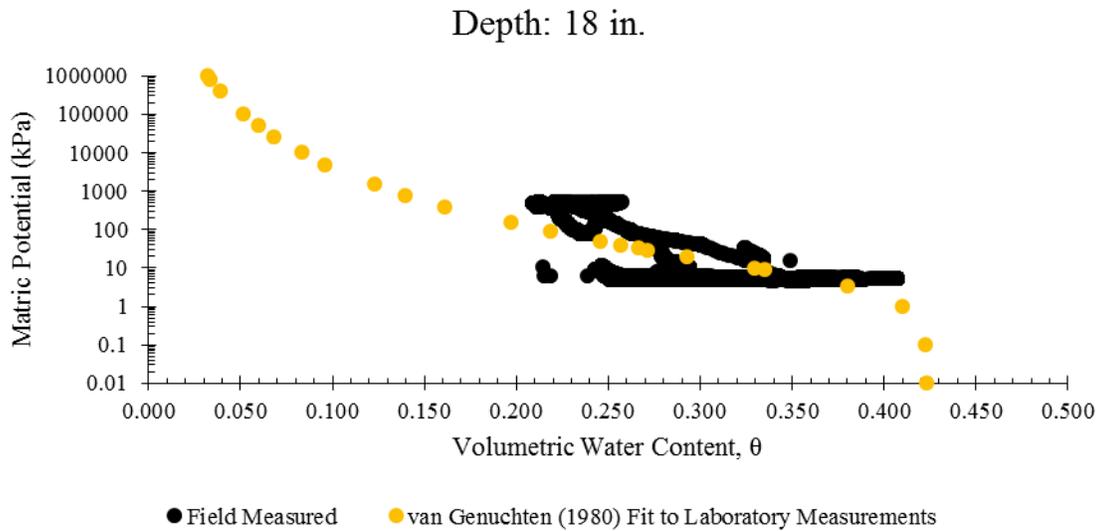
Figure 5.27: Field SWCC and van Genuchten (1980) Fit to Drying Portion of Laboratory Measured SWCC for McBaine, MO Soil at a Depth of 18 in.
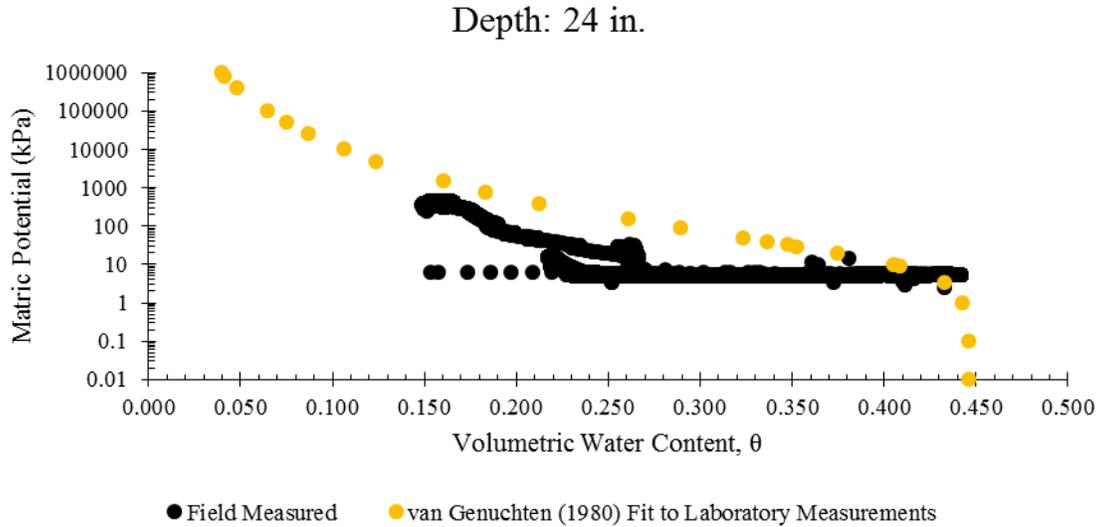
Figure 5.28: Field SWCC and van Genuchten (1980) Fit to Drying Portion of Laboratory Measured SWCC for McBaine, MO Soil at a Depth of 24 in.

5.3.4   Behavior of Soils at McBaine, Missouri Field Site

Laboratory characterization of the McBaine, MO field site soils indicated the potential to shrink-swell over the course of wetting and drying events. Grain-size distributions revealed a large clay-size fraction present in the near surface soils. Indicative of expansive soils were the high Atterberg limits, CEC, and SSA results at depths of 6 in., 12 in., and 18 inches (Table 5.6).

Table 5.11 lists the swell potential for given ranges of plasticity indices (PI's) from Peck et al. (1974). The soil at a depth of 12 in. exhibits high swell potential, while the soil at a depth of 24 in. exhibits low swell potential (Table 5.11). The soil at depths of 6 in. and 18 in. exhibit medium swell potential based on Table 5.11.

The clay mineral kaolinite is non-expansive with typical CEC's ranging from three to 15 meq/100g and SSA's from 10 to 20 m^2/g (Mitchell and Soga, 1976). Smectite is an expansive clay mineral with typical CEC's ranging from 80 to 150 meq/100g and SSA's from 50 to 120 m^2/g (Mitchell and Soga, 1976). However, montmorillonite (highly expansive smectitic clay) can have

SSA's up to 840 m^2/g. Results from the laboratory characterization (Table 5.6) indicate the McBaine, MO soils more closely align with expansive behavior than non-expansive.

Table 5.11: Correlation of Swelling Potential to Plasticity Index from Atterberg Limits (Peck et al., 1974)

Swelling Potential	Plasticity Index (%)	Measured PI (%)
Low	0 to 15	5 at Depth of 24 in.
Medium	10 to 35	20 at Depth of 6 in. and 18 in.
High	35 and Above	45 at Depth of 12 in.

The shrink-swell behavior is consistent with the wide range of calculated dry densities. Dry density determinations were conducted over three different time periods and each time results were different. Two distinct extremes can occur at the McBaine, MO test site; drought and wet, or even flood conditions. The drought conditions and severe precipitation (Figure 5.32) are indicated by the behavior of the nearby pond. The McBaine, MO field site underwent drought during the summer of 2012 (Figure 5.30). A generalized sketch of the hydrologic processes present during drought and wet conditions are shown in Figure 5.31 and Figure 5.33, respectively. The near-surface groundwater table decreases in elevation as the drought conditions are present. Drought presence and the tendency for soils to shrink and swell can form tension cracks and, or slickensides (commonly found in Darwin soils) (Hillel, 1998). Tension cracks were visible throughout the summer months of 2012 as precipitation decreased (Figure 5.34). Tension cracks create preferential flow paths for water to rapidly move downward into the soil as water tends to follow the path of least resistance (Gish and Shirmohammadi, 1991). Over time, given excess moisture, soil expansion from precipitation events will close tension cracks, but the slickensides will remain.

During wet or flood conditions the groundwater table begins to rise back to near-surface levels. The groundwater table rise to near-surface levels was observed by the measured dielectric

constants, and consequently volumetric water contents. Figure 5.29 shows the change in volumetric water content from 11:10 PM to 12:00 AM on March 23rd, 2013, during a rainfall event. The 5TE sensors at a depth of 6 in. first measured a change in dielectric constant and volumetric water content followed by a measured increase by the sensors at a depth of 24 in., 18 in., and 12 in., respectively in that order. The increase in dielectric constant and volumetric water content in the soil at a depth of 24 in. and 18 in. before the soil at a depth of 12 in. increased indicates the complexity of the site.
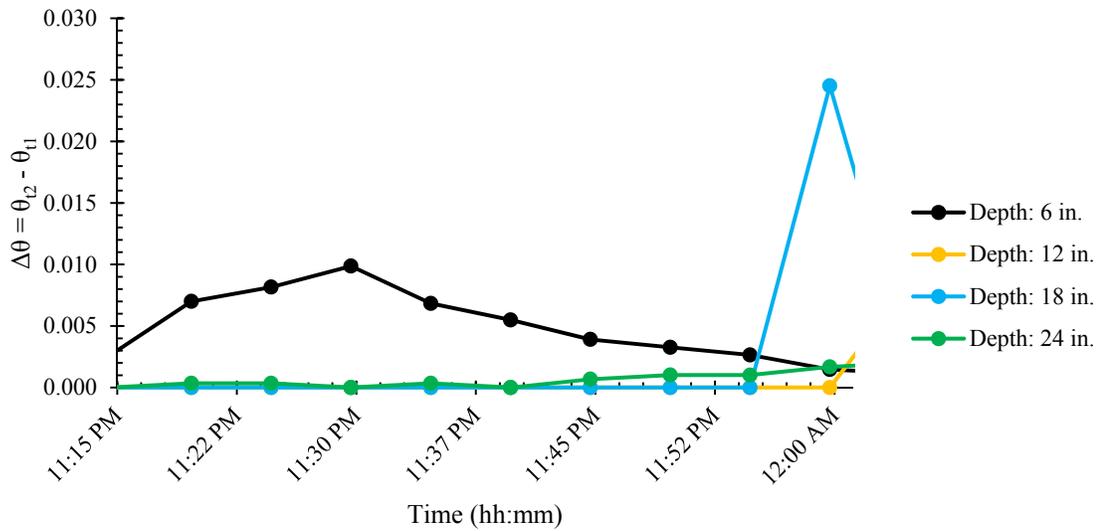
Figure 5.29: Change in Volumetric Water Content over 5 Minute Intervals from 11:15 PM to 12:00 AM due to Rainfall event on March 23rd, 2013

Figure 5.30: Drought Conditions at McBaine, MO Field Site for Receiving only 1.2 in. of Precipitation from June 16th, 2012 thru August 30th, 2012
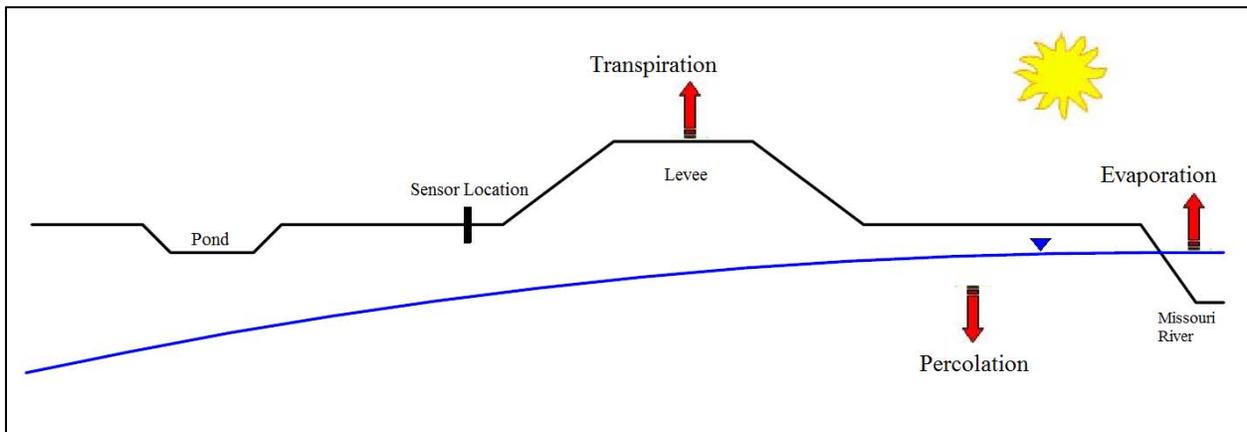
Figure 5.31: Generalized Hydrologic Processes during Drought Conditions

Figure 5.32: Flood Conditions at McBaine, MO Field Site from 8.5 in. of Precipitation from May 19th, 2013 thru May 31st, 2013
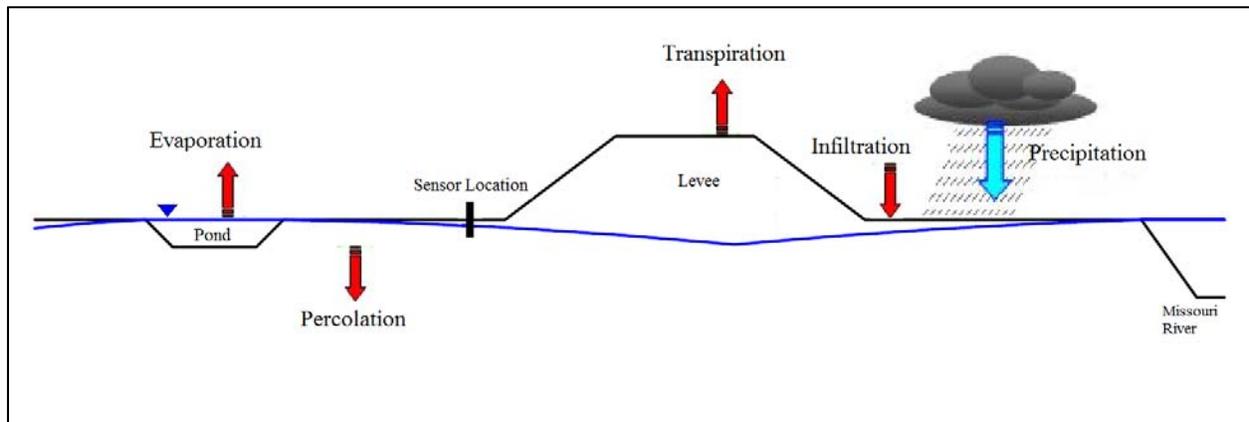
Figure 5.33: Generalized Hydrologic Processes during Wet Conditions

Figure 5.34: Tension Crack near Installed Soil Moisture Sensors at McBaine, MO Field Site

Macropores can also be formed by root growth which create additional pore space and by dry clay soils consisting of large natural aggregates (peds) (Hoogmoed and Bouma, 1980). The blocky soil structure at McBaine, MO is indicative of large soil peds (Figure 5.19). Preferential flow paths created by macropores have the tendency to wet quicker during precipitation events than a soil without. The same can be said once the precipitation event ceases, a soil with macropores will dry quicker than a soil without.

An artificial wetting event using a ring infiltrometer was performed at the McBaine, MO field site on July 9th, 2013 (Figure 5.35). The artificial wetting event investigated the presence of macropores exhibited an extremely quick wetting period, which indicates the presence of macropores. Measured volumetric water content from May 29th, 2013 thru June 3rd, 2013 also indicated the presence of macropores as the soil wetted and dried quickly (Figure 5.36). The "square wave" formed from the quick wetting and drying of the soil was not anticipated as hydraulic conductivity values indicated slow drainage rates. Personal correspondence was made

with Decagon Devices (Decagon, 2012). It was indicated the "square waves" were possibly caused due to flow between the soil peds and entering the space between the "5TE" soil moisture sensor and the soil (Mr. Leo Rivera, personal communication, May 22nd, 2013).
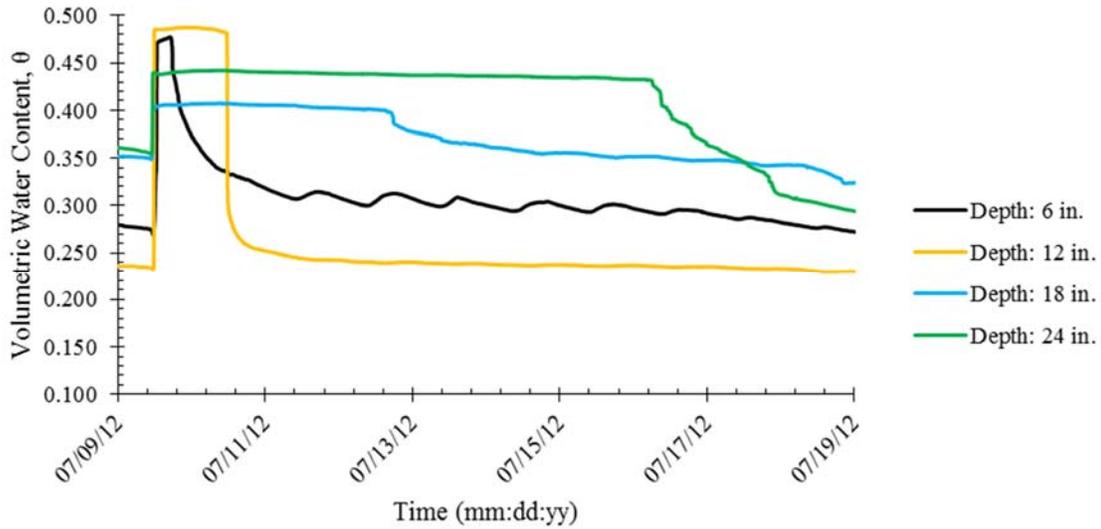
Figure 5.35: Wetting and Drying "Square Wave" from Measured Volumetric Water Content at McBaine, MO Field Site on July 9th, 2013
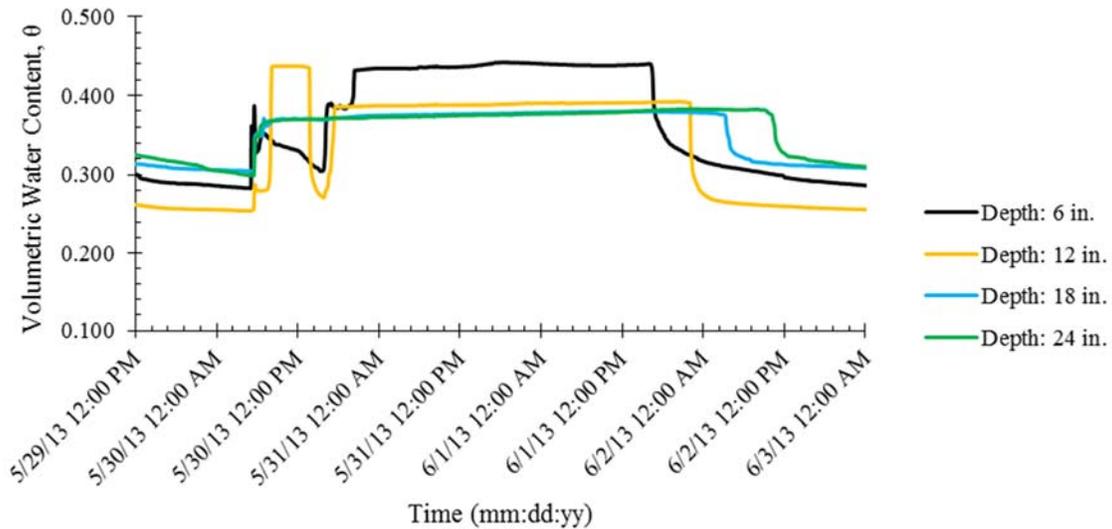
Figure 5.36: Wetting and Drying "Square Wave" from Measured Volumetric Water Contents at McBaine, MO Field Site on May 29th, 2013

130

5.4 Influences Unaccounted for in WinUnSat-H

WinUnSat-H is similar to its earlier version UnSat-H in the sense that it provides accurate approximations of one-dimensional (1-D) vertical water flow in the unsaturated zone (Baca and Magnuson, 1990, Fayer, 2000). However, Fayer (2000) indicated the one-dimensionality was a limitation because water flow is not necessarily vertical. The McBaine, MO field site presented characteristics that indicate flow is not solely vertical. The characteristics creating non-vertical flow were not accounted for in the moisture migration model (WinUnSat-H), and may have affected forecasted volumetric water contents, and subsequently dielectric constants. The one-dimensional capabilities of Win-UnSat-H and the field characteristics not modeled by the computer program were a factor in creating differences between forecasted and measured volumetric water contents, and subsequently dielectric constants, of the McBaine, MO soil.

5.4.1 McBaine, Missouri Field Site Characteristics

Water flowing through inclined soils of differing properties follow refraction laws (Figure 5.38) (Miyazaki, 2005). The McBaine, MO field site is positioned to the east of the Missouri River levee system in an agricultural field (Figure 5.37). From the levee toe outward orthogonally to the east 25 feet the elevation dropped 2.0 feet (8.0 %). The elevation gradient created a slope at the McBaine, MO field site. Visual classification of test pits at McBaine, MO indicated differentiating layers sloped similarly to the ground surface (Figure 5.18). The changing hydraulic conductivity through the layers at the McBaine, MO field site indicate water flow is not entirely vertical. Water flowing through the soil at a depth of 6 in. (k_{sat} of 9.7E-04 cm/s) to the soil at a depth of 12 in. (k_{sat} of 1.5E-04 cm/s) will refract with a resultant of horizontal and vertical as indicated in Figure 5.38; due to the soil at a depth of 12 in. having a lower hydraulic conductivity than the soil at a depth of 6 inches. Water flowing vertically into and through a soil space can enter from above and exit

below. The additional pathways due to changing soil properties create multiple opportunities for flow into and out of the soil space. The additional flow paths for water to travel through a soil space allows the volumetric water content, and subsequently dielectric constant to change more quickly over space and time. Forecasted volumetric water contents did not exhibit the quicker wetting and drying due to the version of WinUnSat-H used in the work herein not having the capabilities to model lateral flow (it is a 1-D model). The rapid increase and decrease of volumetric water contents were measured at the McBaine, MO site and indicated the sloping characteristics at the field site may have had an effect on the differences between forecasted and measured dielectric constants.

Figure 5.37: Instrumentation of McBaine, MO Field Site 25 ft. off East Toe of Missouri River Levee System
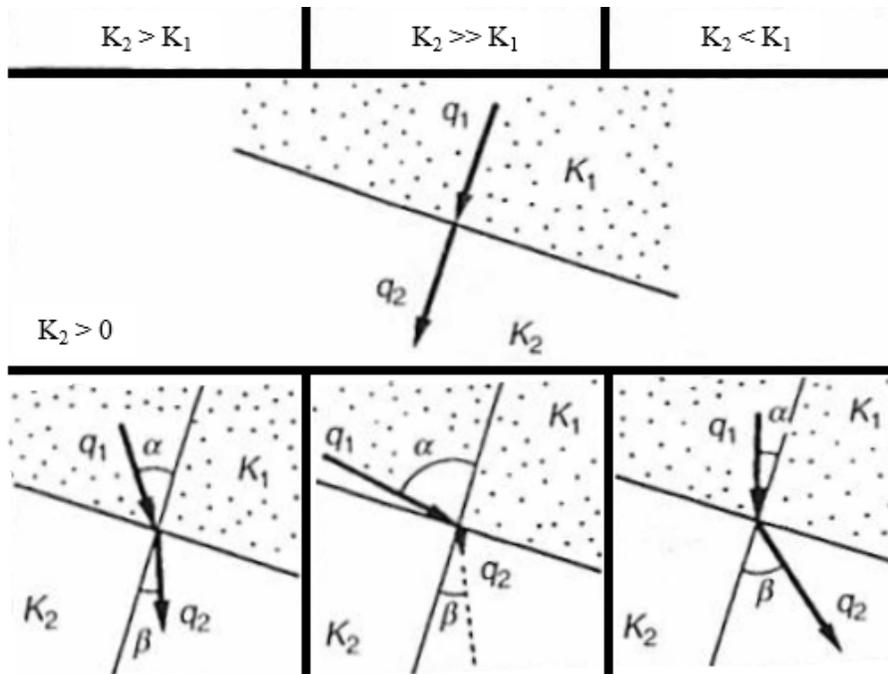
Figure 5.38: Generalized Refraction of Flow through Layered Soil in Slopes (Miyazaki, 2005)

where,

K_1 = hydraulic conductivity of upper soil layer,

K_2 = hydraulic conductivity of lower soil layer,

q_1 = flux through upper soil layer,

q_2 = flux through lower soil layer,

α = angle of incidence flux through upper layer comes in contact with lower layer,

β = refracted angle flux through lower layer follows

5.4.2 Secondary Porosity from Macropores

The tendency of McBaine, MO soils to undergo shrink-swell and the blocky structure presented two difficulties in forecasting the volumetric water contents, and consequently the dielectric constant. Macropore fractures created by the expansion and contraction of soils at the McBaine, MO field site created preferential flow paths for water. The preferential paths created relatively quick entries and exits for water as evident by the rapid change in measured volumetric

water contents and dielectric constants during precipitation and drying periods (Figure 5.35 and Figure 5.36). WinUnSat-H does not have a feature to account for the additional (secondary) porosity. The forecasted dielectric constants shown in Figure 5.2 and Figure 5.3 show slower rates of change following precipitation events than measured dielectric constants (Figure 5.35 and Figure 5.36). The slower rate of change by forecasted values indicate the macropores in the field accelerate the rate of change in volumetric water content, and subsequently dielectric constant, during precipitation and drying events. This effect is not accounted for in WinUnSat-H

5.4.3 Fluctuating Near-Surface Groundwater Table

The presence of a fluctuating near-surface groundwater table creates difficulties in forecasting volumetric water contents with WinUnSat-H due to the upward increase in volumetric water content. With WinUnSat-H being a one-dimensional downward vertical flow program, the upward increase in volumetric water content is ignored by the program and will create differences between forecasted and measured volumetric water contents and consequently dielectric constants.

5.5 Dielectric Constant Predictive Models

The dielectric constant models (Topp et al., 1980, Peplinski et al., 1995) introduced in Chapter 2, were empirically fit to their data sets, which included a wide range of soil types. A wide range of soils were tested, which resulted in substantial model uncertainty associated with the models. This model uncertainty can in turn affect the forecasted dielectric constants.

Forecasted dielectric constants were determined by measuring dielectric constants at the McBaine, MO field site and using the predictive models (Topp et al., 1980, Peplinski et al., 1995) to convert to volumetric water contents. The volumetric water contents determined by the Topp et al. (1980) and Peplinski et al. (1995) model from measured dielectric constants on June 1st, 2013 are shown in Figure 5.39. The calculated volumetric water contents on June 1st, 2013 were

implemented in WinUnSat-H to forecast the volumetric water content. The forecasted volumetric water contents were substituted into the predictive models (Topp et al., 1980, Peplinski et al., 1995) to forecast the dielectric constant of McBaine, MO soils.
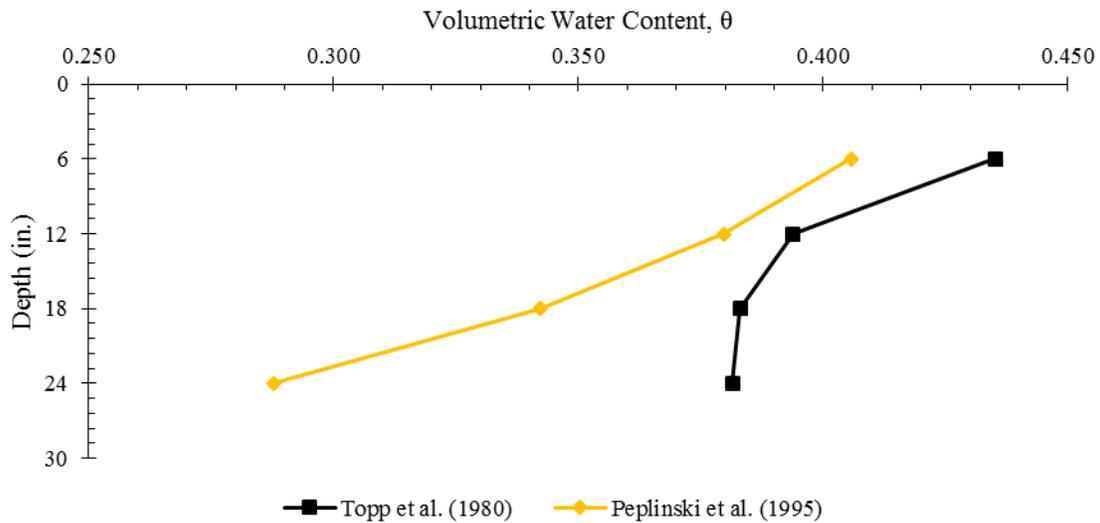
Figure 5.39: Initial Conditions of Back-Calculated Volumetric Water Content using the Topp et al. (1980) and Peplinski et al. (1995) Model versus Depth at McBaine, MO Field Site on June 1st, 2013

The initial volumetric water contents determined by the models (Topp et al., 1980, Peplinski et al., 1995) from measured dielectric constants on June 1st, 2013 showed decreasing volumetric water contents with decreasing depth. Figure 5.39 shows the differences between each model by their calculated initial volumetric water content. The initial volumetric water contents determined by the Topp et al. (1980) and Peplinski et al. (1995) models were more similar at depths of 6 in. and 12 in. differing 0.029 and 0.014, respectively. Volumetric water contents determined by the Topp et al. (1980) and Peplinski et al. (1995) models were least similar at the depths of 18 in. an 24 in., differing 0.041 and 0.093, respectively. Differences in the initial conditions create differences throughout forecasts of volumetric water content, and subsequently dielectric constant.

The differences between forecasted and measured dielectric constants (Figure 5.4 and Figure 5.5) of the McBaine, MO soil were greatest in the soil with high clay content (depth of 12

in.) and lowest in the soil with high sand content (depth of 24 in.). Topp et al. (1980) and Peplinski et al. (1995) revealed similar findings when testing sands and clay (Figure 2.5, Figure 2.6. The soil with high clay content showed large variation with their fit equations than soil with high sand content.

Topp et al. (1980) and Peplinski et al. (1995) also indicated the soil's SSA had an effect on the dielectric constant of soil even though they did not include the property in their models (Figure 2.9). The soil at a depth of 12 in. had the highest SSA (217 m^2/g), as well as the highest differences between forecasted and measured dielectric constants The soil at a depth of 24 in. had the lowest SSA (129 m^2/g) as well as the smallest differences between forecasted and measured dielectric constants. The differences between forecasted and measured dielectric constants show a correlation with the soil's SSA.

5.6   Meteorological Measurements

Meteorological conditions measured at the McBaine, MO field site were implemented into WinUnSat-H to forecast the soil's volumetric water content, and subsequently dielectric constant over time. Differences between forecasted and measured dielectric constants presented the opportunity to discuss the measured meteorological input's accuracy. The accuracy of the McBaine, MO measurements have an effect on the forecasted changes in moisture, and subsequently forecasted dielectric constant, over time. Measured meteorological conditions from three nearby weather stations, managed by the University of Missouri, were compared with McBaine, MO measurements (Table 5.12). The spatial location of the three weather stations with respect to the McBaine, MO field site are shown in Figure 5.40.

WinUnSat-H utilizes daily values of the meteorological data as inputs, and because of that, comparisons were made with daily meteorological values. Comparisons were made by taking the

136

average of measurements made by the three MU weather stations. The average measurements of

MU weather stations were then plotted versus McBaine, MO field site measurements (Table 5.13).

Table 5.13 lists the slope and y-intercept of the linear best-fit equation for each meteorological

comparison. A one to one linear relationship exhibits identical measurements by the averaged MU

values and McBaine, MO values. The daily comparisons (Appendix B) provided the opportunity

to see the spatial and temporal variations in meteorological conditions, but more importantly serve

the purpose of indicating the accuracy the McBaine, MO meteorological measurements have to

forecast the dielectric constant of soils. The spatial and temporal variations are attributed to the

differences between MU weather stations and the McBaine, MO field site and not the inaccuracy

of the McBaine, MO meteorological measurements.

Table 5.12: Locations of Weather Stations and their Distance to McBaine, MO Field Site

Site	Latitude (N)	Longitude (W)	Distance to McBaine, MO (miles)
Sanborn Field	38° 56' 32.28"	92° 19' 13.42"	8.4
Capen Park	38° 55' 45.25"	92° 19' 16.67"	8.0
Jefferson Farms	38° 54' 25.17"	92° 16' 11.91"	10.5
McBaine, MO	38° 53' 49.25"	92° 27' 53.07"	-
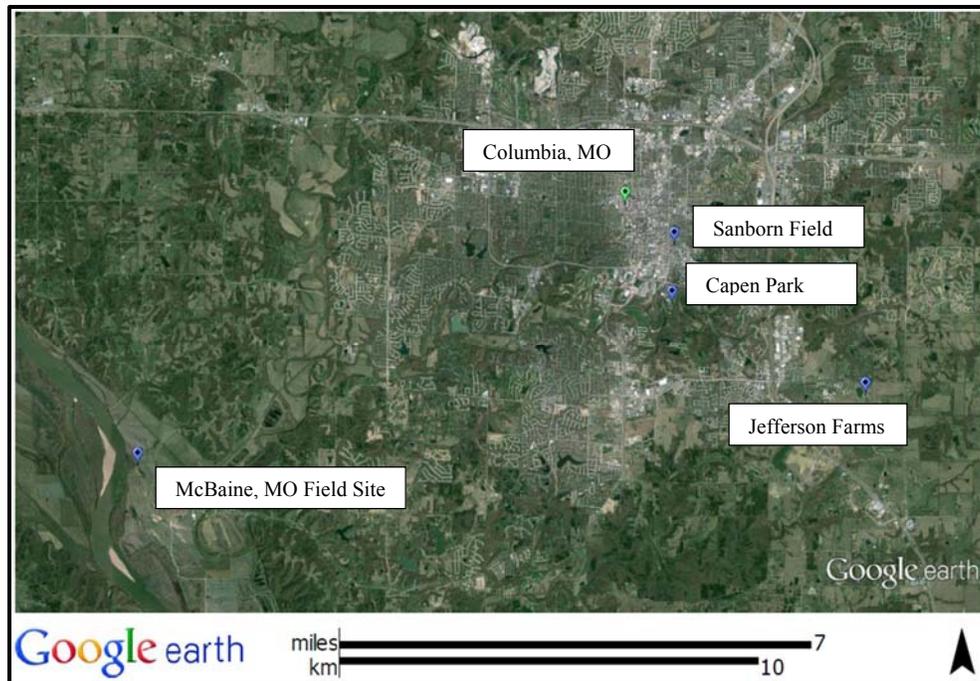
Figure 5.40: McBaine, MO Field Site and MU Weather Stations used to Compare Measured Meteorological Conditions (Google Maps, 2013)

Table 5.13: Slope and y-intercept of Linear Equation for Comparisons of Meteorological Measurements between McBaine, MO Field Site and MU Weather Stations

Meteorological Measurement	*Slope (No.)*	*y-intercept (No.)*
One-to-One Relationship	1.00	0.00
Maximum Daily Air Temperature (°F)	0.95	0.75
Minimum Daily Air Temperature (°F)	0.99	-0.24
Average Daily Dew Point Temperature (°F)	0.98	-1.19
Total Daily Solar Radiation (Langleys)	1.29	-41.91
Average Daily Wind Speed (mph)	0.78	2.04
Total Daily Precipitation (in.)	0.79	0.01

5.7   Summary

The forecasted and measured dielectric constants at the McBaine, MO field site were different. The laboratory characterization of McBaine, MO soils and what was observed at the

field site indicated the soil's tendency to shrink-swell during wetting and drying events. The expansive nature and blocky structure created macropores for water to preferentially flow. The inability of WinUnSat-H to model moisture migration through soils with macropores was indicated by the differences between forecasted and measured dielectric constants. The predictive models (Topp et al., 1980, Peplinski et al., 1995) and their empirically derived equation's also created differences between the forecasted and measured dielectric constants. The measured McBaine, MO meteorological data were compared to three surrounding weather stations. The comparisons indicated McBaine, MO measurements were comparable to the three weather stations measurements. The discussion brought to light elements of the McBaine, MO field site that were not accounted for in the forecasted dielectric constants, but were accounted for in the measured dielectric constants. Differences between the forecasted and measured dielectric constants are attributed to these findings.

6 Conclusions

6.1 Summary

Some nondestructive testing (NDT) techniques in civil engineering applications employ electromagnetic (EM) wave methods. These techniques have proven to be effective for many applications including investigating and characterizing the subsurface, identifying steel reinforcement locations in pavements, and testing the integrity of concrete foundations. Civil engineering subsurface characterizations typically propagate EM waves in the radio to microwave range (3 kHz to 300 GHz).

The real part of relative permittivity (dielectric constant) is a measure of the soil's ability to be polarized by an electrical field and determines the EM's wave velocity. The dielectric constant of a soil impacts properties of refracted and reflected EM energy. Numerous studies have shown the dielectric constant of a soil is strongly dependent on the amount of moisture in the medium (Okrasinski et al., 1978). Constantly changing meteorological conditions and soil properties affect the amount of moisture, and thus affect the dielectric constant, of soil.

The objective of this project was to quantify the effectiveness of forecasted dielectric constants for soil based on meteorological data. *In situ* measurements of the soil's dielectric constant were used to check and compare with forecasted dielectric constants of soil. Dielectric constants were forecasted by coupling empirical dielectric constant predictive models with a soil moisture migration model.

Soil moisture and meteorological sensors were installed on April 23rd, 2012, at a site near McBaine, Missouri (MO) to provide 'ground-truth' data for forecasted dielectric constants of near-surface soils (upper two feet) and their changes with time. Laboratory testing was conducted to determine properties of soils from the McBaine, MO field site. Samples representative of the soil

140

at depths of 6 in., 12 in., 18 in., and 24 in. below ground surface (BGS) were collected and returned to the University of Missouri Soil Characterization and Geotechnical Engineering Laboratory for physical testing.

The McBaine, MO soil's dielectric constant was forecasted over the time period of June 1st, 2013 thru June 30th, 2013. The time period represented field events where measured volumetric water content, and dielectric constant, changed over time. Volumetric water contents, forecasted using the soil moisture migration (WinUnSat-H), were implemented in dielectric constant predictive models (Topp et al., 1980, Peplinski et al., 1995) to forecast the soil's dielectric constant for various depths and time.

Measured dielectric constants on June 1st, 2013 at McBaine, MO were used to establish the initial conditions for the soil moisture migration model. The initial volumetric water contents were input into WinUnSat-H, after which the soil's volumetric water content versus depth were forecast over the time period of June 1st, 2013 thru June 30th, 2013. Forecasted volumetric water contents were substituted into the dielectric constant predictive models (Topp et al., 1980, Peplinski et al., 1995) to forecast dielectric constants over depth and time.

Results of the forecasted and measured dielectric constants at the McBaine, MO field site were compared to quantify the effectiveness of forecasting dielectric constants of soil at the field site. Additionally, the McBaine, MO soil properties and measured meteorological data were examined to determine their role in the differences between forecasted and measured dielectric constants.

6.2   Conclusions

The soil at the McBaine, MO field site exhibits expansive behavior. Atterberg limits, cation exchange capacities, and specific surface areas (SSA's) indicated the soil at depths of 6 in.,

12 in., and 18 in. (which had clay contents greater than 25 percent), were in the ranges commonly exhibited by soils with expansive behavior.

Changes in the soil conditions due to shrinking and swelling from changing moisture conditions led to the observed soil's blocky structure (Figure 5.19) and tension cracks (macropores) (Figure 5.31) forming during dry periods. The macropores became preferential paths resulting in measured volumetric water contents, and consequently dielectric constants, showing rapid increases and decreases; as evidenced by their "square wave" response over time (Figure 5.32 and Figure 5.33). The moisture migration model's inability to account for soil macropores, and the resulting rapid flow of water into or out of the soil, caused forecasted volumetric water contents, and consequently dielectric constants to show 'smoothed' behavior over time, rather than the abrupt (square wave) response measured values exhibited.

The dielectric constant predictive models developed by Topp et al. (1980) and Peplinski et al. (1995) are more reliable for soils with lower specific surface areas (less than 20 m^2/g), as indicated in Chapter 2. The soil at depths of 6 in., 12 in., and 18 in. showed higher SSA's than the soil at a depth of 24 in. (Table 4.3). Converting between dielectric constant and volumetric water content using the predictive models resulted in forecasted dielectric constants being less reliable than measured values.

The inability of the moisture migration model to account for the expansive behavior of the McBaine, MO soils, along with the dielectric constant predictive models being less reliable in the soils with increased (greater than 25 percent) clay-size fraction, led to forecasted dielectric constants being consistently greater than measured dielectric constants (Figure 5.2 and Figure 5.3). The forecasted and measured dielectric constants of the McBaine, MO soils showed that as the soil's sand content decreases (especially below 50 percent) and clay content increases, the

percentage difference between forecasted and measured dielectric constants increased (Table 5.1). The agreement between forecasted and measured dielectric constants at their respective depth are as follows:

- The best agreement between forecasted and measured dielectric constants was seen in the soil at a depth of 24 in. below ground surface, which had 61 percent sand and 16 percent clay by grain-size fraction. The differences between forecasted and measured dielectric constants at a depth of 24 in. were less than five (percentage difference less than 20 percent) throughout the simulated month of June 2013.

- The soil at a depth of 18 in. below ground surface, which had 29 percent sand and 28 percent clay, showed less agreement between forecasted and measured dielectric constants than the soil at a depth of 24 inches. The differences between forecasted and measured dielectric constants at a depth of 18 in. were less than 10 (percentage difference between 20 and 80 percent) throughout the simulated month of June 2013.

- The least agreement between forecasted and measured dielectric constants was seen in the soil at a depth of 12 in. below ground surface, which had 6 percent sand and 57 percent clay by grain-size fraction. The differences between forecasted and measured dielectric constants at a depth of 12 in. were 10 to 15 (percentage difference between 80 and 100 percent) throughout the simulated month of June 2013.

- The soil at a depth of 6 in. below ground surface, which had 31 percent sand and 26 percent clay, showed less agreement between forecasted and measured dielectric constants than the soil at a depth of 24 inches. The differences between forecasted and measured dielectric constants at a depth of 6 in. were less than 10 (percentage difference between 20 and 80 percent) throughout the simulated month of June 2013.

6.3 Practical Implications

This study has shown that site selection and the conditions that occur at a given site have huge implications on forecasting the dielectric constant of soil. Understanding the complexity of the processes at a site and how they change over time are imperative in developing accurate dielectric constant forecasts. In the case of the McBaine, MO test site, the expansive nature of the soils and the fluctuating near-surface groundwater table, among other factors, played roles in creating differences between forecasted and measured dielectric constants. These differences were created due in large part because the moisture migration model could not simulate expansive soils or fluctuating near-surface groundwater table. Developing an understanding of the site and its processes can lead to more accurate methods of analyses, which will lead to more accurate forecasted dielectric constants.

The nature in which a soil behaves to changing meteorological conditions is also important when forecasting the dielectric constant of soil. A soil's water content can change rapidly; day to day, hour to hour, even minute to minute (Figure 5.32 and Figure 5.33). The rapid and large changes a soil's volumetric water content (Figure 4.6) can undergo, make it necessary to model those changes to increase the accuracy of forecasted dielectric constants. Current limitations of moisture migration modeling, constrain dielectric constant forecasts on a daily basis. *In situ* dielectric constants have shown changes to be on a smaller time scale (minutes and hours) during periods of rapidly changing soil moisture; soil moisture is the only parameter that can change rapidly enough to show similar changes in dielectric constant.

6.4 Recommendations

Recommendations for further development on forecasting the dielectric constants of soil follow:

- It is recommended when dielectric constants are forecasted in clays, to use a predictive model that accounts for the wide range of clay minerals. The Topp et al. (1980) and Peplinski et al. (1995) models are more reliable for soils with high sand content than soils with high clay content (Figure 2.5 and Figure 2.6). Hilhorst's (1998) dielectric constant predictive model includes the soil's specific surface area and soil water characteristic curve, which are used to describe clay. Applying a predictive model that accounts for the clay minerals, could lead to better agreement between forecasted and measured dielectric constants in clay; however, Hilhorst's (1998) model was not compared to measured dielectric constants of soils in this research to provide definitive comparisons.

- An alternative to using a dielectric constant predictive model for determining initial volumetric water contents from measured dielectric constants would be to use measured volumetric water contents for initial conditions in the soil moisture migration modeling. Measured volumetric water contents should increase the accuracy of the forecasted volumetric water contents, and dielectric constants.

- A more comprehensive moisture migration model is suggested to improve accurate forecast the volumetric water content, and subsequently dielectric constant, of soil. A moisture migration model that not only accounts for one-dimensional water flow, but two-dimensions, similar to the H.E.L.P. model (Schroeder et al., 1994), and three- dimensions, similar to the HYDRUS model (Yu and Zheng, 2010), should produce more accurate forecasts of the soil's dielectric constant.

  Finally, it is recommended that the work included in this thesis be expanded to monitoring sites with large sand and silt contents. Due to the variability of climates and soil, there is a need for more 'ground-truth' data under various meteorological and soil conditions.

Monitoring field sites with large sand and silt contents, and forecasting their dielectric constants can be used in conjunction with the work included in this thesis to provide a more comprehensive understanding of dielectric constant forecasts for soil.

References

Abidin, K. (2002). "Evaluation of Soil Porosity Using a Low MHz Range Dielectric Constant." *Turkish J. Eng. Env. Sci.*, 26 (1).

ASTM D584 (2010). "Standard Test Methods for Specific Gravity of Soil Solids by Water Pycnometer." *ASTM Geotechnical Testing*.

ASTM D2216 (2010). "Standard Test Methods for Laboratory Determination of Water (Moisture) Content of Soil and Rock by Mass." *ASTM Geotechnical Testing*.

ASTM D2487 (2011). "Standard Practice for Classification of Soils for Engineering Purposes (Unified Soil Classification System)." *ASTM Geotechnical Testing*.

ASTM D2937 (2011). "Standard Test Methods for Density of Soil in Place by the Drive-Cylinder Method." *ASTM Geotechnical Testing*.

ASTM D4318 (2010). "Standard Test Methods for Liquid Limit, Plastic Limit, and Plasticity Index of Soils." *ASTM Geotechnical Testing*.

ASTM D5084 (2010). "Standard Test Methods for Measurement of Hydraulic Conductivity of Saturated Porous Materials Using a Flexible Wall Permeameter." *ASTM Geotechnical Testing*.

Baca, R. G. and Magnuson, S. (1990). Independent Verification and Benchmark Testing of the UnSat-H Computer Code, Version 2.0. Idaho National Engineering Laboratory.

Baker, J. M. and Allmaras, R. R. (1990). "System for Automating and Mutliplexing Soil Moisture Measurement by Time-Domain Reflectometry." *Soil Sci. Soc. Am. J.* 54 (1).

Behari, J. (2005). "Microwave Dielectric Behavior of Wet Soils." Anamaya Publishers. 1 (1).

Bowders, J.J., Koerner, R.M. and Lord, A.E. (1982). "Buried Container Detection Using Ground Probing Radar." *J. of Hazardous Materials*. 7 (1).

Bowders, J.J., Koerner, R.M. and Lord, A.E. (1983). "Potential Use of GPR in Assessing Groundwater Pollution in Partially and Fully Saturated Soils." *Proc.* of the American Geophysical Union Spring Conference, May 31st – June 4th, Philadelphia, PA. 1 (1).

Bowders, J.J., Lord, A.E. and Koerner, R.M. (1982). "Sensitivity Study of a Ground Probing Radar System." *Geotechnical Testing Journal*. 5 (1).

Bungey J.H. and Millard, S. G. (2006). "Testing of Concrete in Structures." Surrey University Press. 1 (1).

Burt, R. (2004). *Soil Survey Laboratory Methods Manual*, Soil Survey Investigations Report No. 42 Version 4.0. Natural Resources Conservation Service, U.S. Department of Agriculture.

CARES (2013). "CARES Map Room." < http://ims.missouri.edu/moims2008/> (October 10th, 2013).f

Cerato, A. B. and Lutenegger, A. J. (2002). "Determination of Surface Area of Fine-Grained Soils bythe Ethylene Glycol Monoethyl Ether." *Geotechnical Testing Journal*. 25 (3).

Curtis J. O. (2001). "A Durable Laboratory Apparatus for the Measurement of Soil Dielectric Properties." *Instrumentation and Measurement: IEEE Transactions*. 50 (5)

Decagon Devices (2012). "Decagon Devices." <http://www.decagon.com/> (May 26th, 2013)

Dobson, M. C., Ulaby F. T., Hallikainen M. T., and El-Rayes M. A. (1985). "Microwave Dielectric Behavior of Wet Soil – Part II: Dielectric Mixing Models." *Geoscience and Remote Sensing, IEEE Transactions*. 23 (1).

Doorenbos, J., Pruitt, W. O., (1977). "Guidelines for Predicting Crop Water Requirements." *Food and Agr. Org.* Irrigation and Drainage Paper. 24 (1).

Fayer, M. J. (2000). "UnSat-H Version 3.0: Unsaturated Soil Water and Heat Flow Model, Theory, User Manual, and Examples." Pacific Northwest National Laboratory.

Feddes, R. A., Kowalik, P. J., and Zaradny, H. (1978). "Simulation of Field Water Use and Crop Yield." Pudoc, Centre Agr. Publ. Doc. Wageningen. 1 (1).

Gish, T. J. and Shirmohammadi A. (1991). "Preferential Flow: Proc. of the National Symposium, December 16th – 17th, Chicago, Illinois." *American Soc. of Agric. Eng.*

Google Maps (2013). "Google Maps." <http://maps.google.com > (August 10th, 2013).

Hendrickx, J. M. H., Curtis, J., Lensen, H. A., and Harmon, R. (2003). "Worldwide distribution of soil dielectric and thermal properties." *Proc.* SPIE 5089, Detection and Remediation Technologies for Mines and Minelike Targets VIII. 1 (1).

Hilhorst, M. A. (1998). "Dielectric Characterisation of Soil." Dissertation, Wageningen Agricultural University (WAU).

Hillel, D. (1980). "Applications of Soil Physics." Academic Press. 1 (1).

Hillel, D. (1982). "Introduction to Soil Physics." Academic Press. 1 (1).

Hillel, D. (1998). "Environmental Soil Physics: Fundamentals, Applications, and Environmental Considerations." Academic Press. 1 (1).

Hoogmoed W. B. and Bouma, J. (1980). "A Simulation Model for Predicting Infiltration into Cracked Clay Soil." *Soil Sci. Soc. Am. J.* 44 (3).

Koerner, R.M., Lord, A.E., Bowders, J.J. (1981). "Utilization and Assessment of a Pulsed RF System to Monitor Subsurface Liquids." *Proc.* of the National Conference on Management of Uncontrolled Hazardous Waste Sites, October 28th – 30th, Washington, DC, HMCRI. 1 (1).

Koerner, R. M., Lord, A. E., Bowders, J. J., and Dougherty, W. W. (1982). "CW Microwave Location of Voids Beneath Paved Areas." *J. of Geot. Eng.* 108 (1).

Lu, N. and W. J. Likos (2004). "Unsaturated Soil Mechanics." John Wiley and Sons. 1 (1).

Mitchell, J. K., and Soga, K. (2005). "*Fundamentals of Soil Behavior.*" John Wiley and Sons. 1 (1).

Miyazaki, T. (2005). "*Water Flow in Soils.*" Taylor and Francis Group. 1 (2).

McQueen, I. S. and Miller, R. F. (1974). "Approximating Soil Moisture Characteristics from Limited Data: Empirical Evidence and Tentative Model." *Water Resources Research*. 10 (3).

Mualem, Y. (1976). "A New Model for Predicting the Hydraulic Conductivity of Unsaturated Porous Media." *Water Resources Research*. 12 (3).

NASA (2013). "Electromagnetic Spectrum Diagram." <mynasadata.larc.nasa.gov/science-processes/electromagnetic-diagram/> (May 26th, 2013).

NRCS, USDA (2013). "Official Soil Series Descriptions." <https://soilseries.sc.egov.usda.gov/osdname.asp> (September 20th, 2013).

Okrasinski, T. A., Koerner, R. M., Lord, A. E. (1978). "Dielectric Constant Determination of Soil at L Band Microwave Frequencies." *ASTM Geotechnical Testing*.

Paltineau, I. C. and Starr, J. L. (1997). Real-Time Soil Water Dynamics Using Multisensor Capacitance Probes: Laboratory Calibration." *Soil Sci. Soc. Am. J.* 61 (6).

Peck, R. B., Hanson, W. E. and Thornburn T. H. (1974). "*Foundation Engineering.*" John Wiley And Sons. 1 (1).

Penman, H. L. (1948). "Natural Evaporation from Open Water, Bare Soil and Grass." *Proc.* Of the Royal Society of London, Series A, Mathematical and Physical Sciences. 193 (1032).

Peplinski, N. R., Ulaby, F. T. and Dobson, M. C. (1995). "Dielectric Properties of Soils in the 0.3 − 1.3 GHz Range." *Geoscience and Remote Sensing: IEEE Transactions*. 33 (3).

Perry-Hill, M. J., Sutter, R. T. and Davidson, M. W. (2006). "Basic Electromagnetic Wave Properties." <micro.magnet.fsu.edu/primer/java/wavebasics/> (May 26th, 2013).

Philip J. R. (1957). "Numerical Solution of Equations of the Diffusion Type with Diffusivity Concentration-Dependent. II." *Australian J. of Physics*. 10 (1).

Richards, L. A. (1931). "Capillary Conduction of Liquids through Porous Mediums." Physics. 1 (5).

Schindler, U., Durner, W., von Unold, G., Muller, L. and Wieland, R. (2010). "The Evaporation Method: Extending the Measurement Range of Soil Hydraulic Properties using the Air-Entry Pressure of the Ceramic Cup." *J. of Plant Nutrition and Soil Sci*. 47 (1).

Schroeder, P.R., Dozier, T.S., Zappi, P.A., McEnroe, B.M., Sjostrom, J.W. and Peyton, R.L. (1994). "The Hydrologic Evaluation of Landfill Performance (HELP) model: Engineering Documentation for Version 3." United States Environmental Protection Agency Risk Reduction Engineering Laboratory.

Schwab, G. O., Fangmeier, D. D., Elliot, W. J. and Frevert, R. K. (1993). "*Soil and Water Conservation Engineering.*" John Wiley and Sons. 1 (4).

Starr, J. L. and I. C. Paltineau (1998). "Real-time Soil Water Dynamics over Large Areas using Multisensor Capacitance Probes and Monitoring System." *Soil and Tillage Research*. 47 (1).

Thomas, A. M. (1966). "*In Situ* Measurement of Moisture in Soil and Similar Substances by Fringe Capacitance." *J. of Sci. Instruments*. 43 (1).

Topp, G. C., Davis, J. L., and Annan, A. P. (1980). "Electromagnetic Determination of Soil Water Content: Measurements in Coaxial Transmission Lines." *Water Resources Research*. 16 (3).

Troch, P. A., Vandersteene, F., Su, Z. and Hoeben, R. (1996). "Estimating Microwave Observation Depth in Bare Soil through Muti-Frequency Scatterometry." 1st EMST User Workshop *Proceedings*, Ispra, Italy.

USDA (2004). *Soil Survey Laboratory Methods Manual*. U.S. Govt. Print. Office, Washington, D.C., United States Department of Agriculture.

van Genuchten, M. T. (1980). "A Closed-Form Equation for Predicting the Hydraulic Conductivity of Unsaturated Soils." *Soil Sci. Soc. Am. J.* 44 (5).

Yu, C. and Zheng C. (2010). "HYDRUS: Software for flow and transport modeling in variably saturated Media." *Ground Water.* 48 (6).

Appendix

A. Sensor Calibrations

A.1 "5TE" Soil Moisture Sensor

Measurement Speed: 150 (ms) milliseconds

Operating Temperature Range: -40 °C to 50 °C

Power Requirements: 3.6 to 15 Volts Direct Current, 0.3 mA quiescent, 10 mA during 150

ms measurement

A.1.1 Dielectric Constant

Accuracy: +/- 1 ε' from 1 to 40 (soil range), +/- 15 percent from 40 to 80

Resolution: 0.1 ε' from 1 to 20, < 0.75 ε' from 20 to 80

Range: 1 (air) to 80 (water)

A.1.2 Volumetric Water Content

Accuracy: +/- 0.03 m^3/m^3 (+/- 3 percent volumetric water content) if electrical conductivity

is < 10 dS/m

Resolution: 0.0008 m^3/m^3 (0.08 percent volumetric water content)

Range: 0 percent to 100 percent

A.1.3 Electrical Conductivity

Accuracy: +/- 10 percent from 0 to 7 dS/m

Resolution: 0.01 dS/m from 0 to 7 dS/m, 0.05 dS/m from 7 to 23 dS/m

Range: 0 to 23 dS/m

A.1.4 Soil Temperature

Accuracy: +/- 1 °C

Resolution: 0.1 °C

Range -40 °C to 50 °C

A.2 "MPS-2" Soil Potential Sensor

Measurement Speed: 150 ms

Operating Temperature Range: - 40 °C to 50 °C

Power Requirements: 3.6 to 15 Volts Direct Current, 0.3 mA quiescent, 10 mA during 150

ms measurement

Equilibration Time: 10 minutes to 1 hour depending on soil material

A.2.1 Matric Potential

Accuracy: +/- 25 percent from -5 kPa to -100 kPa, +/- 35 percent up to -300

Resolution: 0.1 kPa

Range: -5 kPa to -500 kPa

A.2.2 Soil Temperature

Accuracy: +/- 1 °C

Resolution: 0.1 °C

Range -40 °C to 50 °C

A.3 VP-3 Relative Humidity/Air Temperature Sensor

Measurement Speed: 300 ms

Operating Temperature Range: -40 °C to 80 °C

Power Requirements: 3.6 to 15 Volts Direct Current, 0.3 mA quiescent, 10 mA during 150

ms measurement

A.3.1   Relative Humidity

Accuracy:

Humidity [%RH]	0°C	10°C	20°C	30°C	40°C	50°C	60°C	70°C	80°C
100%	±5%	±5%	±5%	±5%	±5%	±5%	±5%	±6%	±10%
95%	±5%	±5%	±4%	±4%	±4%	±4%	±4%	±5%	±8%
90%	±5%	±4%	±2%	±2%	±3%	±3%	±4%	±5%	±8%
85%	±5%	±4%	±2%	±2%	±3%	±3%	±4%	±5%	±8%
80%	±4%	±4%	±2%	±2%	±3%	±3%	±3%	±4%	±6%
75%	±4%	±4%	±2%	±2%	±3%	±3%	±3%	±4%	±6%
70%	±4%	±4%	±2%	±2%	±3%	±3%	±3%	±4%	±6%
65%	±4%	±4%	±2%	±2%	±3%	±3%	±3%	±4%	±6%
60%	±4%	±3%	±2%	±2%	±2%	±2%	±2%	±3%	±5%
55%	±4%	±2%	±2%	±2%	±2%	±2%	±2%	±3%	±5%
50%	±4%	±2%	±2%	±2%	±2%	±2%	±2%	±3%	±5%
45%	±4%	±2%	±2%	±2%	±2%	±2%	±2%	±3%	±4%
40%	±4%	±2%	±2%	±2%	±2%	±2%	±2%	±3%	±4%
35%	±4%	±3%	±2%	±2%	±2%	±2%	±2%	±3%	±4%
30%	±4%	±3%	±2%	±2%	±2%	±2%	±2%	±3%	±4%
25%	±4%	±3%	±2%	±2%	±2%	±2%	±2%	±3%	±4%
20%	±4%	±4%	±2%	±2%	±3%	±3%	±3%	±3%	±4%
15%	±5%	±4%	±2%	±2%	±3%	±3%	±4%	±4%	±5%
10%	±8%	±5%	±3%	±3%	±4%	±4%	±4%	±5%	±8%
5%	±8%	±8%	±5%	±5%	±5%	±5%	±5%	±6%	±10%
0%	±12%	±12%	±5%	±5%	±6%	±6%	±6%	±10%	±12%

Temperature [°C]

Figure A.3.1: Accuracy of Relative Humidity Measurements for Decagon Devices (Decagon, 2012) "VP-3" Sensor

Resolution: 0.1 percent relative humidity

Range: 0 percent to 100 percent

A.3.2   Air Temperature

Accuracy:

Temperature Accuracy (°C)
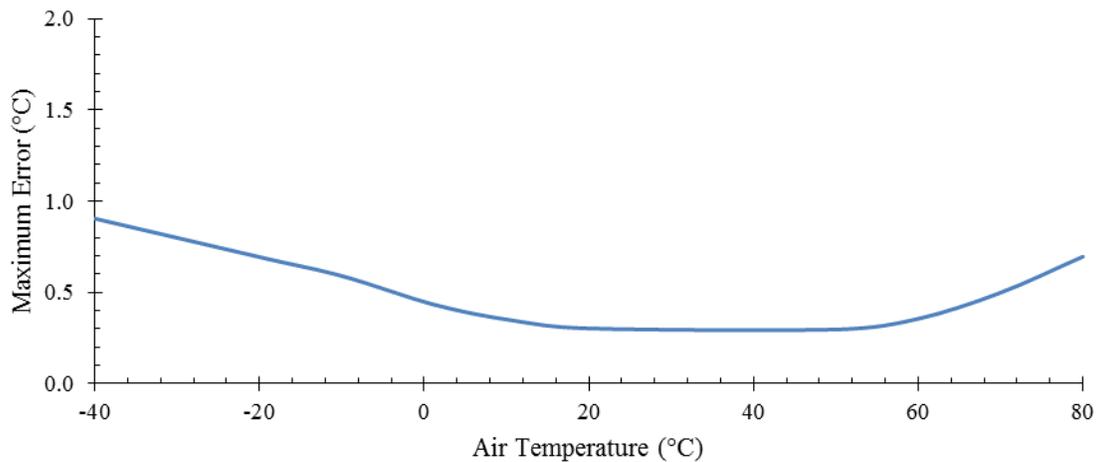
Resolution: 0.1 °C

Range: -40 °C to 80 °C

A.4 Davis Cup Anemometer

A.4.1 Wind Speed

Accuracy: +/- 5 percent

Resolution: 0.45 m/s (1 mph)

Range: 0 to 58 m/s (129 mph)

A.4.2 Wind Direction

Accuracy: 7 °

Resolution: 1 °

Range: 0 ° to 360 °

A.5 "PYR" Total Solar Radiation Sensor

Accuracy: +/- 5 percent

Resolution: N/A

Operating Temperature Range: -40 °C to 60 °C

Spectral Range: 380 nm to 1120 nm

Measurement Range: 0 W/m^2 to 1750 W/m^2

Field of View: 180 °

A.6   "ECRN-50 Low-Resolution Rain Gauge

Single Spoon Tipping Bucket

Resolution: 1 mm

Operating Temperature Range: 0 °C to 60 °C

A.7   "EM50" Digital/Analog Data logger

Input Channels: 5, each supporting 12-bit analog, 32-bit digital, or pulse sensors

Data Storage: 1 MB (36,000 scans of all 5 ports)

Operating Temperature Range: -40 °C to 60 °C

B. Meteorological Measurements

B.1 Maximum Daily Air Temperature

The maximum daily air temperature measured at the MU weather stations versus McBaine, MO field site are shown in Figure B.1. Maximum air temperature measurements at the MU weather stations and McBaine, MO field site followed the one to one relationship closely; having minor differences. Daily differences of maximum air temperature between the MU weather stations and McBaine, MO field site are shown in Figure B.2. The average daily difference was -1.3 °F indicating McBaine, MO collectively measured higher values than the MU weather stations. The greatest daily difference occurred on February 24th, 2013 when the difference was 19.7 °F (71.3 °F compared to 51.6 °F) higher than the MU weather stations. The greatest difference on February 24th, 2013 was caused by snow covering the McBaine, MO sensor.

The linear best-fit equation for the one to one relationship has a slope of 1.0 and intercepts the y-axis at 0.00 °F (Figure B.1). The linear best-fit equation for the compared measurements has a slope of 0.95 and intercepts the y-axis at 0.75 °F (Figure B.1). The maximum daily air temperature comparisons between the MU weather stations and McBaine, MO have slopes and intercepts similar to the one to one relationship.
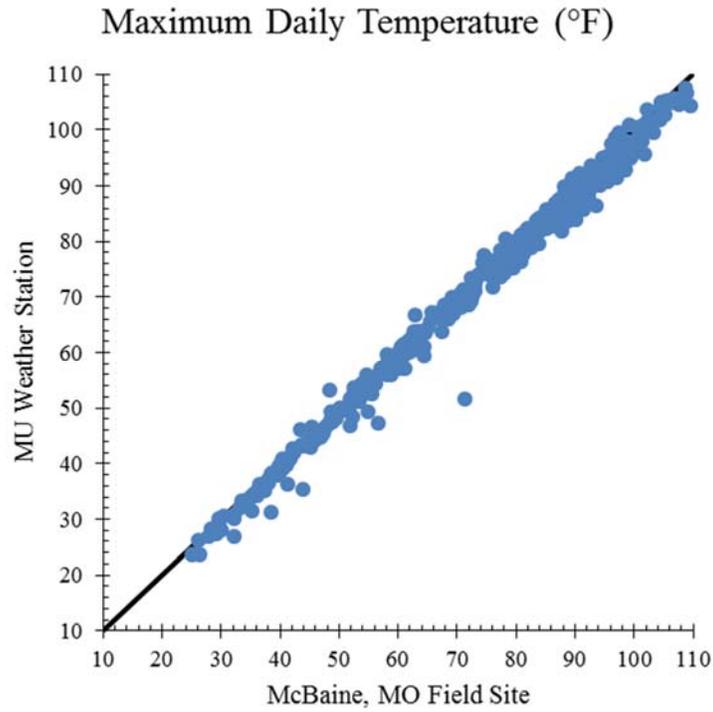
Figure B.1: Maximum Daily Air Temperature Measurements of MU Weather Stations versus McBaine, MO Field Site
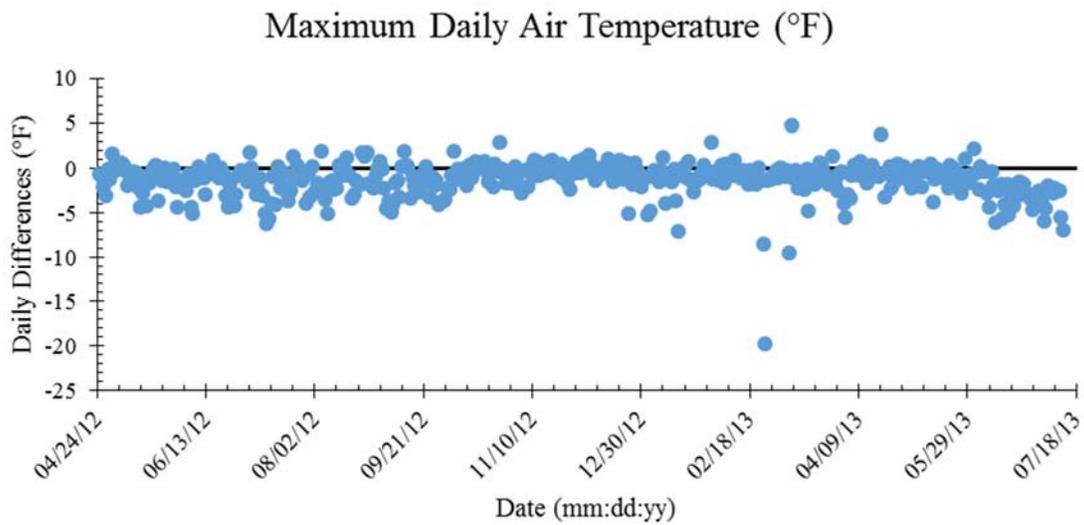
Figure B.2: Daily Differences of Maximum Air Temperature between MU Weather Stations and McBaine, MO Field Site

157

**B.2   Minimum Daily Air Temperature**

The minimum daily air temperature measured at the MU weather stations versus McBaine, MO field site are shown in Figure B.3. Minimum air temperature measurements at the MU weather stations and McBaine, MO field site followed the one to one relationship closely; having only minor differences. The one to one relationship agrees more closely at higher minimum daily temperatures than lower; the MU weather stations measured higher daily minimum temperatures. Daily differences of minimum air temperature between the MU weather stations and McBaine, MO field site are shown in Figure B.4. The average daily difference was -1.4 °F indicating McBaine, MO collectively measured higher values than the MU weather stations. The greatest daily difference occurred on February 24th, 2013, similar to the greatest maximum daily air temperature difference, when McBaine, MO measured 8.2 °F (0.8 °F compared to 8.6 °F) lower than the MU weather stations. The greatest difference on February 24th, 2013 was caused by snow covering the McBaine, MO sensor.

The linear best-fit equation for the one to one relationship has a slope of 1.0 and intercepts the y-axis at 0.00 °F (Figure B.3). The linear best-fit equation for the compared measurements has a slope of 0.99 and intercepts the y-axis at -0.24 °F (Figure B.3). The minimum daily air temperature comparisons between the MU weather stations and McBaine, MO have slopes and intercepts similar to the one to one relationship.
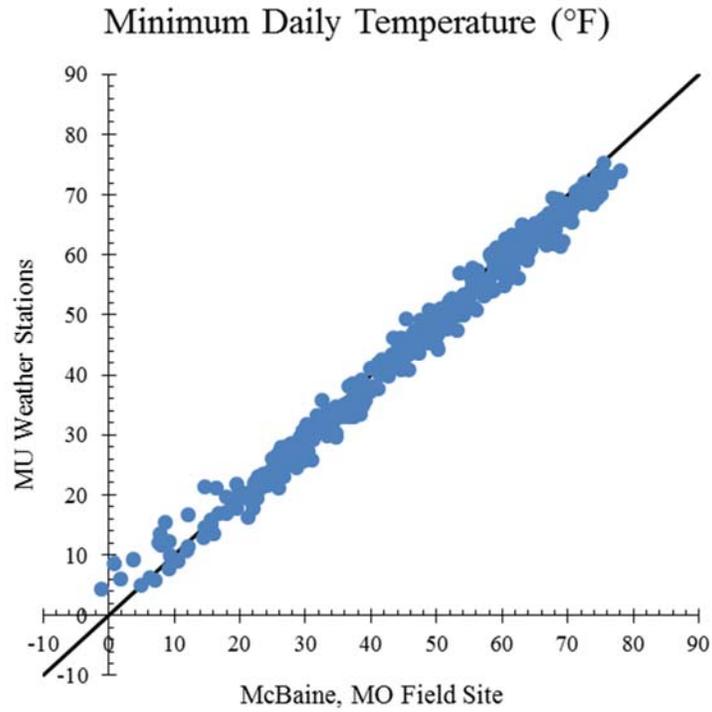
Figure B.3: Minimum Daily Air Temperature Measurements of MU Weather Stations versus McBaine, MO Field Site
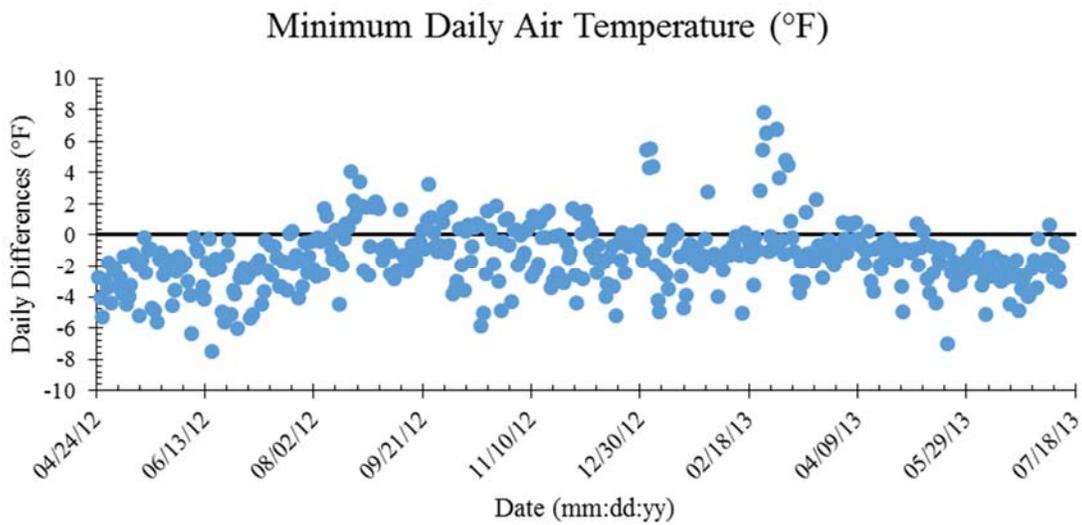

Figure B.4: Daily Differences of Minimum Air Temperature between MU Weather Stations and McBaine, MO Field Site

B.3   Average Daily Dew Point Temperature

The average daily dew point temperature measured at the MU weather stations versus McBaine, MO field site are shown in Figure B.5. Daily dew point temperature measurements at the MU weather stations and McBaine, MO field site followed the one to one relationship. Daily differences of dew point temperature between the MU weather stations and McBaine, MO field site are shown in Figure B.6. The average daily differences were -2.0 °F indicating McBaine, MO collectively measured higher values than the MU weather stations. The greatest daily differences between the MU weather stations and McBaine, MO field site were less than 8.0 °F. The average daily dew point temperatures measured at the MU weather stations and McBaine, MO agreed with each other well.

The generally higher dew point temperatures measured at McBaine, MO are attributed to the additional sources of moisture (nearby pond and Missouri River) available to the atmosphere within the river valley. The easier access to moisture for the McBaine, MO atmosphere resulted in higher dew point temperatures than the MU weather stations.

The linear best-fit equation for the one to one relationship has a slope of 1.0 and intercepts the y-axis at 0.00 °F (Figure B.5). The linear best-fit equation for the compared measurements has a slope of 0.98 and intercepts the y-axis at -1.19 °F (Figure B.5). The daily dew point temperature comparisons between the MU weather stations and McBaine, MO have slopes and intercepts similar to the one to one relationship.
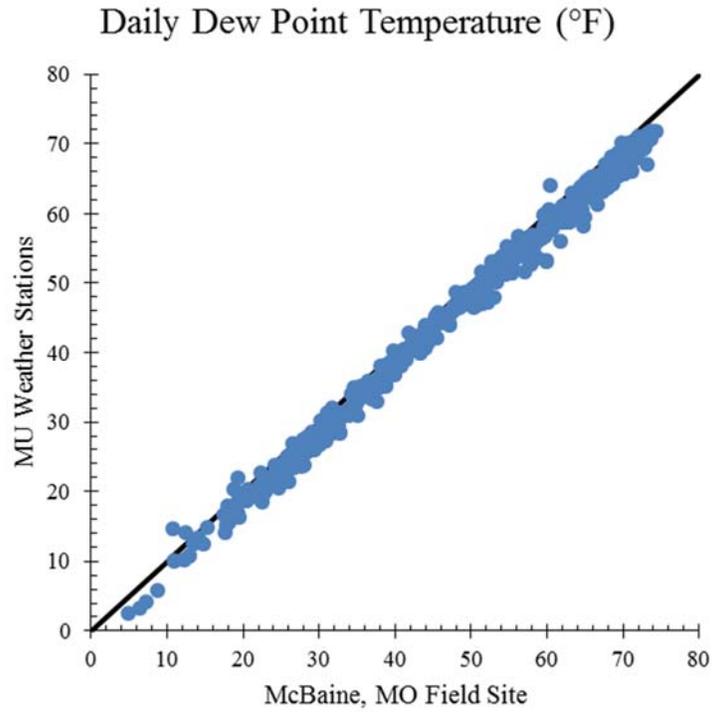
Figure B.5: Daily Dew Point Temperature Measurements of MU Weather Stations versus McBaine, MO Field Site
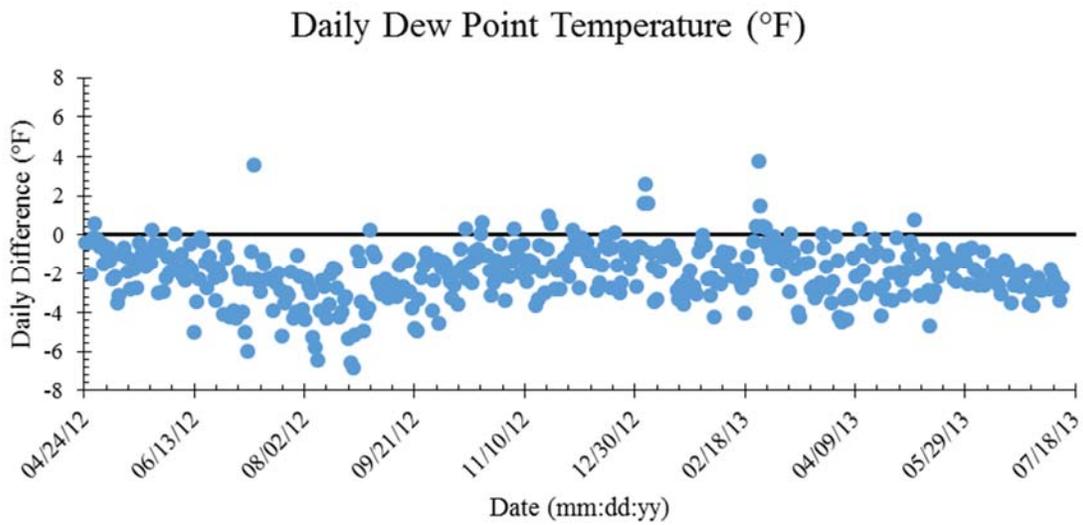
Figure B.6: Daily Differences of Minimum Air Temperature between MU Weather Stations and McBaine, MO Field Site

B.4   Total Daily Solar Radiation

The total daily solar radiation measured at the MU weather stations versus McBaine, MO field site are shown in Figure B.7. Total daily solar radiation measurements at the MU weather stations and McBaine, MO field site followed the one to one relationship at lower daily solar radiation, but at higher daily solar radiation the MU weather stations consistently measured higher. Daily differences of total solar radiation between the MU weather stations and McBaine, MO field site are shown in Figure B.8. The average daily differences were 34.3 Langley's indicating MU weather stations collectively measured higher values than the McBaine, MO field site. The greatest daily differences between the MU weather stations and McBaine, MO field site were less than 250 Langleys. The total daily solar radiation measured at the MU weather stations and McBaine, MO agreed with each other well until the spring warming season arrived.

Through a personal phone conversation with Dr. Pat Guinan of the University of Missouri, it was noted a different solar radiation sensor is used at the MU weather stations than at the McBaine, MO field site. The MU weather stations are installed with Campbell Scientific's (Campbell, 2013) "CMP3-L" pyranometer. The "CMP3-L" has a spectral range of 310 nm to 2800 nm (range up to 2000 W/m^2), whereas the Decagon Devices (Decagon, 2012) "PYR" pyranometer only has a spectral range of 380 nm to 1120 nm (range up to 1750 W/m^2). The daily differences suggest that during the spring and summer season, when the sun's angle of incidence is larger and days are longer, the MU weather stations can measure higher values than McBaine MO.

The lower total solar radiation measurements indicate lower than expected evapotranspiration (as determined from Penman, 1948 equation) occurring at McBaine, MO. Due to this lower than expected moisture loss into the atmosphere, forecasted moisture change, and

subsequently dielectric constant after precipitation events, decreased more slowly than measured results indicated.

The linear best-fit equation for the one to one relationship has a slope of 1.0 and intercepts the y-axis at 0.00 °F (Figure B.7). The linear best-fit equation for the compared measurements has a slope of 1.29 and intercepts the y-axis at -41.91 Langleys (Figure B.7). The total daily solar radiation comparisons between the MU weather stations and McBaine, MO do not have slopes or intercepts similar to the one to one relationship.
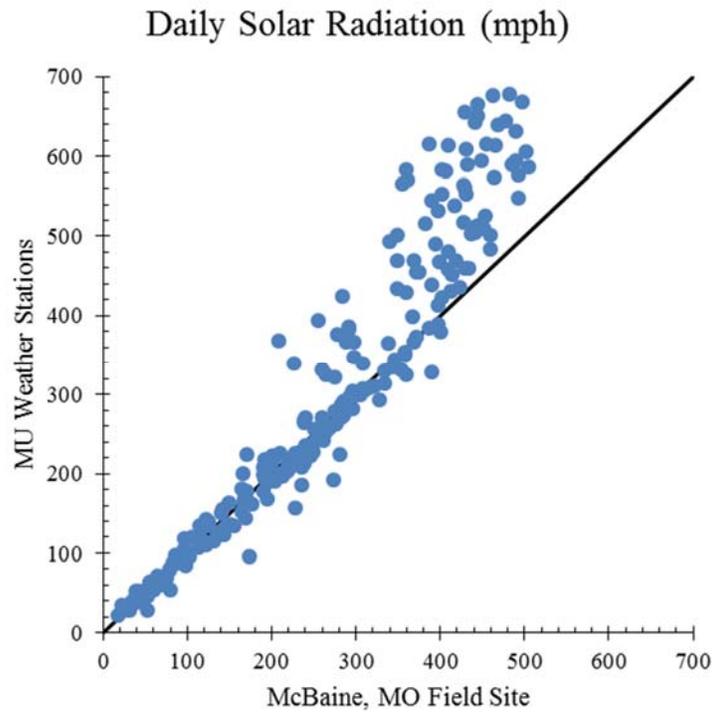
Figure B.7: Total Daily Solar Radiation Measurements of MU Weather Stations versus McBaine, MO Field Site

163
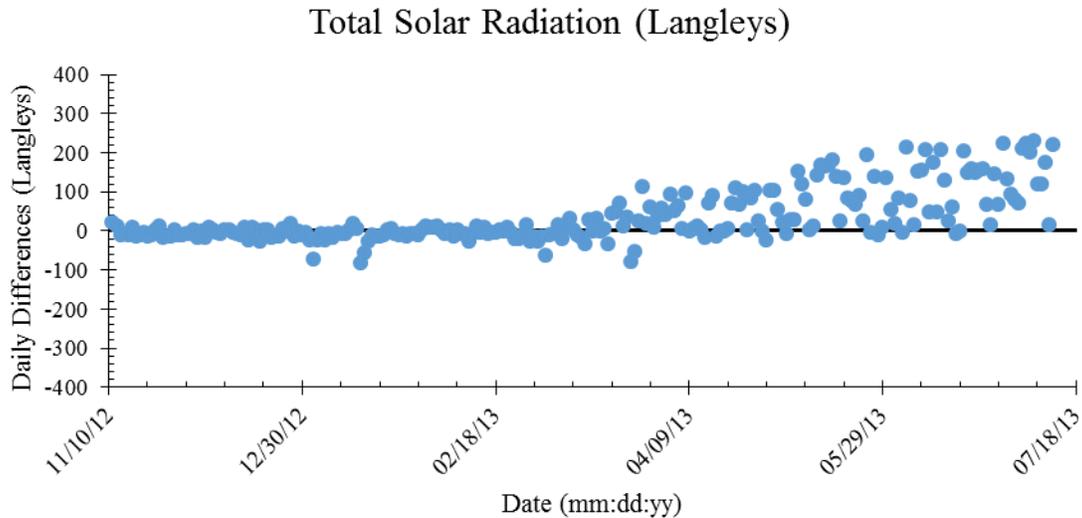
Figure B.8: Daily Differences of Total Solar Radiation between MU Weather Stations and McBaine, MO Field Site

B.5   Average Daily Wind Speed

The average daily wind speed measured at the MU weather stations versus McBaine, MO field site are shown in Figure B.9. Average daily wind speed measurements at the MU weather stations and McBaine, MO field site followed an increasing linear trend, but not the one to one relationship indicating identical measurements. Daily differences of average wind speed between the MU weather stations and McBaine, MO field site are shown in Figure B.8. The average daily differences were 1.3 mph indicating MU weather stations collectively measured higher values than the McBaine, MO field site. The greatest daily difference between the MU weather stations and McBaine, MO field site was 7.4 mph on December 20th, 2012, but typically did not exceed 4 mph. The average daily wind speed measured at the MU weather stations and McBaine, MO agreed with each other well.

The instrumentation installed at McBaine, MO is located near the Missouri River Levee System which runs from north to south at the field site location. Wind measurements at McBaine, MO are generally lower as the levee acts as a wall against the generally eastward blowing winds.

164

The MU weather stations are positioned in open fields not experiencing the cover McBaine, MO exhibits; Sanborn is near an open athletic field, Capen Park and Jefferson Farms are positioned in open grass fields.

The linear best-fit equation for the one to one relationship has a slope of 1.0 and intercepts the y-axis at 0.00 °F (Figure B.9). The linear best-fit equation for the compared measurements has a slope of 0.78 and intercepts the y-axis at 2.04 mph (Figure B.9). The average daily wind speed comparisons between the MU weather stations and McBaine, MO do not have slopes similar to the one to one relationship. The disagreement is expected due to the site characteristics impeding wind measurements at the McBaine, MO field site.
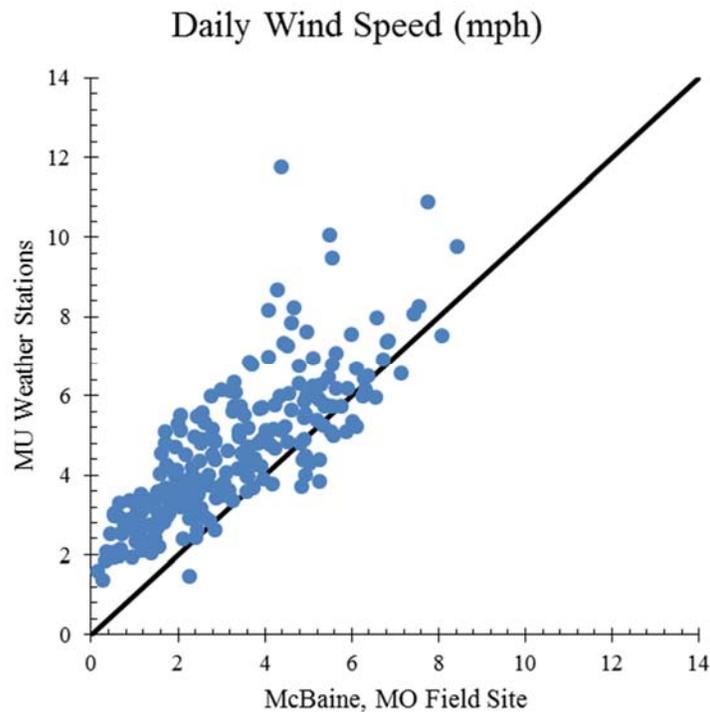
Figure B.9: Average Daily Wind Speed Measurements of MU Weather Stations versus McBaine, MO Field Site

165
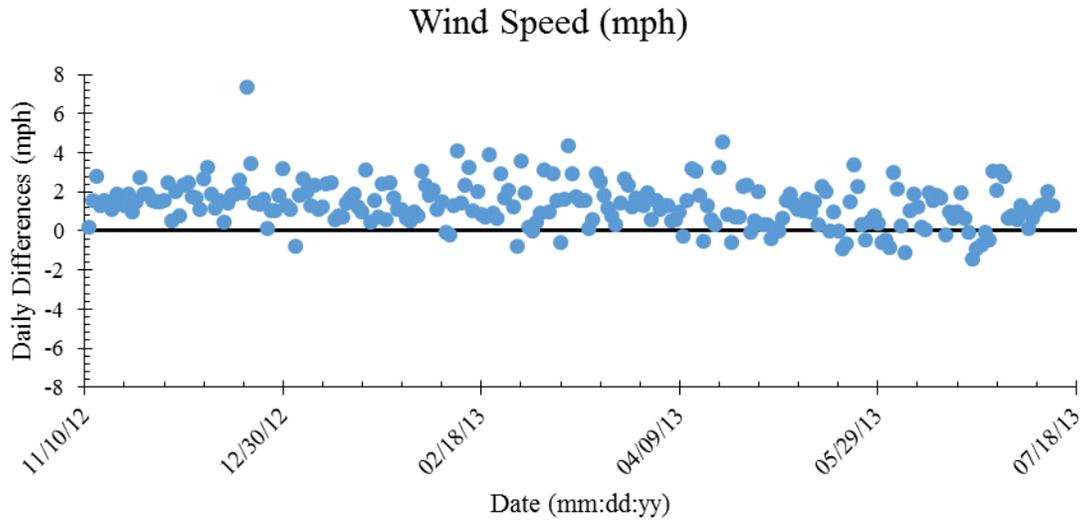
Figure B.10: Daily Differences of Average Wind Speed between MU Weather Stations and McBaine, MO Field Site

B.6 Total Daily Precipitation

The total daily precipitation measured at the MU weather stations versus McBaine, MO field site are shown in Figure B.11. Total daily precipitation measurements at the MU weather stations and McBaine, MO field site followed an increasing trend, but not the one to one relationship indicating identical measurements. Daily differences of total daily precipitation between the MU weather stations and McBaine, MO field site are shown in Figure B.12. The average daily differences when a precipitation event occurred were -0.3 in. indicating McBaine, MO collectively measured higher values than the MU weather stations. The greatest daily difference between the MU weather stations and McBaine, MO field site was 1.5 in. on May 20th, 2013, but typically did not exceed 0.5 inches. The total daily precipitation measured at the MU weather stations and McBaine, MO agreed with each other well.

The linear best-fit equation for the one to one relationship has a slope of 1.0 and intercepts the y-axis at 0.00 °F (Figure B.9). The linear best-fit equation for the compared measurements has a slope of 0.79 and intercepts the y-axis at 0.01 in. (Figure B.9). The total daily precipitation

comparisons between the MU weather stations and McBaine, MO do not have slopes similar to the one to one relationship. However, the spatial and temporal variations of precipitation producing weather systems are great as their strength and areal coverage are constantly changed. The spatial and temporal variations are attributed to the differences between MU weather stations and the McBaine, MO field site and not the inaccuracy of the McBaine, MO sensor.
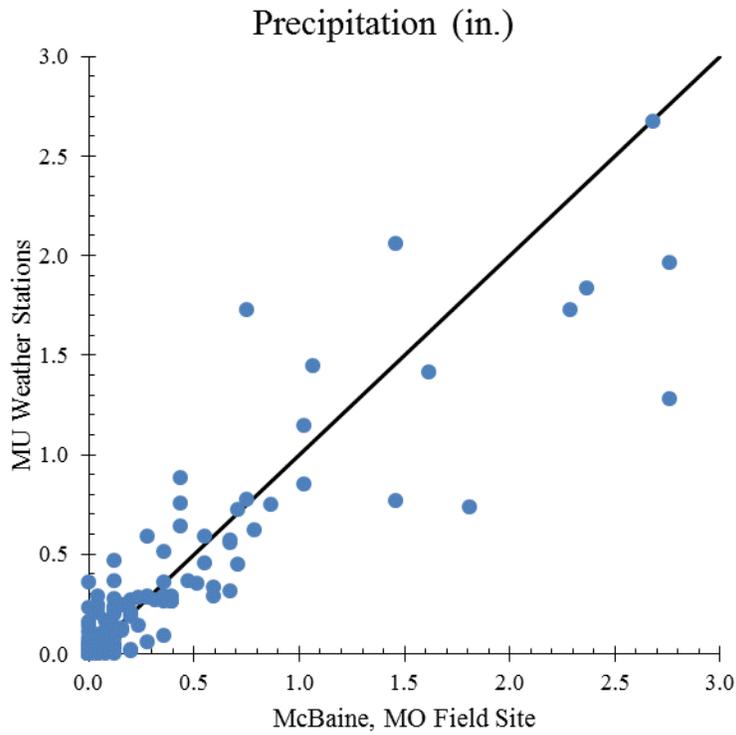
Figure B.11: Total Daily Precipitation Measurements of MU Weather Stations versus McBaine, MO Field Site
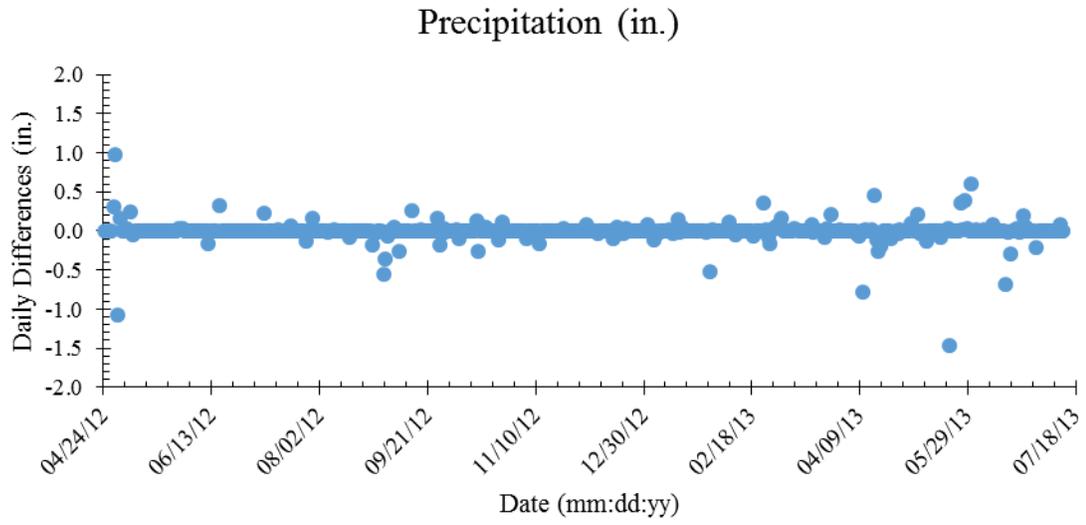
Figure B.12: Daily Differences of Average Wind Speed between MU Weather Stations and McBaine, MO Field Site